

# 博士論文

**Swelling Behaviors of Polyelectrolytes Gels  
with Alternating Neutral/Highly Charged Sequences  
under Various Environmental Conditions**

(中性/高電荷シーケンスを交互に導入した  
高分子電解質ゲルの多様な環境下での膨潤特性)

湯 健

## Preface

The present doctoral dissertation has been written based on research carried out at The University of Tokyo from 2018 to 2021 under the direction of Professor Takamasa Sakai, Professor Ung-il Chung and Dr. Takuya Katashima at Department of Bioengineering, School of Engineering, The University of Tokyo.

First, I would like to express my sincere gratitude to my supervisor, Professor Takamasa Sakai for kind guidance and for many opportunities throughout my life in laboratory. The first day I went to the laboratory, he gave me a book and told me to enjoy Japan. I cannot forget the help and encouragement from him. He guided me into polymer gels and has given me his knowledge generously. Especially, he taught me about ideas and attitudes towards science. Without his guidance, I could not have gone onto the doctoral course.

I would also like to deeply thank Professor Ung-il Chung. During the past three years, he taught me how to improve my English skills and the attitudes for making the slides and writing the papers. His encouragements always support me for overcoming the research problems. I really appreciate his instruction.

I am also grateful to Dr. Takuya Katashima for his valuable advices and instructive discussions. He is not only a teacher but also a friend for me. He helped me to establish the foundation of my research interest and always encouraged me. He taught me how to define the problem, carry out the experiment, and design the structure of the paper. He is always kind for helping me solving many problems. Thanks to Dr. Takuya Katashima, I could achieve this work and have a lot interest for the polymer gels.

I would also like to acknowledge valuable advices and helpful discussions given by Dr. Xiang Li, Professor Mitsuhiro Shibayama, Dr. Naoyuki Sakumichi at The University of Tokyo. I would like to show my greatest appreciation to Mr. Yoshiro Mitsukami and Mr. Yuki Yokoyama at the Nippon Shokubai Co., Ltd for supporting the materials. I could not accomplish this dissertation without their cooperation.

I express my gratitude to Emeritus Prof. Gerald Manning at Rutgers University. He gave me a lot fruitful discussions and aroused my interest for the polyelectrolyte gels.

I would like to thank all the members of Tei/Sakai laboratory. I thank for their encouragement and the times spent together. With their kind helps,

I have an unforgettable experience in Japan. I also thanks all members of the Shibayama laboratory.

Last of all, I wish to express my deepest appreciation to my family for all support, affectionate encouragement and understanding.

Jian Tang

Department of Bioengineering

School of Engineering

The University of Tokyo

February 2021

## Table of contents

<b>Chapter 1. General introduction .....</b>	<b>8</b>
<b>Chapter 2. Swelling behaviors of hydrogels with alternating neutral/highly charged sequences in monovalent salt solutions .....</b>	<b>21</b>
<b>2.1. Introduction .....</b>	<b>21</b>
<b>2.2. Materials and Methods .....</b>	<b>27</b>
A. Preparation of prepolymers .....	27
B. Fabrication of Tetra-PAA-PEG gels .....	27
C. Rheological measurements after gelation .....	27
D. Ultraviolet-visible light (UV-vis) spectroscopy .....	28
E. Swelling experiments .....	28
F. Rheological properties of the swollen and deswollen gels .....	29
<b>2.3. Theoretical Description of the Equilibrium Swelling State .....</b>	<b>31</b>
<b>2.4. Results and Discussion .....</b>	<b>35</b>
A. Design of Tetra-PAA-PEG gels with controlled reaction time .....	35
B. Examination of network homogeneity .....	36
C. Relationship between the swelling and external environment .....	41
D. Effect of counterion condensation on swelling .....	45
<b>2.5. Conclusions .....</b>	<b>52</b>
<b>Appendix .....</b>	<b>53</b>

<b>References .....</b>	<b>66</b>
<b>Chapter 3. Effect of nonlinear elasticity on the swelling behaviors of Tetra-PAA-PEG gels in monovalent salt solutions .....</b>	<b>72</b>
<b>3.1. Introduction .....</b>	<b>72</b>
<b>3.2. Materials and Methods .....</b>	<b>75</b>
A. Fabrication of Tetra-PAA-PEG Gels.....	75
B. Rheological Measurements after Gelation .....	75
C. Swelling Experiments .....	76
<b>3.3. Results and Discussion .....</b>	<b>78</b>
A. Effect of neutral segments lengths on the swelling behaviors .....	78
B. Effect of neutral segments lengths on the mechanical properties .....	79
C. Effect of finite extensibility of polymer chains on the swelling behaviors.....	84
D. Applicability of the modified F-R-D-M model for the conventional polyelectrolyte gels .....	90
<b>3.4. Conclusion .....</b>	<b>95</b>
<b>Appendix .....</b>	<b>96</b>
<b>Reference .....</b>	<b>103</b>
<b>Chapter 4. Swelling behaviors of Tetra-PAA-PEG gel in divalent salt solutions .....</b>	<b>106</b>
<b>4.1. Introduction .....</b>	<b>106</b>

<b>4.2. Experimental</b> .....	<b>109</b>
A. Fabrication of Tetra-PAA-PEG Gels.....	109
B. Swelling Experiments .....	109
C. Rheological Properties of the swollen and deswollen gels .....	110
D. Small-angle X-ray scattering (SAXS).....	111
<b>4.3. Result and discussions</b> .....	<b>112</b>
A. Effect of pH on the swelling behaviors (divalent salt).....	112
B. Effect of divalent salt concentration on the swelling behaviors.....	115
C. Effect of divalent salt concentration on the mechanical properties.....	116
<b>4.4. Conclusion</b> .....	<b>123</b>
<b>Reference</b> .....	<b>124</b>
<b>Chapter 5. Summary and Conclusion</b> .....	<b>126</b>
<b>List of publications</b> .....	<b>130</b>
<b>List of presentations</b> .....	<b>131</b>

## Chapter 1. General introduction

Polymer gels consist of an elastic cross-linked network and solvents filling the interstitial spaces of the network. Due to the characteristic structure, polymer gels look like solid material but exhibit a flexible response after applying stress or strain and can undergo deformation depending on the environment. Polyelectrolyte gels is a charged polymer network with fixed ions on the polymer chains and contain solvent with mobile ions localized in the network frame. Compared with neutral polymer gels, polyelectrolyte gels always exhibit significant water-absorbing ability but do not dissolve in water. The swelling properties of polyelectrolyte gel are sensitive to the external solvent environment, i.e., the pH value, the salt concentration, and salt types. The swelling behaviors of the sodium polyacrylate gel strongly depend on the kind of salt. The swelling ratios of the sodium polyacrylate gel smoothly decrease with the increase of monovalent salt concentration (NaCl, KCl, CsCl), while the swelling ratios of gel reduce much faster in a divalent salt solution (CaCl<sub>2</sub>, SrCl<sub>2</sub>, BaCl<sub>2</sub>). Due to unique swelling properties, the polyelectrolyte gels have attracted considerable interest in bioengineering. For example, the macroscopic muscle-like actuators, drug delivery, biosensors, active membranes separation, and scaffolds for tissue engineering are similar to the similar multi-responsive swelling behaviors as biological systems.<sup>1-3</sup> These swelling properties relate to the polyelectrolyte gel structure and have been investigated for an extended period.

The Flory can describe the equilibrium swelling behaviors of neutral polymer gels–Rehner model, in which the total free energy is minimum in the equilibrium

swelling state.<sup>4</sup> According to the model, the total free energy ( $F$ ) is the sum of the elastic free energy ( $F_{el}$ ) and mixing free energy ( $F_{mix}$ ). In their pioneering works, Flory and co-workers assumed that elastic free energy has a Neo-Hookean-type potential<sup>4,5</sup>, which originated from the rubber elasticity and resisted the gel's deformation. Flory and Huggins estimated the mixing free energy using the lattice approximation<sup>6,7</sup>, which derives from the polymer-solvent interaction and prevents the polymer network from collapsing. The elastic pressure ( $\Pi_{el}$ ) originated from elastic free energy, and the mixing pressure ( $\Pi_{mix}$ ) derived from mixing free energy described the equilibrium swelling state of the neutral gel via these assumptions.<sup>8-11</sup>

Regarding the polyelectrolyte gels, the interaction between the ions within the gel needs to be considered. There are always two main kinds of interactions inside the polyelectrolyte gel: the Coulomb energy between two fixed ions with the same charge and the electrostatic interaction between the counterions and fixed ions with the opposite charge. The free energy derived from the Coulombic interactions always contributes to the electrostatic repulsion between the fixed ions on the polymer chain, leading to the expansion of the polyelectrolyte gel.<sup>12</sup> This electrostatic repulsion between the fixed ions is strongly influenced by the pH and ionic strength. Conventionally, this contribution to the gel expansion is small and is negligible, especially when salt is added to the external solvent. The latter electrostatic interaction between the fixed ions and mobile ions with opposite charges relates to estimating the effective fixed ion concentration. When the ion-ion interaction is small, compared with thermal energy, a part of counterions are not distributed evenly throughout the network

but tend to remain in the vicinity of the fixed ions on the polymer chains, and forming an ionic atmosphere following the Debye–Hückel approximation,<sup>13,14</sup> which was derived within the framework of linearized Poisson–Boltzmann equation. The rest part of the counterions can freely move within the gel. In the case of ion-ion interaction being larger than the thermal energy, a portion of counterions bind with the fixed ion and reduce their effective thermodynamic concentration, known as counterion condensation.<sup>15,16</sup> Manning improved the previous counterion condensation theory and developed a series of empirical formulations that can describe the counterions' distribution.<sup>17</sup> Manning proposed a critical dimensionless parameter for deciding whether the counterion condensation occurs or not. If the fixed ion density is small, compared with the critical value, the counterion condensation will not occur, and the distribution of counterions follow the Debye–Hückel approximation like the former case; on the other hand, if the fixed ion is larger than the critical value, a portion of counterions will condense on the fixed ion and become localized around the network strand, leading to the decrease of the effective fixed ion concentration. The uncondensed counterions are assumed to follow the Debye–Hückel approximation. This distribution makes it possible to know the displacement probability between any two arbitrary charges in the chain. Here, I can understand the distribution of freely moving and restricted mobile ions inside the gel via the above theories.

The ionic contribution was derived from the free energy caused by the difference in the free mobile ion concentrations inside and outside the gels ( $F_{\text{ion}}$ ); this effect is well known as the Donnan equilibrium.<sup>18</sup> Mobile ions can be condensed in a medium with

fixed ions when the medium is connected to the external solution due to the Donnan potential. This ionic free energy can contribute to the osmotic pressure of the free mobile ions, which is known as ionic pressure ( $\Pi_{\text{ion}}$ ). Therefore, the contribution to the expansion of the polyelectrolyte gel is always considered derived from the heterogeneous distribution of free mobile ions concentrations inside and outside the gel, which can be fully understood by the Donnan equilibrium theory.

Ricka and Tanaka<sup>19</sup> proposed a model by combining the Flory–Rehner model with the Donnan equilibrium (F-R-D model) to describe the swelling behaviors of weak polyelectrolyte gels. In this model, the sum of the elastic pressure, mixing pressure, and ionic pressure equals 0 when the polyelectrolyte gel is reaching the equilibrium swelling state. This model successfully described many experimental results of polyelectrolyte gel with relatively low charge density,<sup>20–25</sup> in which the charge density is small, compared with the critical concentration of Manning's counterion condensation theory, the ion-ion interaction is weaker than the thermal energy, and the distribution of mobile ions follow the Debye–Hückel approximation. However, this model does not work well for polyelectrolyte gel with a high charge density, in which the counterion condensation occurs. Simply considering this problem, the wrong estimation of ionic pressure causes the failure of the F-R-D model for describing the swelling behaviors of polyelectrolyte gel.

In contrast, the counterion condensation has not been considered inside this model. Although there have been some attempts to examine the applicability of Manning's model for describing the swelling behaviors of polyelectrolyte gels, a significant

deviation between the predictions and experimental results still exists,<sup>26,27</sup> which is attributed to the heterogeneity of polymer gel, whose structure was not precisely controlled and the distribution of the fixed ions was heterogeneous.<sup>28</sup> Conventionally, the polyelectrolyte gels are prepared via the random copolymerization of charged and neutral monomers with cross-linkers. (Figure 1-1). Due to the reactivities, the ionic monomers and neutral monomers are expected to be randomly localized on the polymer strand, resulting in the areas with sparse and dense fixed ions.<sup>28,29</sup> The charge density is high in dense regions and counterion condensation can occur, resulting in the decrease of the concentration of both effective fixed ion and free mobile ions. (Figure 1-2). However, the bulk charge density of the gel does not satisfy the requirement of the critical charge density in Manning's theory, which suggests there is no counterion condensation occurring inside the gel. This contradiction between the theory and the real situation always lead to the misunderstanding of the relationship between structure and properties of polyelectrolyte gel. It is impossible to evaluate the real heterogeneous distribution of charges inside the polyelectrolyte; thus the validation of the theories is often inhibited. In order to fully understand the relationship between the structure and the swelling properties of polyelectrolyte gels, it is important to design a polyelectrolyte gel with well-controlled heterogeneous distribution of charge as a model for validating the theories.

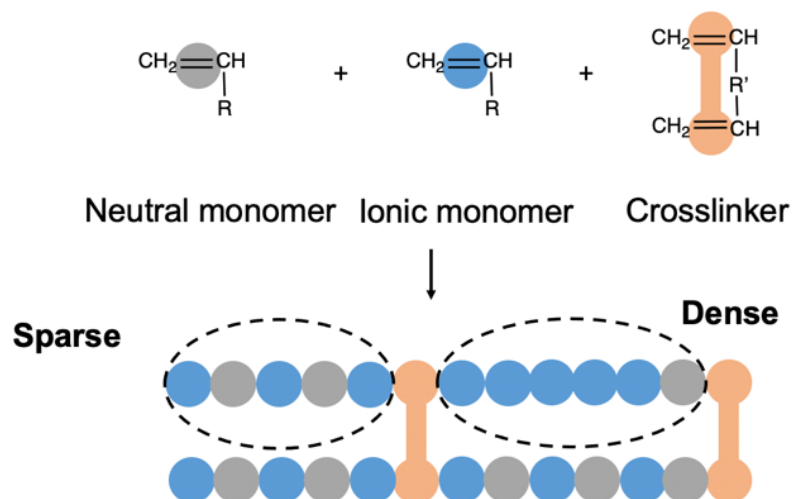


**Figure 1-1.** Schematic illustrations of the preparation of conventional polyelectrolyte gel via random copolymerization.

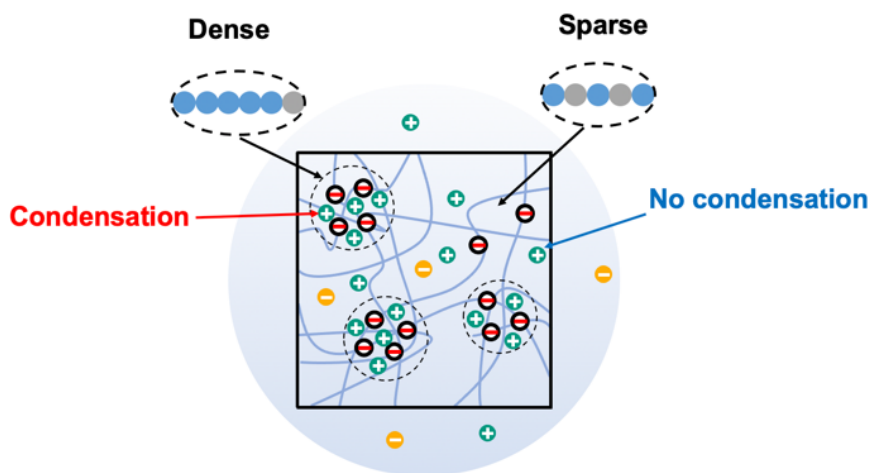


**Figure 1-2.** Schematic illustrations of charge distribution inside the polyelectrolyte gel.

In the last decades, we have designed and fabricated a nearly-ideal polymer network structure using tetra-armed poly(ethylene glycol) as prepolymers, which is known as “Tetra-PEG gel”.<sup>30</sup> Tetra-PEG gel is formed by AB-type crosslink-coupling

of two tetra-armed prepolymers with mutually reactive end groups. As the tetra-armed building blocks were precisely synthesized via anionic polymerization, the resultant networks were expected to have a regular network structure with four-arm cross-linking points and a uniform strand length.<sup>31</sup> <sup>1</sup>H multiple-quantum nuclear magnetic resonance,<sup>32</sup> Fourier transform infrared spectroscopy,<sup>33</sup> Ultraviolet-visible light spectroscopy,<sup>34</sup> small-angle neutron scattering, static light scattering<sup>35,36</sup> and mechanical test<sup>37-43</sup> was performed to confirm the controllability of the network structure. Recently, tetra-armed poly(acrylic acid) gel (Tetra-PAA gel) was successfully fabricated using the end-linking of tetra-armed prepolymers via click chemistry.<sup>44,45</sup> According to small-angle neutron scattering and small-angle X-ray scattering studies, Tetra-PAA gel in the uncharged state had a similar concentration fluctuation as that in an un-cross-linked solution, suggesting that the heterogeneous distribution of polymer segments was highly suppressed, which is similar as the conventional Tetra-PEG gels. These studies indicate that a polyelectrolyte gel with a uniform network structure can be formed via the AB type crosslink-coupling reaction. Based on our previous experience, I synthesized a regular polyelectrolyte gel (Tetra-PAA-PEG gel) with alternating neutral/highly charged sequences by tetra-thiol-terminated poly(ethylene glycol) (Tetra-PEG-SH) and tetra-maleimide-terminated poly(acrylic acid) (Tetra-PAA-MA) via the click chemistry. (Figure 1-3)

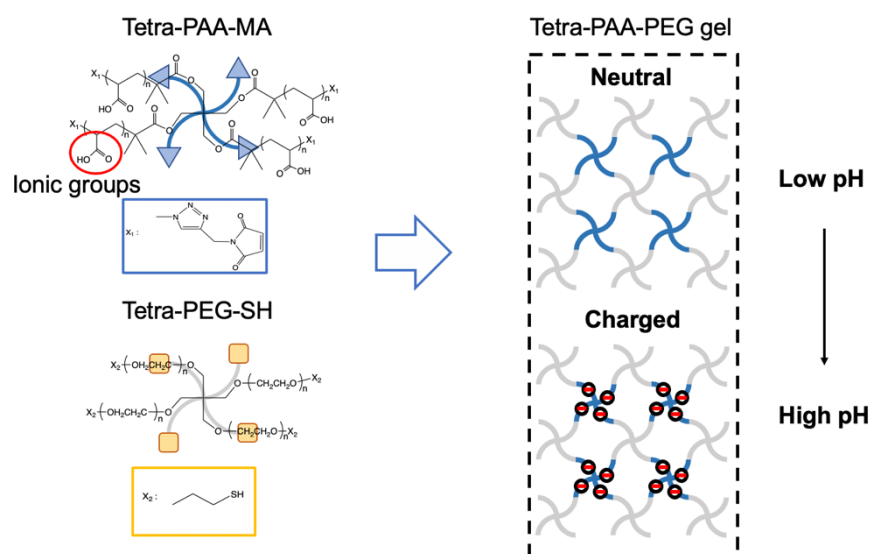


**Figure 1-3.** Schematic illustrations of preparation of Tetra-PAA-PEG gels.

In order to understand the effect of heterogeneous distribution of fixed ions on the swelling behaviors of Tetra-PAA-PEG gel, the main aims in the dissertation are summarized as follows:

- 1) To design and fabricate a regular polyelectrolyte gel with well-controlled heterogeneous distribution of fixed ions and examine the homogeneity of the network structure;
- 2) To clarify the swelling behaviors of highly charged polyelectrolyte gel in monovalent salt solutions;
- 3) To clarify the effect of the lengths of neutral segments on the swelling behaviors of highly charged polyelectrolyte gel in monovalent salt solutions;
- 4) To clarify the swelling behaviors of highly charged polyelectrolyte gel in divalent salt solutions;

The contents of this dissertation are as follows:

**Chapter 1:** General introduction

**Chapter 2:** Tetra-PAA-PEG gel is formed by AB-type crosslink-coupling of tetra-thiol-terminated poly(ethylene glycol) (Tetra-PEG-SH) and tetra-maleimide-terminated poly(acrylic acid) (Tetra-PAA-MA) via click chemistry. The gelation condition is optimized by tuning the pH of the buffer solution. The network homogeneity is examined based on mechanical and spectroscopic measurements. The relationship between the heterogeneous distribution of fixed ions and the monovalent salt solution's swelling properties is investigated based on the Flory-Rehner theory, considering both Donnan equilibrium and counterion condensation effect (F-R-D-M model).

**Chapter 3:** I control the molecular weight ( $M_w$ ) of Tetra-PEG-SH and investigate the effect of neutral segment lengths on the mechanical and swelling properties of Tetra-PAA-PEG gel. The effect of the finite extensibility of the network strand on the swelling behaviors is precisely deduced.

**Chapter 4:** The swelling behaviors of Tetra-PAA-PEG gel in divalent solutions are investigated. The contribution from the aggregation structure between the calcium ions and acrylic acid groups to the elasticity of the gel is clarified. Furthermore, the applicability of the F-R-D-M model for describing the swelling behaviors in divalent salt solutions is estimated.

**Chapter 5:** Conclusion.

## References

- (1) Drury, J. L.; Mooney, D. J. *Biomaterials* **2003**, *24* (24), 4337–4351.
- (2) Toh, W. S.; Loh, X. J. *Mater. Sci. Eng. C* **2015**, *45*, 690–697.
- (3) Slaughter, B. V; Khurshid, S. S.; Fisher, O. Z.; Khademhosseini, A.; Peppas, N. *Adv. Mater.* **2009**, *21* (32-33), 3307–3329.
- (4) Flory, P. J. *Principles of Polymer Chemistry*; Cornell University Press, 1953.
- (5) Flory, P. J.; Rehner, J. *J. Chem. Phys.* **1943**.
- (6) Huggins, M. L. *Ann. N. Y. Acad. Sci.* **1942**, *43* (1), 1–32.
- (7) Flory, P. J. Thermodynamics of High Polymer Solutions. *J. Chem. Phys.* **1942**, *10* (1), 51–61.
- (8) López-León, T.; Fernández-Nieves, A. *Phys. Rev. E, Soft Matter Phys.* **2007**, *75* (1), 1–8.
- (9) Fernández-Barbero, A.; Fernández-Nieves, A.; Grillo, I.; López-Cabarcos, E. *Phys. Rev. E.* **2002**, *66* (5), 10.
- (10) Lietor-Santos, J.-J.; Sierra-Martin, B.; Vavrin, R.; Hu, Z.; Gasser, U.; Fernandez-Nieves, A. *Macromolecules* **2009**, *42* (16), 6225–6230.
- (11) Lopez, C. G.; Richtering, W. *Soft Matter* **2017**, *13* (44), 8271–8280.
- (12) Dusek, K. *J. Polym. Sci.* **1975**, *13*, 253–262.
- (13) Freedman, H. L. *Ionic Solutions Theory*. Wiley Interscience: New York 1962.
- (14) Bockris, J. O. O'M.; Reddy, AKN *Modern Electrochemistry*, Vol. 2. Plenum Press, New York 1970.
- (15) Oosawa, F. *J. Polym. Sci.* **1957**, *23* (103), 421–430.

- (16) Kotin, L.; Nagasawa, M. *J. Chem. Phys.* **1962**, *36* (4), 873–879.
- (17) Manning, G. S. *J. Phys. Chem.* **1981**, *85* (11), 1506–1515.
- (18) Donnan, F. G.; Guggenheim, E. A. *Zeitschrift für Phys. Chemie* **1932**, *162* (1), 346–360.
- (19) Rička, J.; Tanaka, T. *Macromolecules* **1984**, *17* (12), 2916–2921.
- (20) Çaykara, T.; Akçakaya, I. *Eur. Polym. J.* **2006**, *42* (6), 1437–1445.
- (21) Hirotsu, S.; Hirokawa, Y.; Tanaka, T. *J. Chem. Phys.* **1987**, *87* (2), 1392–1395.
- (22) Ikkai, F.; Suzuki, T.; Karino, T.; Shibayama, M. *Macromolecules* **2007**, *40* (4), 1140–1146.
- (23) Okay, O.; Sariişik, S. B.; Zor, S. D. *J. Appl. Polym. Sci.* **1998**, *70* (3), 567–575.
- (24) Baker, J. P.; Blanch, H. W.; Prausnitz, J. M. *Polymer (Guildf)*. **1995**, *36* (5), 1061–1069.
- (25) Shibayama, M.; Ikkai, F.; Inamoto, S.; Nomura, S.; Han, C. C. *J. Chem. Phys.* **1996**, *105* (10), 4358–4366.
- (26) Jeon, C. H.; Makhaeva, E. E.; Khokhlov, A. R. *Macromol. Chem. Phys.* **1998**, *199* (12), 2665–2670.
- (27) Liu, X.; Tong, Z.; Hu, O. *Macromolecules* **1995**, *28* (11), 3813–3817.
- (28) Zeldovich, K. B.; Khokhlov, A. R. *Macromolecules* **1999**, *32* (10), 3488–3494.
- (29) Dušek, K.; Prins, W. *Fortschritte der Hochpolym.* **2006**, *6*, 1–102.
- (30) Sakai, T.; Matsunaga, T.; Yamamoto, Y.; Ito, C.; Yoshida, R.; Suzuki, S.; Sasaki, N.; Shibayama, M.; Chung, U. Il. *Macromolecules* **2008**, *41* (14), 5379–5384.
- (31) Kamata, H.; Li, X.; Chung, U. Il; Sakai, T. *Adv. Healthc. Mater.* **2015**, *4* (16),

- 2360–2374.
- (32) Lange, F.; Schwenke, K.; Kurakazu, M.; Akagi, Y.; Chung, U. Il; Lang, M.; Sommer, J. U.; Sakai, T.; Saalwächter, K. *Macromolecules* **2011**, *44* (24), 9666–9674.
- (33) Akagi, Y.; Katashima, T.; Katsumoto, Y.; Fujii, K.; Matsunaga, T.; Chung, U. Il; Shibayama, M.; Sakai, T. *Macromolecules* **2011**, *44* (14), 5817–5821.
- (34) Yoshikawa, Y.; Sakumichi, N.; Chung, U. Il; Sakai, T. *Soft Matter* **2019**.
- (35) Matsunaga, T.; Sakai, T.; Akagi, Y.; Chung, U. Il; Shibayama, M. *Macromolecules* **2009**, *42* (4), 1344–1351.
- (36) Matsunaga, T.; Sakai, T.; Akagi, Y.; Chung, U. Il; Shibayama, M. *Macromolecules* **2009**, *42* (16), 6245–6252.
- (37) Katashima, T.; Sakurai, H.; Chung, U. il; Sakai, T. *Nihon Reoroji Gakkaishi* **2019**, *47* (2), 61–66.
- (38) Sakai, T.; Akagi, Y.; Kondo, S.; Chung, U. *Soft Matter* **2014**, *10* (35), 6658–6665.
- (39) Akagi, Y.; Sakurai, H.; Gong, J. P.; Chung, U. Il; Sakai, T. *J. Chem. Phys.* **2013**, *139* (14), 1–7.
- (40) Li, X.; Nakagawa, S.; Tsuji, Y.; Watanabe, N.; Shibayama, M. *Sci. Adv.* **2019**, *5* (12), 1–8.
- (41) Fujiyabu, T.; Yoshikawa, Y.; Chung, U. il; Sakai, T. *Sci. Technol. Adv. Mater.* **2019**, *20* (1), 608–621.
- (42) Akagi, Y.; Gong, J. P.; Chung, U. Il; Sakai, T. *Macromolecules* **2013**, *46* (3),

- 1035–1040.
- (43) Akagi, Y.; Katashima, T.; Sakurai, H.; Chung, U. Il; Sakai, T. *RSC Adv.* **2013**, *3* (32), 13251–13258.
- (44) Oshima, K.; Mitsukami, Y. *Polymer (Guildf)*. **2016**, *100*, 134–142.
- (45) Oshima, K.; Fujimoto, T.; Minami, E.; Mitsukami, Y. *Macromolecules* **2014**, *47* (21), 7573–7580.

## Chapter 2. Swelling behaviors of hydrogels with alternating neutral/highly charged sequences in monovalent salt solutions

### 2.1. Introduction

Polyelectrolyte gels are a network structure that consists of both polymer networks with fixed ions on network strands and a solvent with mobile counterions. In contrast to electrically neutral gels, polyelectrolyte gels can always swell or shrink to a significant degree, depending on the external solution's pH value and ionic strength.<sup>1-4</sup> For example, a polyacrylamide-acrylic acid gel is a representative of polyelectrolyte gels with pKa of 4.2. In the conventional studies, they investigated the swelling ratio of the polyacrylamide-acrylic acid gel in the presence of various types of salts, i.e., NaCl, CaCl<sub>2</sub>, AlCl<sub>3</sub>, etc. Therefore, we utilize polyelectrolyte gels in commercial applications, including diapers, soil modifiers, and seawater desalination. Moreover, polyelectrolyte gels' multi-responsive swelling behaviors are similar to biological systems such as nerve excitation, muscle contraction, and cell locomotion. Many attempts to utilize polyelectrolyte gels for drug delivery, soft actuators, and tissue engineering.<sup>5-8</sup>

The Flory–Rehner model can describe the equilibrium swelling behaviors of hydrogels, in which the equilibrium swelling state requires the minimum of the total free energy.<sup>9</sup> According to the description of the model, the total free energy ( $F$ ) for the polyelectrolyte gel is the sum of the free energy of elastic deformation ( $F_{el}$ ), the free energy of mixing ( $F_{mix}$ ), and the free energy caused by the imbalance concentration distribution of the mobile ions inside and outside the gels ( $F_{ion}$ ). Flory and co-workers

assumed to describe the elastic free energy by the Neo-Hookean-type model<sup>9,10</sup>. They estimated the mixing free energy based on the lattice model,<sup>11,12</sup> and the Donnan equilibrium determines the ionic free energy.<sup>13</sup> Mobile ions condense in a medium with fixed ions when the external solution connects with the medium. Ricka and Tanaka<sup>14</sup> proposed combining the Flory–Rehner model with the Donnan equilibrium (F-R-D model) to describe the polyelectrolyte gels’ swelling behaviors. Many experimental studies tried to validate the Flory–Rehner model with the Donnan equilibrium. They often utilized the polyelectrolyte gels obtained via radical random polymerizations, such as polyacrylamide-acrylic acid,<sup>14</sup> poly(*N*-isopropyl acrylamide),<sup>15,16</sup> poly(*N*-isopropyl acrylamide-co-acrylic acid),<sup>17–19</sup> acrylamide-based,<sup>20–24</sup> poly(vinyl imidazole)<sup>25</sup> and poly (acrylamide-co-acrylic acid and trimethyl-*N*-acryloyl-3-aminopropyl ammonium chloride) gels<sup>26</sup>. The model succeeded in describing the swelling behaviors of polyelectrolyte gels with relatively low charge density. On the other hand, some research showed that the F-R-D model does not work well for polyelectrolyte gels with a high charge density. Höpfner et al.<sup>27</sup> observed the model prediction’s deviation with increasing the fixed ions’ density. They found that the F-R-D model overestimated the equilibrium swelling ratio by up to 30%. Katchalsky et al.<sup>28</sup> suggested that the substantial deviation from the classical Donnan equilibrium theory may be due to a significant decrease in the mobile ions’ activity coefficient in the ionized polyelectrolyte.

Most probably, the overestimation of the contribution of counterions can lead to these deviations. The relationship between the ion-ion interaction and thermal

fluctuation influences the ionic contribution. When the ion density is low, the ion-ion interaction is small compared with the thermal energy. The distribution of ions follows the Boltzmann distribution, which in accord with the Debye-Hückel limiting law.<sup>29-31</sup> This agrees with Tanaka's original situation, where he assumed a weakly charged flexible gel and the Donnan equilibrium are applicable. However, when the distance between neighboring fixed ions is small, the counterions' binding force becomes more significant than the thermal fluctuation.<sup>32-34</sup> In this condition, the counterions are localized around the network strands. Many experiments reported this phenomenon as an abnormally low osmotic pressure of the polymer "solution" for the first time. Oosawa<sup>35</sup> suggested that when a portion of the counterions inside the highly charged polyelectrolyte solution became condensed, the fixed ion concentration decreased significantly. This phenomenon is currently known as counterion condensation. Kotin and Nagasawa attempted to estimate the bound fraction of the fixed ions' counterions based on the Poisson-Boltzmann distribution. They propose a mathematical expression for describing the degree of counterion condensation.<sup>36</sup> Manning developed a series of empirical formulations and improved the previous condensation theory.<sup>37</sup> In Manning's approach, the density of fixed ions on the polymer chains cannot exceed a specific critical value, depending on the neighboring fixed ions' distance.

A few studies also examined Manning's model's applicability to describe the swelling behaviors of polyelectrolyte gels. They found that the model may still produce a significant deviation concerning the swelling ratio.<sup>3,38</sup> Recent works mentioned that polymer gels' heterogeneity, including the aggregation structures<sup>39,40</sup> and the fixed ions'

heterogeneous distribution could lead to the deviation. Researchers conventionally prepared the polyelectrolyte gels via the random copolymerization of the ionic/neutral monomers. They expected the ionic monomers to localize on a strand, owing to the differences in the monomers' reactivities, with areas of dense and sparse fixed ions.<sup>41,42</sup> However, it is impossible to evaluate the accurate heterogeneous distribution of charges, inhibiting the associated theories' validation. To fully understand polyelectrolyte gels' swelling behaviors, we need gels with well-controlled block structures.

In 2008, our group designed and fabricated a polymer gel with a well-controlled network structure via an AB-type crosslinking between two tetra-armed polyethylene glycols, which is known as the Tetra-PEG gel.<sup>43,44</sup> We expect to obtain the resultant networks with an ideal network structure with tetra-functional crosslinking points and a uniform strand length by precisely synthesizing the tetra-armed building blocks via anionic polymerization. As elucidated in our previous reports, we confirm the network structures' controllability using <sup>1</sup>H multiple-quantum nuclear magnetic resonance, Fourier transforms infrared spectroscopy and mechanical tests.<sup>45-47</sup> Thus, the Tetra-PEG gels' fabrication method is expected to be a reasonable one to fabricate polymer gels with well-controlled block structures. Recently, Tetra-armed polyacrylic acid (PAA) and Tetra-functional PAA gels were successfully synthesized by Oshima et al. using the end-linking of Tetra-PAA via click chemistry.<sup>48</sup> According to small-angle neutron scattering (SANS) and small-angle X-ray scattering (SAXS) studies, concentration fluctuation of Tetra-PAA gel in the uncharged state is similar to that in an un-crosslinked solution. This result suggested that the polymer segments'

heterogeneous distribution was negligible. The network structure of Tetra-PAA gels is identical to the conventional Tetra-PEG gels. The gel in the charged state showed a scattering peak owing to the characteristics of the polyelectrolyte.<sup>49</sup> These studies indicated that I could fabricate a regular polyelectrolyte gel via the AB-type crosslinking reaction.

In this work, I synthesize regular polyelectrolyte gels with alternating neutral/highly charged sequences and investigate the influence of the heterogeneous distribution of fixed ions on the swelling behaviors. We synthesize the neutral and charged tetra-functional segments composed of polyethylene glycol (Tetra-PEG) and polyacrylic acid (Tetra-PAA) for fabricating the regular polyelectrolyte gels. The click chemistry creates the network between the mutually reactive maleimide and thiol end groups of the Tetra-PEG and Tetra-PAA, respectively (the Tetra-PAA-PEG gel shown in Figure 2-1). It's worth noting that the previous Tetra-PEG gels<sup>43</sup> and Tetra-PAA gel<sup>48</sup> should be different from the Tetra-PAA-PEG gel, which should have alternating neutral/charged sequences. The reason is that the Tetra-PEG gel is entirely neutral, while all the monomers of the Tetra-PAA gel are charged depending on the external solution conditions. I investigate the Tetra-PAA-PEG gel based on mechanical and spectroscopic measurements; then, we analyze the swelling behaviors of Tetra-PAA-PEG gel under tuned external solutions. By comparing the observed swelling ratios with the theoretical model predictions that consider both the Donnan equilibrium and the counterion condensation effects, I can reveal the molecular mechanism of the swelling of highly charged polyelectrolyte gels.

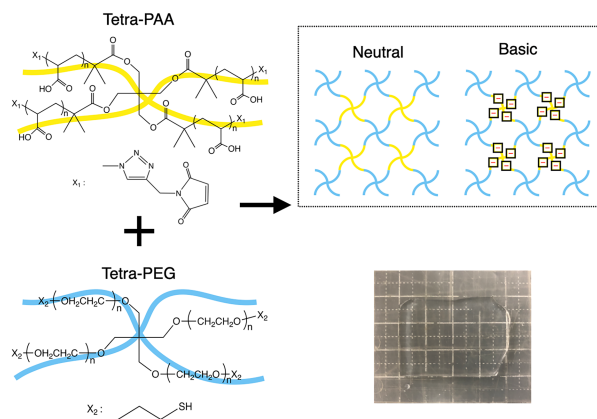


**Figure 2-1.** Schematic Illustration of the Tetra-PAA-PEG gel design and the optical image, where yellow and blue parts represent the polyacrylic acid and polyethylene glycol units, respectively.

## 2.2. Materials and Methods

### A. Preparation of prepolymers

The Tetra-thiol-terminated polyethylene glycol (Tetra-PEG-SH) was purchased from NOF CORPORATION (Tokyo, Japan). Tetra-maleimide-terminated poly(acrylic acid) (Tetra-PAA-MA) was synthesized via the click reaction of Tetra-azide-terminated poly(*tert*-butyl acrylate) (Tetra-PtBuA-N<sub>3</sub>)<sup>48</sup> with *N*-propargylmaleimide in the presence of copper wire and subsequent deprotection of PtBuA with trifluoroacetic acid. The details of the synthesis of Tetra-PAA-MA are described in Section 1 of Supporting Information. The molar masses of Tetra-PEG-SH and Tetra-PAA-MA were  $2.0 \times 10^4$  g mol<sup>-1</sup> and  $1.9 \times 10^4$  g mol<sup>-1</sup>, respectively.

### B. Fabrication of Tetra-PAA-PEG gels

Equivalent molars of Tetra-PEG-SH and Tetra-PAA-MA were dissolved in citrate-phosphate buffer solution. The buffer solutions' pH were set to 3.0, 5.1, 5.9, and 7.1 to achieve different reaction rates, and the ionic strength of the buffer solutions was 100 mM. In order to obtain the same molar concentrations, Tetra-PEG-SH and Tetra-PAA-MA concentrations were set to 64.7 g L<sup>-1</sup> and 60.0 g L<sup>-1</sup>, respectively. These concentrations were slightly above the overlapping concentrations for each polymer. Equal amounts of the prepolymer solutions were mixed for 30 s and poured into the silicone mold at room temperature. In this study, 48 h were given for the completion of each reaction.

### C. Rheological measurements after gelation

Tetra-PAA-MA and Tetra-PEG-SH's mixed solution was poured into the interstice of

the double cylinder of a rheometer (MCR301; Anton Paar, Graz, Austria) at 25°C. In the cylinder, 48 h were given for the completion of the reaction at 25 °C, after mixing. After the gelation reaction, I measured the angular frequency ( $\omega$ ) dependence of the storage modulus ( $G'$ ) and loss modulus ( $G''$ ) with a strain amplitude ( $\gamma$ ) of 1.0% at 25 °C. The value of  $\gamma$  was determined within the linear viscoelastic region.

#### D. Ultraviolet-visible light (UV-vis) spectroscopy

Linear-hydroxyl-terminated polyethylene glycol ( $M_w = 2.0 \times 10^4$  g mol<sup>-1</sup>) was dissolved into the Tetra-PAA-MA polymer solution, which was purchased from FUJIFILM Wako Pure Chemical Corporation (Tokyo, Japan). The linear PEG and Tetra-PAA-MA polymers' molar ratios were the same as those of Tetra-PEG-SH and Tetra-PAA-MA. Turbidity measurements were performed at 500 nm by ultraviolet and visible light absorption spectroscopy (V-670; JASCO). The samples' temperature was controlled to be 25 °C, and the pH of the samples ranged from 1.9 to 12.4.

The reaction conversion ( $p$ ) of the Tetra-PAA-PEG gel was also estimated using ultraviolet and visible light absorption spectroscopy (V-670; JASCO). The Tetra-PAA-MA and Tetra-PEG-SH prepolymer solutions were mixed and stirred for 30 s. The resultant solution was poured into a cuvette with a PTFE cover (optical path length = 5 mm), and the absorption of UV light was measured in the range of 250-350 nm.

#### E. Swelling experiments

The swelling ratio measurements were performed on rectangular films (length: 5.0 mm, thickness: 2.0 mm, and width: 3.0 mm). The specimens were immersed in solutions with pH from 2.0 to 11.0 for 48 h to reach the equilibrium swelling state. I determined

the equilibrium swelling state when the volume change, measured using the microscope (see the later), reached a plateau value. The detailed data is shown in Section 2 of the Supporting Information. The outer solution's pH was adjusted by titrating a HCl (pH = 2.0) or a NaOH solution (pH= 12.0), respectively. I prepared the solutions for the ionic strength-dependence by adding different amounts of NaCl to adjust the ionic strength (10-1000 mM). The Tetra-PAA-PEG gel's swelling ratio was investigated by measuring the volume change of the sample using the encoded stereo microscopes (M165 C, Leica Co.). In this study, the swelling ratio ( $Q$ ) was obtained from volume measurements using

$$Q = V_s/V_0 \quad (2-1)$$

where  $V_s$  and  $V_0$  stand for the swollen and initial volumes of the Tetra-PAA-PEG gel, respectively. The volume change was estimated using the change of the side lengths by assuming isotropic deformation, as given by

$$Q = (L_s/L_0)^3 \quad (2-2)$$

where  $L_0$  is the side length of gel at as-prepared state (= 5.0 mm) and  $L_s$  is the side length of gel sample at equilibrium swelling state (= 2.30-11.3 mm).

#### F. Rheological properties of the swollen and deswollen gels

For the rheological measurement of swollen and deswollen gels, the Tetra-PAA-PEG gel fabrication method was the same as that in the swelling experiment, except that I shaped the gel into a disk. The swollen and deswollen gel samples were set at the measuring plate of a rheometer (MCR301; Anton Paar, Graz, Austria) with a parallel plate fixture having a diameter of 25 mm. The diameter and thickness of the samples at

as-prepared state were 40.0 mm and 1.5 mm, respectively. The as-prepared samples were immersed into the outer solutions with pH 2.0-11.4 and ionic strength of 10 mM for one week to reach the equilibrium swelling state. The angular frequency ( $\omega$ ) dependence of  $G'$  and  $G''$  were measured with  $\gamma=0.01$  at 25 °C. The oscillatory shear strain amplitudes were determined within the range of the linear viscoelasticity for all the tests.

### 2.3. Theoretical Description of the Equilibrium Swelling State

In this section, I use the equations describing the equilibrium swelling state of the polyelectrolyte gels. According to Flory's assumption,<sup>9</sup> we can determine the swelling ratio ( $Q$ ) by three contributions to the swelling pressure of the system: (i) contribution of the elastic free energy followed by the swelling of the network strands,  $\Pi_{el}$ ; (ii) contribution of the free energy originated from the mixing of polymer segments with solvent molecules,  $\Pi_{mix}$ ; and (iii) contribution of the osmotic free energy derived from the imbalanced concentration distribution of the counterions inside and outside the gel,  $\Pi_{ion}$ .<sup>13,50</sup> The sum of the three pressures of the polyelectrolyte gel is zero at the equilibrium swelling state:<sup>17</sup>

$$\Pi = \Pi_{el} + \Pi_{mix} + \Pi_{ion} = 0 \quad (2-3)$$

According to the definition,  $\Pi_{el}$  is a change in the elastic free energy ( $\Delta F_{el}$ ) when changing the number of solvent molecules ( $n_B$ ) with a constant number of polymers in the system ( $n_A$ ), and the expression of  $\Pi_{el}$  is

$$\Pi_{el} = -\frac{1}{V_1} \left( \frac{\partial \Delta F_{el}}{\partial n_B} \right)_{n_A} \quad (2-4)$$

where  $N_A$  is Avogadro's constant,  $V_1$  is the molar volume of the solvent. In this case,  $N_A/V_1$  is the number of solvent molecules in a unit volume. According to Flory's model,<sup>9</sup> which describe the  $\Delta F_{el}$  as<sup>51</sup>

$$\Delta F_{el} = \frac{V_0 G_0}{2} (\alpha_x^2 + \alpha_y^2 + \alpha_z^2 - 3) \quad (2-5)$$

Here,  $V_0$  is the gel's volume at the as-prepared state, and  $G_0$  is the shear modulus of the gel at the as-prepared state.  $\alpha_i$  is the elongation ratio in the  $i$  axis ( $i=x, y, z$ ) of the swollen gel. We can write the elongation ratios by assuming the swelling of the gel is

anisotropic deformation as

$$\alpha_x = \alpha_y = \alpha_z = \alpha = Q^{\frac{1}{3}} = \left(\frac{V}{V_0}\right)^{\frac{1}{3}} \quad (2-6)$$

where  $Q$  and  $V$  are the gel's swelling ratio (equation (2-1)) and volume at swollen state, respectively. Substituting equations (2-5) and (2-6) into equation (2-4), the following equation is obtained and expressed as

$$\Pi_{el} = -\frac{1}{V_1} \left( \frac{\partial \Delta F_{el}}{\partial n_B} \right)_{n_A} = -\frac{1}{V_1} \left( \frac{\partial \Delta F_{el}}{\partial \alpha} \right)_{n_A} \left( \frac{\partial \alpha}{\partial n_B} \right)_{n_A} = -\frac{1}{V_1} \frac{3V_0 G_0}{2} 2\alpha \left( \frac{\partial \alpha}{\partial n_B} \right)_{n_A} \quad (2-7)$$

Here,

$$\alpha^3 = \frac{V}{V_0} = \frac{V_0 + n_B V_1}{V_0} \quad (2-8)$$

Therefore, I can rewrite the  $\Pi_{el}$  as

$$\Pi_{el} = -G_0 Q^{-\frac{1}{3}} \quad (2-9)$$

$\phi$  is the polymer volume fraction in the gel at the equilibrium swelling state, and  $\phi_0$  is the polymer volume fraction in the gel at the as-prepared state. In equation (2-9), the term  $G_0 Q^{-\frac{1}{3}}$  equal to the shear modulus of the gel at the swollen state. Thus, measuring the gel's shear modulus at swollen state by rheological measurement is a method to validate the  $\Pi_{el}$ .

In the case of the mixing pressure, when we assume the polymerization degree of gel is infinite, we can calculate  $\Pi_{mix}$  by using the lattice approximation as<sup>9</sup>

$$\Pi_{mix} = -\frac{RT}{V_1} [\ln(1 - \phi) + \phi + \chi \phi^2] = -\frac{RT}{V_1} \left[ \ln \left\{ 1 - \left( \frac{\phi_0}{Q} \right) \right\} + \left( \frac{\phi_0}{Q} \right) + \chi \left( \frac{\phi_0}{Q} \right)^2 \right] \quad (2-10)$$

where  $V_1$  is the solvent's molar volume, and  $\chi$  is the Flory-Huggins interaction parameter between the polymer and solvent.

Due to the fixed ions on the polymer chains, a portion of the mobile counterions in the external solution can diffuse into the gel. The fixed ions can attract some of these counterions to keep the neutrality. In this case, the mobile ion concentrations inside and outside of the gel are imbalanced at the equilibrium state. Thus, the expression of  $\Pi_{\text{ion}}$  is obtained and shown as,<sup>13</sup>

$$\Pi_{\text{ion}} = RT \sum_i (C_i - C_i') \quad (2-11)$$

where  $C_i$  and  $C_i'$  are the concentrations of the mobile ions inside and outside of the gel. Here, the subscript  $i$  indicates the mobile ions' types. Donnan equilibrium determines the concentration ratio of mobile ions inside and outside of the gel as

$$\frac{C_i}{C_i'} = K^{Z_i} \quad (2-12)$$

where  $K$  is the so-called Donnan ratio, and  $Z_i$  is the valency of mobile ions.

Substituting equations (2-9), (2-10), and (2-11) into equation (2-3), the equilibrium swelling ratio ( $Q$ ) is achieved when the swelling pressure is zero:

$$-G_0 Q^{-\frac{1}{3}} - \frac{RT}{V_1} \left[ \ln \left\{ 1 - \left( \frac{\phi_0}{Q} \right) \right\} + \left( \frac{\phi_0}{Q} \right) + \chi \left( \frac{\phi_0}{Q} \right)^2 \right] + RT \sum_i C_i' (K^{Z_i} - 1) = 0 \quad (2-13)$$

In this equation,  $K$  is a function of  $Q$ , which is determined by considering the charge balance equation inside the gel, given as<sup>14</sup>

$$\sum_i Z_i K^{Z_i} C_i' + Z_a \frac{[\text{COOH}]_0}{Q \left( 1 + \frac{K C_{\text{H}}'}{K_a} \right)} = 0 \quad (2-14)$$

where  $Z_a$  is the valence of fixed ions,  $[\text{COOH}]_0$  is the total concentration of the fixed ions at the non-ionized state,  $C_{\text{H}}'$  is the concentration of protons in the external solution, and  $K_a$  is the dissociation equilibrium constant. In this equation, the first term on the left side is the concentration of mobile ions, and the second term is the

concentration of fixed ions on the polymer chain. Finally, we can determine the  $Q$  by satisfying equations (2-13) and (2-14) as a function of pH ( $C_H'$ ).

## 2.4. Results and Discussion

### A. Design of Tetra-PAA-PEG gels with controlled reaction time

Following the Tetra-PEG gel fabrication method, I fabricated the Tetra-PAA-PEG gel by employing two tetra-armed prepolymers with the mutually reactive end groups of maleimide and thiol. The buffer solution's pH can control the reaction rate between the end groups maleimide and thiol by altering the buffer solutions' pH. To optimize the gelation condition, I investigated the effect of pH on the gelation time. Table 2-1 shows the gelation time against the pH of the buffer solution. The Tetra-PAA-PEG gel's gelation time decreased from 940 s to 240 s with increasing the pH value. A high pH is preferred for the maleimide-thiol reaction because the ionized thiol concentration increases with an increase of pH.<sup>52-54</sup> In the high pH region ( $5.1 < \text{pH} < 7.0$ ), I successfully obtained the transparent gels.

On the other hand, when  $\text{pH} < 3.0$ , the solution became turbid, and the gelation did not occur. The tendency was further observed in the UV-Vis spectra, as shown in Figure 2-2. The mixture transmittance ( $T$ ) decreased when  $\text{pH} < 3.8$ , suggesting the aggregation formed via an interpolymer complex between PAA and PEG.<sup>55,56</sup> This reflected that hydrogen bonds between PAA and PEG forms under acidic conditions<sup>57,58</sup> and promoted aggregation structure. In contrast, the aggregation structure is not formed in a polymer solution solely with PAA or PEG. In this study, I chose a citrate-phosphate buffer solution with  $\text{pH}=5.9$  and an ionic strength of 100 mM for fabricating the Tetra-PAA-PEG gel.

**Table 2-1.** Gelation time of the Tetra-PAA-PEG gel under different pH conditions with an ionic strength of 100 mM. The symbol – means that gelation did not occur.

Group number	pH of buffer solution	Ionic strength of buffer solution / mM	Gelation time / s
1	4.3	100	–
2	5.1	100	940
3	5.9	100	610
4	7.0	100	240

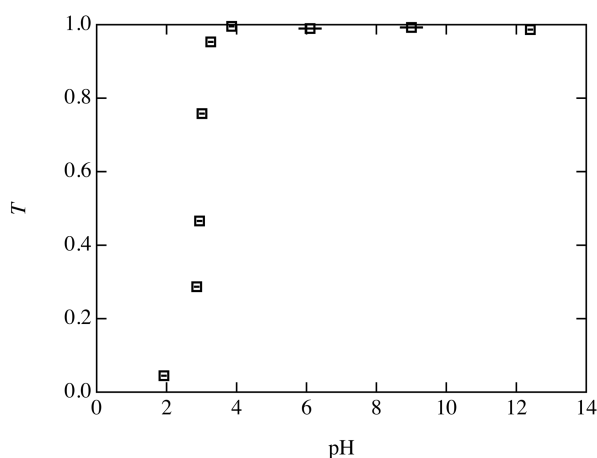


**Figure 2-2.** The transmittance of the Tetra-PAA-MA/PEG mixed solution as a function of pH values in deionized water. The molar ratio of Tetra-PAA-MA to PEG is the same as that of Tetra-PAA-MA to Tetra-PEG-SH.

#### B. Examination of network homogeneity

We performed UV spectroscopy to investigate the reaction conversion ( $p$ ) of the Tetra-PAA-PEG gel. Figure 2-3 shows the time-development of pure maleimide absorption during the gelation reaction. According to our recent studies, the unreacted maleimide group's absorption peak occurs at around 300 nm.<sup>59</sup> However, the absorption peaks originating from PAA had a severe overlap under the same wavelength. To assess the time-development of the reaction between the maleimide and thiol groups, I subtracted

the contribution of PAA from the experimentally obtained spectrum. We show the detailed procedure in Section 5 of Supporting Information. Then, the peak intensity at 310 nm was purely derived from the maleimide groups, as shown in Figure 2-3. The concentration of the maleimide in the gel can be estimated by

$$A_{310} = \varepsilon_{310}l[\text{MA}] \quad (2-15)$$

[MA] is the unreacted maleimide's concentration.  $l$  is the cell's thickness.  $\varepsilon_{310}$  is the molar absorption coefficient for maleimide. We used the concentration change of the maleimide to estimate the reaction conversion ( $p$ ) as

$$p = \frac{[\text{MA}]_0 - [\text{MA}]}{[\text{MA}]_0} \quad (2-16)$$

Inserting equation (2-15) into equation (2-16), the reaction conversion was estimated to be 0.71, suggesting that one prepolymer chain has one unreacted chain on average. This value is lower than that of the conventional Tetra-PEG gels ( $\sim 0.9$ ).<sup>45</sup> This difference can be attributed to an insufficient hetero-reaction between PEG and PAA. It's worth noting that we can accommodate the effect of incomplete reaction in the theoretical prediction. The gel fraction is estimated to be approximated 99 % by the Bethe approximation<sup>60,61</sup>, suggesting that it did not critically influence the following analysis.

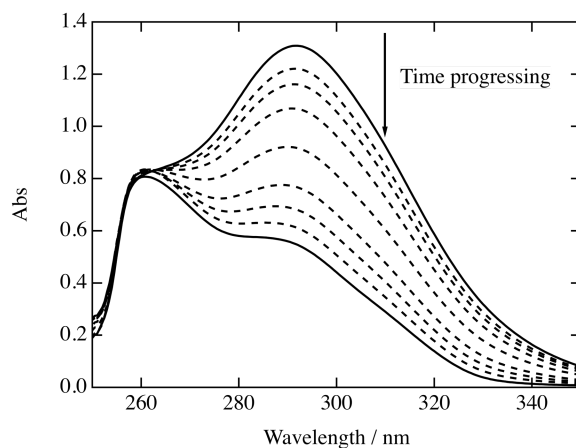


**Figure 2-3.** Time-development of pure maleimide absorption at 310 nm during the gelation reaction. The spectra range from 1 min to 16 h (as represented by solid lines).

Figure 2-4 shows the angular frequency-dependence of the storage and loss moduli of the Tetra-PAA-PEG gel after the completion of the reaction. The storage modulus was independent of the angular frequency and was more than 100 times higher than the loss modulus. This result indicated that the gel was elastic with little viscoelastic energy dissipation. The storage modulus at the rubbery plateau region,  $G_0$  was estimated to be  $4.29 \times 10^3$  Pa.

It remains unclear how to describe the relationships between the structural parameters and the Tetra-PAA-PEG gel's elasticity.  $\chi$  parameter of Tetra-PAA-PEG gel was estimated to be 0.46 (See Section 4.2 of Appendix), which was close to those of Tetra-PEG gel ( $=0.475$ )<sup>62</sup> and of PAA ( $= 0.47$  at ionization degree of 6%)<sup>63</sup>. Furthermore, the Kuhn segment size of the PEG and PAA is 0.7 nm and 0.64 nm.<sup>64,65</sup> These values are also close, suggesting that the Tetra-PAA-PEG gel in the deionized

state has a similar value of the  $\chi$  parameter and the flexibility to that of the Tetra-PEG gel. Thus, I assume to describe the Tetra-PAA-PEG gel's elasticity the same as that of the Tetra-PEG gel, which is known to possess an ideal network structure. If this assumption is confirmed, it gives evidence that the Tetra-PAA-PEG gel has a uniform network structure with uniformly distributed crosslinking points and an almost identical strand length. According to our previous studies using the Tetra-PEG gel, I can write  $G_0$  as

$$G_0 = g(\nu - \mu) \quad (2-17)$$

where  $g$  is a function depending on the prepolymer concentration ( $C$ ) and temperature.<sup>45</sup> Under the condition of the overlapping of prepolymers, it is empirically known that  $g$  is approximately equal to  $nk_B T$ .<sup>66</sup> Here  $n$ ,  $k_B$ , and  $T$  are the number density of tetra-functional prepolymers, Boltzmann constant, and absolute temperature, respectively.

In equation (2-17),  $\nu$  and  $\mu$  are the numbers per prepolymer of the elastically active network strands and the crosslinks, respectively. Adopting the Bethe approximation, I can write  $\nu$  and  $\mu$  as a reaction conversion function ( $p$ ).<sup>67,68</sup> Under the stoichiometric mixing condition, I can presume that the reaction is an AA-type reaction of the 4-armed prepolymer instead of an AB-type reaction.<sup>69</sup> Thus, the probability of one arm of a 4-armed prepolymer being unconnected to the percolated network,  $P(F)$ , is expressed as

$$P(F) = \left(\frac{1}{p} - \frac{3}{4}\right)^{\frac{1}{2}} - \frac{1}{2} \quad (2-18)$$

Using equation (2-18), I can derive the probability of 3-functional or 4-functional crosslink (i.e.,  $P(X_3)$  or  $P(X_4)$ ) from a 4-armed prepolymer as

$$P(X_3) = \binom{4}{3} \cdot P(F) \cdot [1 - P(F)]^3 \quad (2-19)$$

$$P(X_4) = [1 - P(F)]^4 \quad (2-20)$$

In this case, I can rewrite  $\nu$  and  $\mu$  as:

$$\mu = P(X_3) + P(X_4) \quad (2-21)$$

$$\nu = \frac{3}{2} \cdot P(X_3) + 2 \cdot P(X_4) \quad (2-22)$$

By inserting equations (2-21) and (2-22) into equation (2-17) with assuming  $g \cong nk_B T$ , I can calculate  $G_0$  to be  $3.84 \times 10^3$  Pa, which is close to the experimental result ( $G_0 = 4.29 \times 10^3$  Pa). Based on these results, I can consider the Tetra-PAA-PEG gel to have a regular network structure composed of uniform network strands, although each crosslink has one dangling chain on average. Regarding the distribution of charged species, the PAA and PEG units connected alternately because Tetra-PAA only reacted with Tetra-PEG and vice versa. The Tetra-PAA-PEG gel demonstrates regularly alternating neutral/highly charged sequences and is, thus, an ideal model polyelectrolyte gel for examining the effect of counterion condensation.

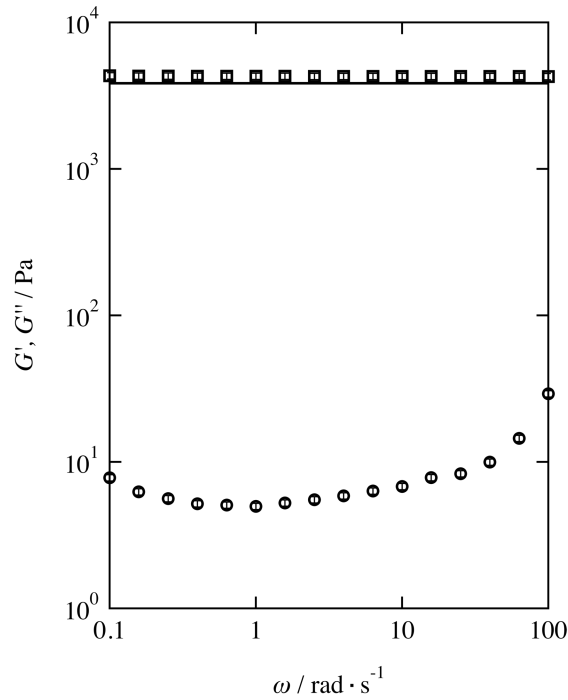


**Figure 2-4.** Angular frequency-dependence ( $\omega$ ) of the storage modulus  $G'$  (squares) and loss modulus  $G''$  (circles) of the Tetra-PAA-PEG gel in the as-prepared state. The solid line represents the predicted results ( $3.84 \times 10^3$  Pa) from equation (2-17).

### C. Relationship between the swelling and external environment

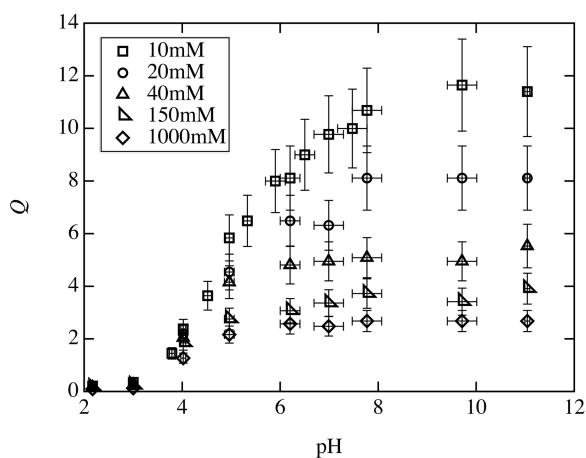
Figure 2-5(A) shows the pH-dependence of the Tetra-PAA-PEG gel's swelling ratio in salt solutions with tuned ionic strengths. The swelling ratio increased with an increasing pH, with a drastic increase around pH=5.9 that corresponded to the Tetra-PAA-MA polymer's pKa. In contrast, the swelling ratio decreased with increasing of the ionic strength. These results are consistent with the conventional polyacrylic acid gels' swelling behaviors, suggesting that the Donnan equilibrium dominates the swelling

behavior.<sup>70–75</sup> Notably, all the salt concentrations were much larger than the fixed ions, where the Donnan equilibrium works well.

Figure 2-5(B) compares the experimental results with the Flory–Rehner model's predictions with the Donnan equilibrium (F-R-D model). Here, we estimated the value of  $\chi$  to be 0.46 from the swelling ratio at high pH and high ionic strength limits, where the ion pressure  $\Pi_{\text{ion}}$  is negligible. I note that we can estimate  $\chi$  parameter at low pH and low salt concentration region, where the ion pressure is insignificant. The Tetra-PAA-PEG gel at a low pH region was not transparent, attributed to hydrogen bonds forming between PAA and PEG. This heterogeneous structure prevented the precise estimation of the  $\chi$  parameter. Thus, I had no choice but to obtain the  $\chi$  parameter at high pH and salt concentration limit, where the hydrogen bond is negligible at  $\text{pH} > 4.0$ . Except for the  $\chi$  parameter, I utilized the experimentally obtained parameters such as  $G$ ,  $\varphi$ , pH, and salt concentrations.

The swelling ratio's theoretical prediction was much higher than the experimentally observed  $Q$ . It suggests the underestimation of  $\Pi_{\text{el}}$  or overestimation of  $\Pi_{\text{mix}}$  or  $\Pi_{\text{ion}}$ . We present the detailed discussion in Sections 4 of the Appendix.

(A)



(B)

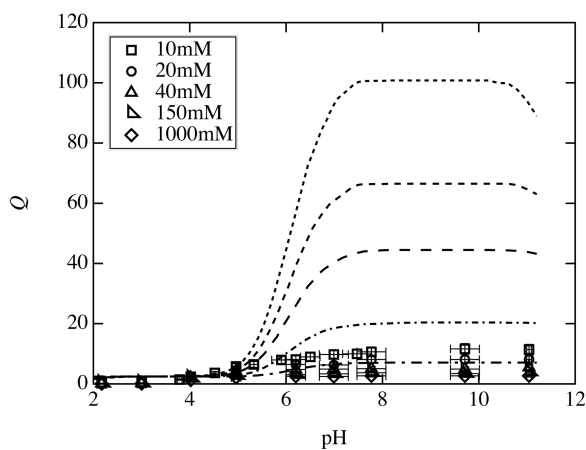


**Figure 2-5.** (A) pH-dependence of the swelling ratio of the Tetra-PAA-PEG gel in salt solutions with different ionic strengths of 10 mM (square), 20 mM (circle), 40 mM (triangle), 150 mM (isosceles right triangle), and 1000 mM (rhombus). We fabricated the Tetra-PAA-PEG gel in a citrate-phosphate buffer solution with pH=5.9 and a strength of 100 mM. (B) Comparing experimental results with the Flory–Rehner model predictions with the Donnan equilibrium (dashed lines) (F-R-D model). The predictions under 10, 20, 40, 150, and 1000 mM are represented from top to bottom.

To investigate the discrepancy between the experimental results and theoretical predictions, I first validated the elastic free energy ( $\Pi_{el}$ ). By measuring the shear modulus at swollen state ( $G_{eq}$ ) as a function of the swelling ratio ( $Q$ ), as shown in Figure 2-6,  $G_{eq}$  decreased with increasing  $Q$ . In the range of  $Q > 1$ , we found the power-law exponent  $1/3$ , which agrees with the predictions from equation (2-9). These results confirmed the validity of  $\Pi_{el}$  at highly swollen states. Notably, in the deswollen state ( $Q < 1$ ),  $G$  deviated significantly from that of equation (2-9). This unexpected deswollen state may originate from the aggregation structures formed in the gels. The strain is not homogeneously applied in such a heterogeneous system, amplifying the stress in the hard aggregation phase and the soft phase strain.<sup>76,77</sup>

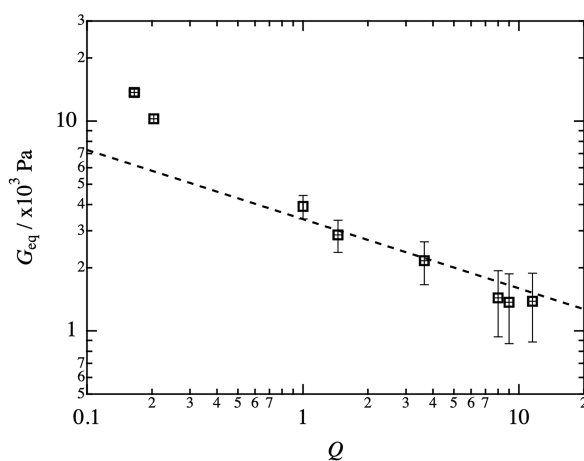


**Figure 2-6.** Double logarithm plot of  $G_{eq}$  and  $Q$  of the equilibrium swollen Tetra-PAA-PEG gels under various pH. The dashed line represents the predictions from equation (2-9).

#### D. Effect of counterion condensation on swelling

According to its definition,  $\chi$  is invariable under a constant temperature, and thus,  $\Pi_{\text{mix}}$  cannot be modified. It is straightforward that the upward deviation can originate from the overestimation of  $\Pi_{\text{ion}}$ . As described in the previous section, similar phenomena were observed and explained due to the occurrence of counterion condensation.<sup>78</sup> Counterion condensation is a phenomenon where counterions are bound to polymer chains, resulting in decreased effective charge density.<sup>35</sup> In Manning's model for a monovalent system, the counterion condensation can be described by the balance between two characteristic lengths: Bjerrum length ( $l_B$ ) and the average contour distance between the neighboring fixed charges of a polymer chain ( $b$ ).<sup>37</sup>  $l_B$  is the separation when the electrostatic energy between unit electrostatic charges becomes equal to the thermal energy, and we can write it as

$$l_B = q^2 / \epsilon k_B T \quad (2-23)$$

where  $q$  is the elementary charge,  $\epsilon$  is the dielectric constant of the solvent, and  $k_B$  is the Boltzmann's constant. When the solvent and ion species are trapped to water and sodium, respectively,  $l_B$  is determined as a constant (7.14 Å at 298 K).<sup>79</sup> Manning defined a characteristic size  $\xi$  as the ratio of  $l_B$  to  $b$  using

$$\xi = l_B / b \quad (2-24)$$

The counterion condensation occurs at  $\xi > 1$ .<sup>80</sup> In the polyacrylic acid gel, the ionization degree increased, and  $b$  decreases with pH.

In general, there are two ways to estimate  $b$ , as shown in Figure 2-7(A). The first method is by calculating the "true" distance between the neighboring fixed ion groups

on the PAA chains, where the fixed ions are localized only on the PAA chains and the PEG chains are negligible. The acrylic acid groups' ionization degree can be estimated from the titration measurement (see Section 3 of Appendix). Under this assumption, I can express  $b$  as a function of pH as

$$b = \frac{L_{\text{PAA}}}{n_{\text{PAA}}} (10^{\text{p}K_{\text{a}} - \text{pH}} + 1) \quad (2-25)$$

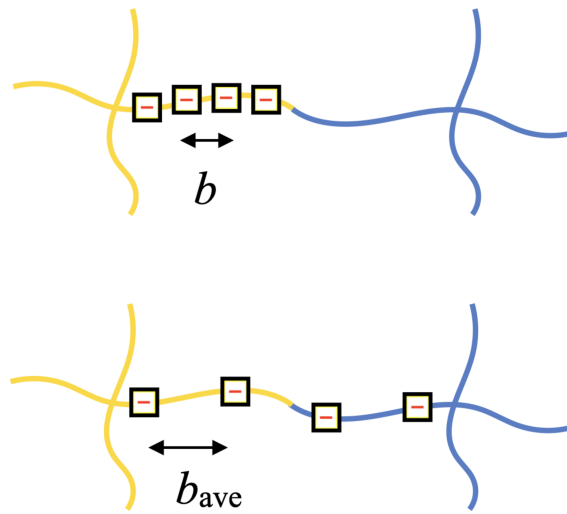
Here,  $L_{\text{PAA}}$  PAA arm's contour length in a tetra-armed polymer and  $n_{\text{PAA}}$  is the number of acrylic acid groups on the PAA arm. The other method assumes that the fixed ions are distributed homogeneously along the strand, which is often considered in conventional studies for random copolymers. I can calculate  $b_{\text{ave}}$  using

$$b_{\text{ave}} = \frac{L_{\text{PAA}} + L_{\text{PEG}}}{n_{\text{PAA}}} (10^{\text{p}K_{\text{a}} - \text{pH}} + 1) \quad (2-26)$$

where  $L_{\text{PEG}}$  is the contour length of the PEG arm in a tetra-armed polymer.

In Figure 2-7(B), lines represent the calculation results using equations (2-25) and (2-26), respectively. I found that  $\zeta$  increased drastically at pH=5.9 and reached a plateau at high pH regions for all results.  $\zeta$  exceeded the unity using equation (2-25), while  $\zeta$  remained below 1 using equation (2-26). In other words, I can predict the counterion condensation from equation (2-25) for the Tetra-PAA-PEG gel, but not from equation (2-26).

(A)



(B)

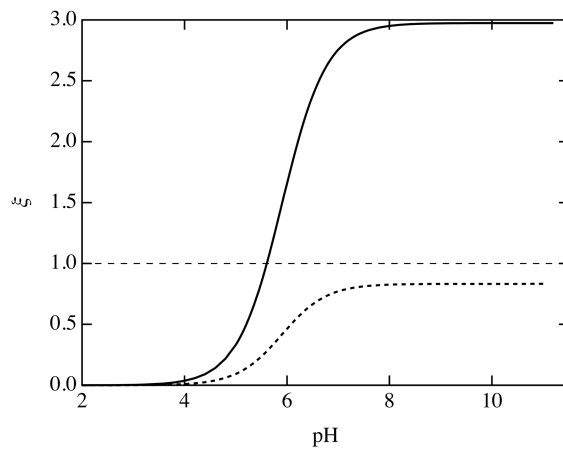


**Figure 2-7.** (A) Two calculation methods of  $b$ . The top panel shows the illustration obtained by assuming that the fixed ions are distributed only on the PAA chains. In contrast, the bottom shows that the immobile ions are distributed homogeneously on both the PAA and PEG chains. (B) Relationships between  $\xi$  and pH, where the solid and dashed lines represent the results from equations (2-25) and (2-26), respectively.

Counterion condensation traps a part of the mobile counterions around the polymer chains. I can derive ionic pressure from the heterogeneous distribution of 'mobile ions' inside and outside the gel. Here, the definition of the mobile ions is the ions, of which distribution obeys the Debye-Hückle approximation. The distribution of the trapped counterions does not follow the Debye-Hückle approximation, which cannot contribute to the ionic pressure. The condensed counterion effectively decreases the fixed ion density, resulting in a decrease in non-condensed mobile ion concentration inside gel by the Donnan equilibrium. Thus, the counterion condensation reduces the polymer chain's net charge density and cannot contribute to  $\Pi_{\text{ion}}$  (Figure 2-8). The effective concentration of the fixed acrylic acid groups reduces, as given by

$$[\text{COOH}]_{0, \text{effective}} = \frac{[\text{COOH}]_0}{2\zeta} \quad (2-27)$$

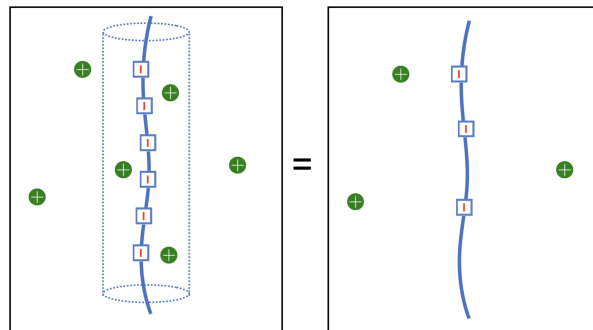


**Figure 2-8.** Schematic illustration of the counterion condensation. The left panel is the actual situation, while the right panel is a practical situation. Counterions within a certain distance from the polymer chains condensed, resulting in reduced active charge density.

The change in effective acrylic acid concentration influences the Donnan equilibrium. Figure 2-9 shows the calculated  $\Pi_{\text{ion}}$  as a function of pH under the condition of  $Q=1$ . I observed that  $\Pi_{\text{ion}}$  increased with the increase of pH and accompanied the acrylic acid's ionization. The apparent acrylic acid concentration decreased when the counterion condensation occurred, and  $\Pi_{\text{ion}}$  was reduced by approximately ten times compared to  $\Pi_{\text{ion}}$  without the counterion condensation. Here, the cases of with/without the counterion condensation correspond to the top and bottom illustrations in Figure 2-7(A), respectively.

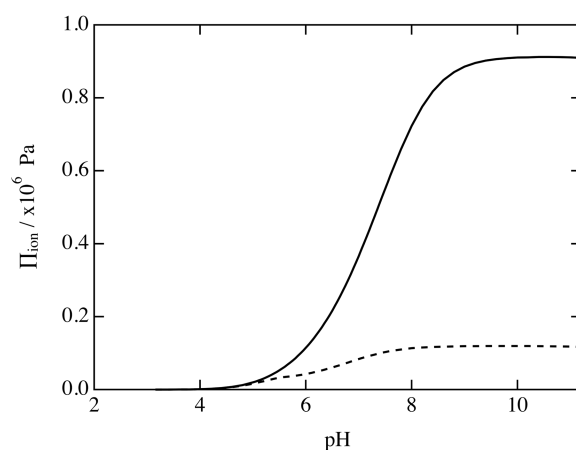


**Figure 2-9.** Ion pressure as a function of pH. Solid and dashed lines represent the calculation without and with counterion condensation, respectively. The ionic strength is ten mM.

In Figure 2-10, I plotted the theoretical predictions with the counterion condensation. The Flory–Rehner model with the Donnan equilibrium’s prediction can well reproduce the swelling behaviors of Tetra-PAA-PEG gels. Notably, the downward deviation at low pH regions originates from PAA and PEG aggregation structure

formation. For the predicted results, the significant slope changes at pH=5.6 arose from the counterion condensation occurrence. On the other hand, when we used  $b_{ave}$ ,  $\zeta$  was below unity even in the high pH region with no counterion condensation, resulting in the same results as those in Figure 2-5(B). These results indicated that the ionic interaction within the network strand's length-scale could determine the counterion condensation occurrence. It is vital to find the correct estimate of  $b$  on this scale for predicting the swelling behaviors of polyelectrolyte gels.

In conventional studies using the random copolymerization of neutral and ionic monomers, they assumed homogeneous distribution of fixed ions. However, ionic monomers do not distribute homogeneously in the polymer chain in real "random" copolymers.<sup>41</sup> The smaller swelling ratio, compared to the Flory–Rehner model's prediction with the Donnan equilibrium observed in the previous studies may originate from the occurrence of counterion condensation at local sequences with dense ionic monomers.

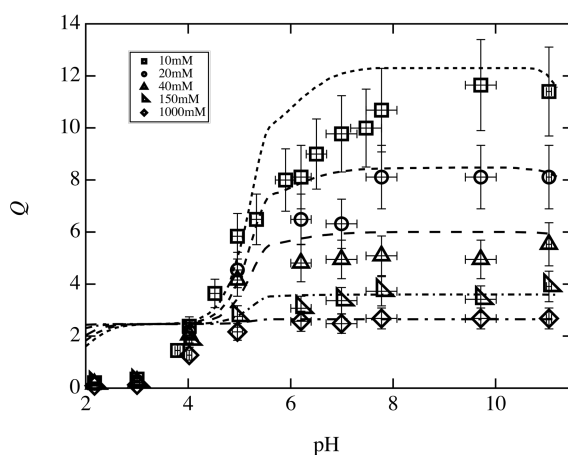


**Figure 2-10.** pH-dependence of the swelling ratio of the Tetra-PAA-PEG gel in

salt solutions with different ionic strengths. Dashed lines are fitting results predicted by the Flory–Rehner model modified using Manning’s model.

## 2.5. Conclusions

I successfully designed and fabricated a Tetra-PAA-PEG gel with alternating neutral/highly charged sequences using the AB-type crosslinking reaction. I measured the UV-vis spectra and mechanical properties to deduce the network structures of the Tetra-PAA-PEG gel. Then, I investigated the swelling behaviors for various pH values and ionic strengths. The significant findings are as follows. (i) The UV-vis measurements indicate that the reaction conversion ( $p$ ) of the end groups was  $\sim 70\%$ ; (ii) The elastic modulus was well reproduced by the same model as the Tetra-PEG gel is known to possess an ideal network structure. This finding indicates that the Tetra-PAA-PEG gel also has a similarly uniform network structure; (iii) The swelling ratio increased with an increasing pH and a decreasing ionic strength when the pH was around 5.9 corresponded to the pKa of the prepolymer chain. This finding indicates that the Donnan equilibrium strongly governs the swelling properties; (iv) I cannot use the Flory–Rehner model with the Donnan equilibrium to estimate the swelling ratio, especially for regions with high pH and low ionic strengths. In contrast, the results obtained based on minimal modification by counterion condensation is consistent with the experimental results. These findings indicate that the ionic interaction within the network strand's length-scale can determine the counterion condensation. It is vital to accurately estimate the distance between the neighboring fixed ions for predicting the swelling behaviors of polyelectrolyte gels.

## Appendix

### 1. Synthesis of Tetra-PAA-MA

#### 1.1. Synthesis of Tetra-PtBuA-MA

Tetra-PtBuA-N3 (10.4 g) and 2,2-bypyridine (720 mg) were dissolved in dichloromethane (110 mL) in a flask filled with nitrogen and shielded from light. *N*-propargyl maleimide (250 mg) was added and the solution was stirred for 20 min in an ice bath. A ball of copper wire ( $\phi$ 0.3 mm x 20 m, YAHATA NEJI CORPORATION) was added and stirring was continued for 1 h in the ice bath and subsequently at room temperature for 7 h. It should be noted that the surface of the copper wire was sanded with sand paper (#600, RIKEN CORUNDUM CO., LTD.) immediately before use. After the copper wire was removed, the solution was evaporated. The residue was dissolved in a small amount of acetone, and to the solution was added water. The precipitate was dissolved in diethyl ether and washed with water. The organic layer was dried over sodium sulfate and evaporated, yielding Tetra-PtBuA-MA (9 g) as a pale gray powder.

#### 1.2. Synthesis of Tetra-PAA-MA

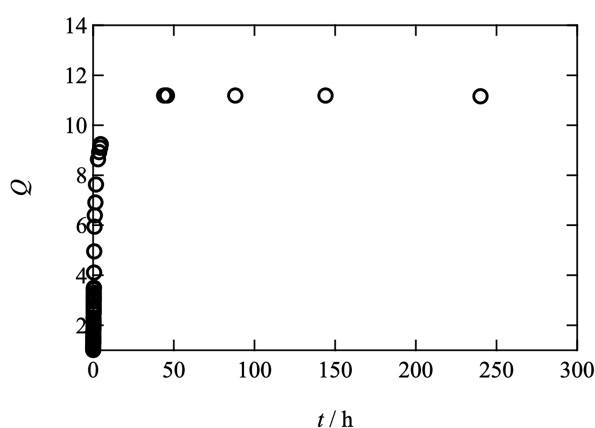
Tetra-PtBuA-MA (1 g) was dissolved in dichloromethane (18 mL) in a flask filled with nitrogen and shielded from light. Trifluoroacetic acid (6 mL) was added. The solution was stirred overnight at room temperature. After the fluid was removed by a pipette, the precipitate was dried in vacuo. The dry solid was washed with dichloromethane, dried in vacuo, and crushed in a mortar. The foregoing procedure was repeated for the

remaining Tetra-PtBuA-MA. The powder was combined, washed with acetone four times, and dried in vacuo, yielding Tetra-PAA-MA (4.3 g) as a white powder.

The chemical structure of the yielding Tetra-PAA-MA was evaluated by  $^1\text{H NMR}$ .  $^1\text{H NMR}$  ( $\text{CD}_3\text{OD}$ ):  $\delta$  7.90-8.15 (m, 4H), 6.86 (bs, 8H), 5.40-5.48 (m, 8H), 4.78-4.81 (m, 8H), 4.12 (bs, 8H), 2.22-2.85 (m, 4nH), 1.48-1.95 (m, (8n+8)H), 1.20 (bs, 24H).

## 2. Time-development of the swelling ratio during swelling test

Supporting figure 1 shows the time-development of the swelling ratio ( $Q$ ) for the Tetra-PAA-PEG gel at pH12. The ionic strength of the external solution was 10 mM.  $Q$  was determined as  $(L_s/L_0)^3$ .  $L_0$  and  $L_s$  are the side length of gel at as-prepared state (= 5.0 mm) and that of the gel sample at equilibrium swelling state, respectively. The equilibrium state of the Tetra-PAA-PEG gel was determined by the volume change of the swollen gel less than 1% for after 48h.

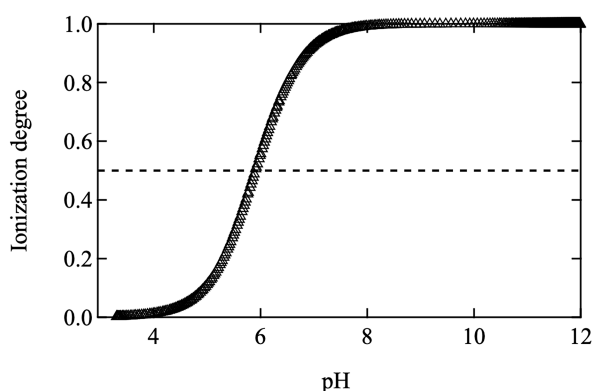


**Supporting figure 1.** Time-development of the swelling ratio ( $Q$ ) for the Tetra-PAA-PEG gel at pH12.

## 3. Potentiometric titration

The polymer solution was prepared by dissolving a weighed amount of Tetra-PAA-MA in deionized water. The ionic strength of the polymer solution was set at 10 mM by adding NaCl salt. The Polymer solution was neutralized by adding a standard 0.02 mol L<sup>-1</sup> NaOH solution. Before the titration measurement, the polymer solution was carefully degassed with nitrogen to prevent the dissolution of CO<sub>2</sub>. Titration measurement was performed using an automatic titrator (COM-1700A; HIRANUMA, Japan) at room temperature with a combination glass electrode.

The obtained results are shown in Supporting figure 2. pKa of Tetra-PAA-MA was determined to be pH5.9, where the ionization degree is 0.5.



**Supporting figure 2.** Experimental potentiometric titration exhibiting the ionization degree of Tetra-PAA-MA as a function of the pH. The ionic strength is equal to 10 mM.

#### 4. Derivation of the total free energy

To obtain the prediction of  $Q$  as a function of pH, I derive three free energies,  $\Pi_{el}$ ,  $\Pi_{mix}$ , and  $\Pi_{ion}$  as follows:

##### 4.1. Elastic free energy $\Pi_{el}$

As shown in eq. (2-9),  $\Pi_{el}$  is expressed by  $G_0$  and  $Q$ .  $G_0$  was the experimental data, obtained by measuring the shear modulus with rheometer.

#### 4.2. Mixing free energy $\Pi_{mix}$

According to equation (2-10),  $\Pi_{mix}$  is a function of  $Q$  and  $\chi$ , because  $\phi_0$  was estimated to be 0.052 from the feed condition.  $\chi$  parameter was estimated from the experimental results for the swelling ratio of the gel at pH9.7 and extremely high ionic strength. In extremely high ionic strength condition, the effect of the fixed ion groups is screened out. Notably, I chose pH9.7, because at low pH region below pH4.0, the Tetra-PAA-PEG gel was not transparent due to the effect of the hydrogen bond between the PAA and PEG chains. There was one report that the hydrogen bond between PAA and PEG is not formed at high pH region.<sup>81</sup> To eliminate the non-ideal condition, I increased pH when I estimated  $\chi$  parameter.

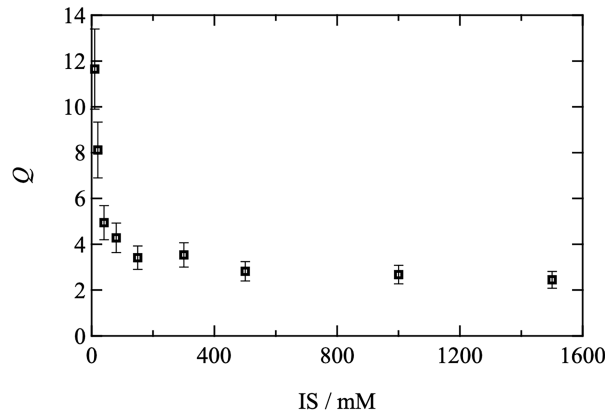
Supporting figure 3 exhibited the dependence of  $Q$  of the Tetra-PAA-PEG gel on the ionic strength at pH9.7.  $Q$  reached a plateau at 1000 mM, which indicates that the effect of the fixed ion groups is screened out and that the ionic pressure is negligible in this condition. Equation (2-3) was expressed by equations (2-9) and (2-10) without considering the ionic pressure, and the balance between elastic pressure and mixing pressure was given as

$$-G_0 Q^{-\frac{1}{3}} - \frac{RT}{V_1} \left[ \ln \left\{ 1 - \left( \frac{\phi_0}{Q} \right) \right\} + \left( \frac{\phi_0}{Q} \right) + \chi \left( \frac{\phi_0}{Q} \right)^2 \right] = 0 \quad (\text{A-2-1})$$

Equation (A-2-1) is rewritten as

$$\chi = -\frac{\frac{G_0 V_1}{RT} Q^{-\frac{1}{3}} + \ln\left\{1 - \left(\frac{\phi_0}{Q}\right)\right\} + \left(\frac{\phi_0}{Q}\right)}{\left(\frac{\phi_0}{Q}\right)^2} \quad (\text{A-2-2})$$

Using equation (A-2-2) and the experimental data of  $Q$  at IS =1500mM,  $\chi$  parameter was calculated to be 0.46. When I calculate  $Q$  for various pH and ionic strength, I utilized this value.



**Supporting figure 3.** Ionic strength-dependence of swelling ratio of Tetra-PAA-PEG gel at pH9.7.

#### 4.3. Ionic free energy $\Pi_{\text{ion}}$

According to equation (2-11),  $\Pi_{\text{ion}}$  was determined by the concentration distribution of mobile ions inside and outside of the gel. The total concentration of the mobile ions inside the gel ( $C_m$ ) was estimated based on equation (2-12) and is given as

$$C_m = \sum_i Z_i K^{Z_i} C_i' \quad (\text{A-2-3})$$

Inside the gel, the mobile ions were  $\text{Na}^+$ ,  $\text{H}^+$ ,  $\text{OH}^-$  and  $\text{Cl}^-$ .

$$C_m = K([\text{Na}^+] + [\text{H}^+]) - \frac{[\text{Cl}^-]}{K} \quad (\text{pH} > 7.0) \quad (\text{A-2-4})$$

$$C_m = K[Na^+] - \frac{[Cl^-] + [OH^-]}{K} \quad (\text{pH} < 7.0) \quad (\text{A-2-5})$$

The concentration of the fixed ions inside the gel ( $C_f$ ) is defined by the dissociation equilibrium constant ( $K_a$ ). In this study, the fixed group is the carboxyl group (-COOH).

The concentration of the ionized carboxyl groups is written as

$$[COO^-] = \frac{[COOH]_0}{10^{\text{p}K_a - \text{pH}} + 1} \quad (\text{A-2-6})$$

where  $[COOH]_0$  is the total concentration of the fixed ions. Here,  $\text{p}K_a$  is influenced by the molecular weight and salt concentration.<sup>82,83</sup> Thus, I experimentally measured  $\text{p}K_a$  of the Tetra-PAA-MA polymer based on titration measurements, and the details are given in Section 2 of Appendix. The concentration of fixed ions inside the gel  $C_f$  was given as

$$C_f = Z_a \frac{[COOH]_0}{Q \left( 1 + \frac{K C_H'}{K_a} \right)} \quad (\text{A-2-7})$$

the equation (2-14) was the sum of equations (A-2-3) and (A-2-7).

In the Donnan equilibrium, the distribution of the mobile ion is determined by equation (A-2-3) and the electroneutrality inside the gel, which can be expressed by inserting equations (A-2-3) and (A-2-7) to equation (2-14) as

$$K([Na^+] + [H^+]) - \frac{[COOH]_0}{Q \left( 1 + \frac{K[H^+]}{K_a} \right)} - \frac{[Cl^-]}{K} = 0 \quad (\text{pH} < 7.0) \quad (\text{A-2-8})$$

$$K[Na^+] - \frac{[COOH]_0}{Q \left( 1 + \frac{K[H^+]}{K_a} \right)} - \frac{[Cl^-] + [OH^-]}{K} = 0 \quad (\text{pH} > 7.0) \quad (\text{A-2-9})$$

From equations (A-2-8) and (A-2-9),  $K$  is described as a function of  $Q$  depending on pH:

$$K = \frac{-B + \sqrt{B^2 - 3Ag(Q)} \left( \cos \frac{f(Q)}{3} + \sqrt{3} \sin \frac{f(Q)}{3} \right)}{3A} \quad (\text{A-2-10})$$

where

$$f(Q) = \arccos \frac{2(B^2 - 3Ag(Q))B - 3A(Bg(Q) - 9AC)}{2\sqrt{(B^2 - 3Ag(Q))^3}} \quad (\text{A-2-11})$$

$$g(Q) = -\left(\frac{[\text{COOH}]_0 K_a}{Q} + [\text{H}^+][\text{Cl}^-]\right) \quad (\text{pH} < 7.0) \quad (\text{A-2-12})$$

$$g(Q) = -\left(\frac{[\text{COOH}]_0 K_a}{Q} + [\text{H}^+]( [\text{Cl}^-] + [\text{OH}^-] )\right) \quad (\text{pH} > 7.0) \quad (\text{A-2-13})$$

In equation (A-2-10), the constants,  $A$ ,  $B$ , and  $C$  are expressed below pH7.0:

$$A = ([\text{Na}^+] + [\text{H}^+])[\text{H}^+] \quad (\text{A-2-14})$$

$$B = ([\text{Na}^+] + [\text{H}^+])K_a \quad (\text{A-2-15})$$

$$C = -[\text{Cl}^-]K_a \quad (\text{A-2-16})$$

Above pH7.0, they are expressed as

$$A = [\text{Na}^+][\text{H}^+] \quad (\text{A-2-17})$$

$$B = [\text{Na}^+]K_a \quad (\text{A-2-18})$$

$$C = -([\text{Cl}^-] + [\text{OH}^-])K_a \quad (\text{A-2-19})$$

On the other hand,  $\Pi_{\text{ion}}$  can be expressed by inserting equation (A-2-3) into equation (2-11) as

$$\Pi_{\text{ion}} = RT \left[ (K - 1)([\text{Na}^+] + [\text{H}^+]) + \left(\frac{1}{K} - 1\right)[\text{Cl}^-] \right] \quad (\text{pH} < 7.0) \quad (\text{A-2-20})$$

$$\Pi_{\text{ion}} = RT \left[ (K - 1)[\text{Na}^+] + \left(\frac{1}{K} - 1\right)([\text{Cl}^-] + [\text{OH}^-]) \right] \quad (\text{pH} > 7.0) \quad (\text{A-2-21})$$

$Q$  is determined to make the swelling pressure to be zero. Thus, the ionic contribution (equation (2-11)) is balanced with the sum of the elastic and osmotic contributions (equations (2-9) and (2-10)).

$$G_0 \left(\frac{1}{Q}\right)^{1/3} + \frac{RT}{V_1} \left[ \ln \left\{ 1 - \left(\frac{\phi_0}{Q}\right) \right\} + \left(\frac{\phi_0}{Q}\right) + \chi \left(\frac{\phi_0}{Q}\right)^2 \right] =$$

$$RT \left[ (K - 1)([\text{Na}^+] + [\text{H}^+]) + \left(\frac{1}{K} - 1\right) [\text{Cl}^-] \right] \quad (\text{pH} < 7.0)$$

(A-2-22)

$$G_0 \left(\frac{1}{Q}\right)^{1/3} + \frac{RT}{V_1} \left[ \ln \left\{ 1 - \left(\frac{\phi_0}{Q}\right) \right\} + \left(\frac{\phi_0}{Q}\right) + \chi \left(\frac{\phi_0}{Q}\right)^2 \right] =$$

$$RT \left[ (K - 1)[\text{Na}^+] + \left(\frac{1}{K} - 1\right) ([\text{Cl}^-] + [\text{OH}^-]) \right] \quad (\text{pH} > 7.0)$$

(A-2-23)

From equations (A-2-22) and (A-2-23),  $K$  is described as a function of  $Q$  depending on pH:

$$K = \frac{-h(Q) + \sqrt{(h(Q))^2 - 4ab}}{2a} \quad (\text{A-2-24})$$

where

$$h(Q) = -\frac{G_0 Q^{-1/3}}{RT} - \frac{1}{V_1} \left[ \ln \left\{ 1 - \left(\frac{\phi_0}{Q}\right) \right\} + \left(\frac{\phi_0}{Q}\right) + \chi \left(\frac{\phi_0}{Q}\right)^2 \right] - ([\text{Na}^+] + [\text{Cl}^-] + [\text{H}^+])$$

(pH < 7.0)

(A-2-25)

$$h(Q) = -\frac{G_0 Q^{-1/3}}{RT} - \frac{1}{V_1} \left[ \ln \left\{ 1 - \left(\frac{\phi_0}{Q}\right) \right\} + \left(\frac{\phi_0}{Q}\right) + \chi \left(\frac{\phi_0}{Q}\right)^2 \right] - ([\text{Na}^+] + [\text{Cl}^-] + [\text{OH}^-])$$

(pH > 7.0)

(A-2-26)

In equation (A-2-24), the constants,  $a$  and  $b$  are expressed below pH 7.0;

$$a = [\text{Na}^+] + [\text{H}^+] \quad (\text{A-2-27})$$

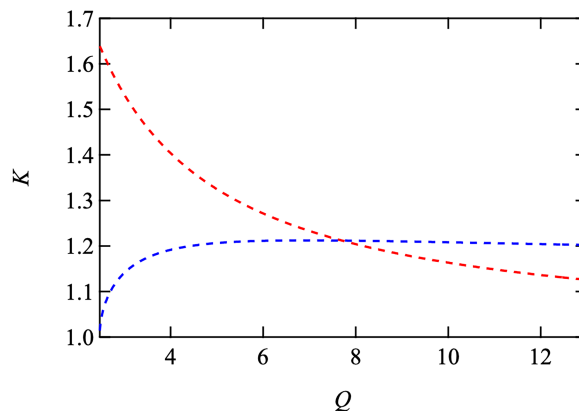
$$b = [\text{Cl}^-] \quad (\text{A-2-28})$$

Above pH 7.0, they are expressed as

$$a = [\text{Na}^+] \quad (\text{A-2-29})$$

$$b = [\text{Cl}^-] + [\text{OH}^-] \quad (\text{A-2-30})$$

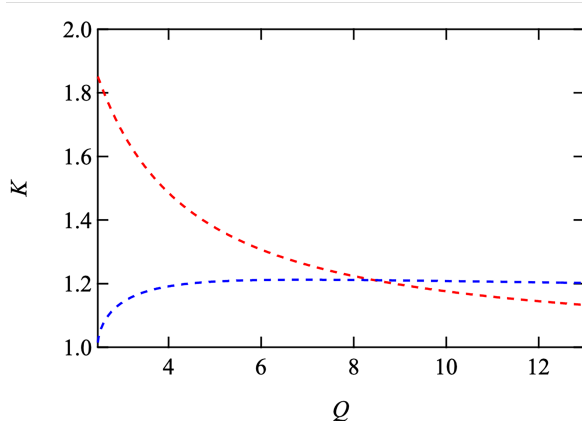
Finally,  $Q$  is determined to satisfy the equations (A-2-10) and (A-2-24). For example, in the case of pH6.0 and salt concentration of NaCl was 20 mM,  $[\text{COOH}]_0 = 0.39 \text{ mol L}^{-1}$ ,  $\zeta = 1.66$ . In the external solution,  $[\text{Na}^+] = [\text{Cl}^-] = 0.02 \text{ mol L}^{-1}$ ,  $[\text{H}^+] = 10^{-6} \text{ mol L}^{-1}$ . By inserting all the values of each parameter into equation (A-2-8), the relationship between  $Q$  and  $K$  was obtained with equation (A-2-10) and shown in supporting figure 4. Considering the counterion condensation,  $[\text{COOH}]_0$  was replaced by  $[\text{COOH}]_{0, \text{effective}}$  of equation (2-27) and the relationship between  $Q$  and  $K$  was obtained with equation (A-2-24) and was shown in supporting figure 4. The crossover point was the solutions of  $Q$  and  $K$ ,  $Q = 7.70$  and  $K = 1.212$ .



**Supporting figure 4.** Relationships between  $K$  and  $Q$ . The red dashed curve exhibited the relationship between  $K$  and  $Q$  obtained from equation (A-2-10); The blue dashed curve exhibited the relationship between  $K$  and  $Q$  obtained from equation (A-2-24). The crossover point was the solution of  $K$  and  $Q$ .

In the case of pH8.0 and salt concentration of NaCl was 20 mM,  $[\text{COOH}]_0 = 0.39 \text{ mol L}^{-1}$ ,  $\zeta = 2.95$ . In the external solution,  $[\text{Na}^+] = [\text{Cl}^-] = 0.02 \text{ mol L}^{-1}$ ,  $[\text{H}^+] =$

$10^{-8}$  mol L<sup>-1</sup>. By inserting all the values of each parameter into equation (A-2-9), the relationship between  $Q$  and  $K$  was obtained with equation (A-2-10) and shown in supporting figure 5. Considering the counterion condensation,  $[\text{COOH}]_0$  was replaced by  $[\text{COOH}]_{0,\text{effective}}$  of equation (A-2-27) and the relationship between  $Q$  and  $K$  was obtained with equation (A-2-24) and was shown in supporting figure 5. The crossover point was the solutions of  $Q$  and  $K$ ,  $Q = 8.44$  and  $K = 1.211$ .



**Supporting figure 5.** Relationships between  $K$  and  $Q$ . The red dashed curve exhibited the relationship between  $K$  and  $Q$  obtained from equation (A-2-10); The blue dashed curve exhibited the relationship between  $K$  and  $Q$  obtained from equation (A-2-24). The crossover point was the solution of  $K$  and  $Q$ .

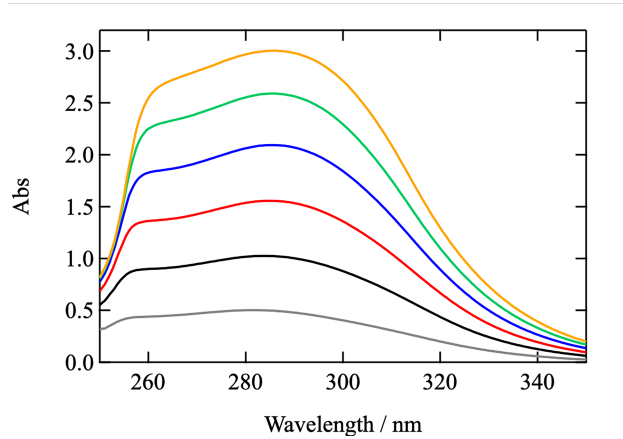
## 5. Detailed analysis of the maleimide peak in UV-vis spectra

Constant amounts of Tetra-PAA-MA and linear PAA (10, 20, 30, 40, 50, 60 g L<sup>-1</sup>) were dissolved in citrate-phosphate buffer solution (pH5.9, 100 mM). The molecular masses of the Tetra-PAA-MA and linear PAA were  $1.9 \times 10^4$  g mol<sup>-1</sup> and  $5.0 \times 10^3$  g mol<sup>-1</sup> (which correspond with the molecular mass of one PAA arm in Tetra-PAA-MA

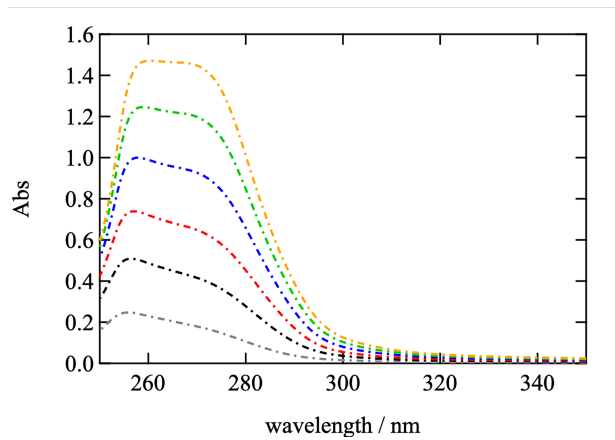
polymer), respectively. Polymer solutions were poured into a cuvette with PTFE cover (optical path length, 5 mm), and the absorption was measured in the range of 250-350 nm. The absorption spectra of the polymer solutions were obtained by ultraviolet and visible light absorption spectroscopy (V-670; JASCO).

Supporting Figures 6 (A) and (B) show the UV-vis absorption spectra for the Tetra-PAA-MA and linear PAA solutions at different concentrations, respectively. Compared with the results of linear PAA, Tetra-PAA-MA showed an additional peak around 300nm, which may be attributed to the maleimide peak. To estimate the contribution from the maleimide groups, I tried to subtract the effect of the acrylic acid from the spectra of the Tetra-PAA-MA, shown in Supporting figure 6 (C). After the subtraction, the peak around the 300 nm became pronounced, which is consistent with our previous study.<sup>84</sup> When I estimate the reaction conversion during the gelation process, I utilize the peak intensity at 310 nm. It is because the UV absorption peak of maleimide at 300 nm overlapped with that of the thioether bond at 250 nm.<sup>45</sup> Before the estimation of the reaction conversion, I confirmed the linearity between the peak intensity at 310 nm and the concentration, shown in Supporting figure 6 (D). Figure 6 (E) shows the time-development of the UV spectra during the gelation process. The peak intensity around 300 nm decreased, accompanied by the progress of the Michael reaction. The unreacted maleimide group shows the absorption peaks around these regions.

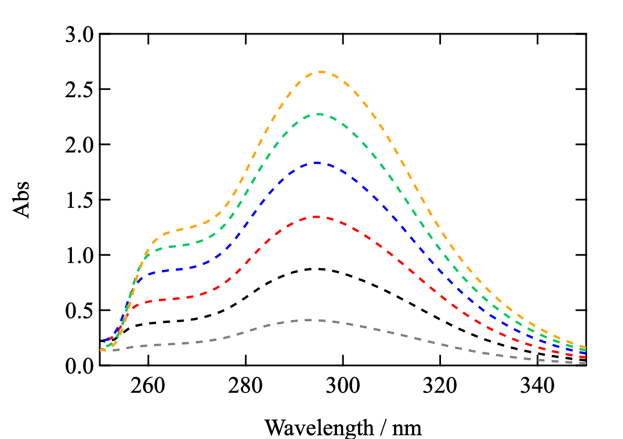
(A)



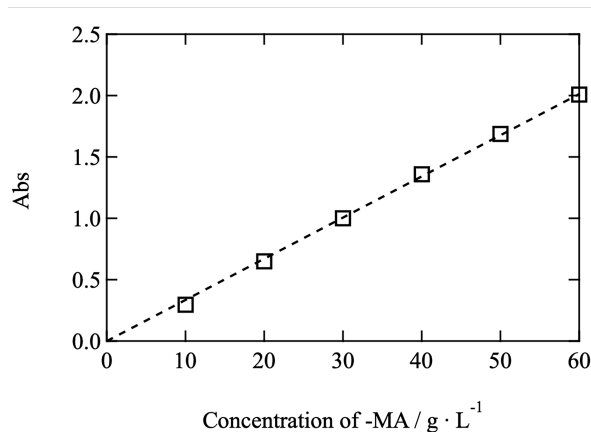
(B)



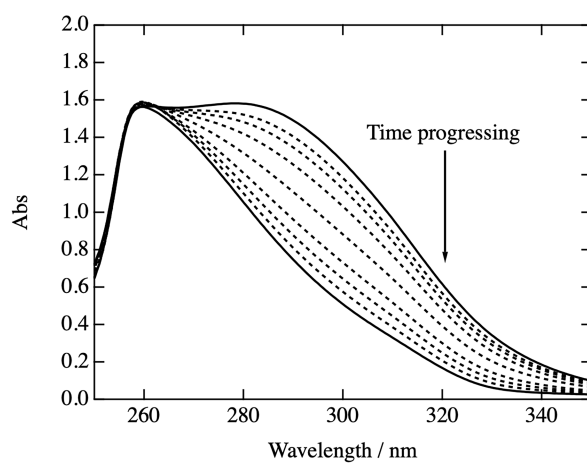
(C)



(D)



(E)



**Supporting figure 6.** Concentration-dependence of the UV-vis absorption spectra of (A) Tetra-PAA-MA, (B) PAA, respectively. Concentration: 10 g L<sup>-1</sup>(gray), 20 g L<sup>-1</sup>(black), 30 g L<sup>-1</sup>(red), 40 g L<sup>-1</sup>(blue), 50 g L<sup>-1</sup>(green), 60 g L<sup>-1</sup>(orange). (C) UV-vis spectra after removing the contribution of the linear PAA from the Tetra-PAA-MA. (D) Relationship between the peak intensity at 310 nm and the PAA concentration. (E) Time-dependence of UV-vis absorption spectra presenting the gelation reaction process of the Tetra-PAA-PEG gel in a citrate-phosphate buffer solution with pH5.9 and ionic strength of the buffer solution equal to 100 mM at 25°C. Spectra ranges from 1 min to 16 h (both are represented as solid lines)

## References

- (1) Schneider, S.; Linse, P. *J. Phys. Chem. B* **2003**, *107* (32), 8030–8040.
- (2) Schneider, S.; Linse, P. *Macromolecules* **2004**, *37* (10), 3850–3856.
- (3) Jeon, C. H.; Makhaeva, E. E.; Khokhlov, A. R. *Macromol. Chem. Phys.* **1998**, *199* (12), 2665–2670.
- (4) Cheng, W. M.; Hu, X. M.; Zhao, Y. Y.; Wu, M. Y.; Hu, Z. X.; Yu, X. T. *E-Polymers* **2017**, *17* (1), 95–106.
- (5) Lenaerts, V. M.; Gurny, R. *Bioadhesive Drug Delivery Systems*; CRC press, 1989.
- (6) Drury, J. L.; Mooney, D. J. *Biomaterials* **2003**, *24* (24), 4337–4351.
- (7) Slaughter, B. V.; Khurshid, S. S.; Fisher, O. Z.; Khademhosseini, A.; Peppas, N. A. *Adv. Mater.* **2009**, *21* (32-33), 3307–3329.
- (8) Toh, W. S.; Loh, X. J. *Mater. Sci. Eng. C* **2015**, *45*, 690–697.
- (9) Flory, P. J. *Principles of Polymer Chemistry*; Cornell University Press, 1953.
- (10) Flory, P. J.; Rehner, J. *J. Chem. Phys.* **1943**, *11* (11), 521–526.
- (11) Huggins, M. L. *Ann. N. Y. Acad. Sci.* **1942**, *43* (1), 1–32.
- (12) Flory, P. J. *J. Chem. Phys.* **1942**, *10* (1), 51–61.
- (13) Donnan, F. G.; Guggenheim, E. A. *Zeitschrift für Phys. Chemie* **1932**, *162* (1), 346–360.
- (14) Rička, J.; Tanaka, T. *Macromolecules* **1984**, *17* (12), 2916–2921.
- (15) Lopez, C. G.; Lohmeier, T.; Wong, J. E.; Richtering, W. *J. Colloid Interface Sci.* **2020**, *558*, 200–210.
- (16) Hirotsu, S.; Hirokawa, Y.; Tanaka, T. *J. Chem. Phys.* **1987**, *87* (2), 1392–1395.

- (17) Shibayama, M.; Tanaka, T. *Adv. Polym. Sci.* **1993**, *109*.
- (18) Shibayama, M.; Ikkai, F.; Inamoto, S.; Nomura, S.; Han, C. C. *J. Chem. Phys.* **1996**, *105* (10), 4358–4366.
- (19) Ikkai, F.; Suzuki, T.; Karino, T.; Shibayama, M. *Macromolecules* **2007**, *40* (4), 1140–1146.
- (20) Baker, J. P.; Blanch, H. W.; Prausnitz, J. M. *Polymer (Guildf)*. **1995**, *36* (5), 1061–1069.
- (21) Aalaie, J.; Vasheghani-Farahani, E. *Iran. Polym. J. (English Ed)*. **2012**, *21* (3), 175–183.
- (22) Okay, O.; Sariisik, S. B. *Eur. Polym. J.* **2000**, *36* (2), 393–399.
- (23) Çaykara, T.; Akçakaya, I. *Eur. Polym. J.* **2006**, *42* (6), 1437–1445.
- (24) Okay, O.; Sariışik, S. B.; Zor, S. D. *J. Appl. Polym. Sci.* **1998**, *70* (3), 567–575.
- (25) Drozdov, A. D. *Int. J. Solids Struct.* **2015**, *64*, 176–190.
- (26) Nakano, Y.; Seida, Y.; Uchida, M.; Yamamoto, S. *JOURNAL of CHEMICAL ENGINEERING of JAPAN*. 1990, pp 574–579.
- (27) Höpfner, J.; Richter, T.; Košovan, P.; Holm, C.; Wilhelm, M. *Intell. Hydrogels* **2013**.
- (28) Katchalsky, A.; Michaeli, I. *J. Polym. Sci.* **1955**, *15* (79), 69–86.
- (29) Reed, C. E.; Reed, W. F. *J. Chem. Phys.* **1992**, *96* (2), 1609–1620.
- (30) Borkovec, M.; Jönsson, B.; Koper, G. J. M. *Surface and colloid science*; Springer, 2001; pp 99–339.
- (31) Aleksandrov, A.; Polydorides, S.; Archontis, G.; Simonson, T. *J. Phys. Chem. B*

- 2010**, *114* (32), 10634–10648.
- (32) Garcés, J. L.; Madurga, S.; Borkovec, M. *Phys. Chem. Chem. Phys.* **2014**, *16* (10), 4626–4638.
- (33) Borkovec, M.; Daicic, J.; Koper, G. J. M. *Proc. Natl. Acad. Sci.* **1997**, *94* (8), 3499–3503.
- (34) Garcés, J. L.; Madurga, S.; Rey-Castro, C.; Mas, F. J. *Polym. Sci. Part B Polym. Phys.* **2017**, *55* (3), 275–284.
- (35) Oosawa, F. *J. Polym. Sci.* **1957**, *23* (103), 421–430.
- (36) Kotin, L.; Nagasawa, M. *J. Chem. Phys.* **1962**, *36* (4), 873–879.
- (37) Manning, G. S. *J. Chem. Phys.* **1969**, *51* (3), 924–933.
- (38) Liu, X.; Tong, Z.; Hu, O. *Macromolecules* **1995**, *28* (11), 3813–3817.
- (39) Okay, O.; Durmaz, S. *Polymer (Guildf)*. **2002**, *43* (4), 1215–1221.
- (40) Melekaslan, D.; Okay, O. *Polymer (Guildf)*. **2000**, *41* (15), 5737–5747.
- (41) Zeldovich, K. B.; Khokhlov, A. R. *Macromolecules* **1999**, *32* (10), 3488–3494.
- (42) Dušek, K.; Prins, W. *Fortschritte Der Hochpolym.* **1969**, *6*, 1–102.
- (43) Sakai, T.; Matsunaga, T.; Yamamoto, Y.; Ito, C.; Yoshida, R.; Suzuki, S.; Sasaki, N.; Shibayama, M.; Chung, U. Il. *Macromolecules* **2008**, *41* (14), 5379–5384.
- (44) Kamata, H.; Li, X.; Chung, U. Il; Sakai, T. *Adv. Healthc. Mater.* **2015**, *4* (16), 2360–2374.
- (45) Yoshikawa, Y.; Sakumichi, N.; Chung, U. Il; Sakai, T. *Soft Matter* **2019**, *15* (25), 5017–5025.
- (46) Lange, F.; Schwenke, K.; Kurakazu, M.; Akagi, Y.; Chung, U. Il; Lang, M.;

- Sommer, J. U.; Sakai, T.; Saalwächter, K. *Macromolecules* **2011**, *44* (24), 9666–9674.
- (47) Fujiyabu, T.; Yoshikawa, Y.; Chung, U. il; Sakai, T. *Sci. Technol. Adv. Mater.* **2019**, *20* (1), 608–621.
- (48) Oshima, K.; Fujimoto, T.; Minami, E.; Mitsukami, Y. *Macromolecules* **2014**, *47* (21), 7573–7580.
- (49) Morishima, K.; Li, X.; Oshima, K.; Mitsukami, Y.; Shibayama, M. *J. Chem. Phys.* **2018**, *149* (16), 163301.
- (50) Procter, H. R.; Wilson, J. A. *J. Chem. Soc. Trans.* **1916**, *109*, 307–319.
- (51) Onuki, A. *Adv. Polym. Sci.* **1993**, *109*, 63–121.
- (52) Northrop, B. H.; Frayne, S. H.; Choudhary, U. *Polym. Chem.* **2015**, *6* (18), 3415–3430.
- (53) Bednar, R. A. *Biochemistry* **1990**, *29* (15), 3684–3690.
- (54) Yoshitake, M.; Kamiyama, Y.; Nishi, K.; Yoshimoto, N.; Morita, M.; Sakai, T.; Fujii, K. *Phys. Chem. Chem. Phys.* **2017**, *19* (44), 29984–29990.
- (55) Kato, N.; Takeda, M.; Sakai, Y.; Uyehara, T. I. *ICAS 2001*; The Japan Society for Analytical Chemistry, 2002.
- (56) Cohen, Y.; Prevysh, V. *Acta Polym.* **1998**, *49* (10–11), 539–543.
- (57) Khutoryanskiy, V. V.; Dubolazov, A. V.; Nurkeeva, Z. S.; Mun, G. A. *Langmuir* **2004**, *20* (9), 3785–3790.
- (58) Szabó, Á.; Szanka, I.; Tolnai, G.; Szarka, G.; Iván, B. *Polymer (Guildf)*. **2017**, *III*, 61–66.

- (59) Morel, F.; Decker, C.; Jönsson, S.; Clark, S. C.; Hoyle, C. E. *Polymer (Guildf)*. **1999**, *40* (9), 2447–2454.
- (60) Katashima, T.; Urayama, K.; Chung, U. Il; Sakai, T. *J. Chem. Phys.* **2015**, *142* (17), 1–12.
- (61) Li, X.; Tsutsui, Y.; Matsunaga, T.; Shibayama, M.; Chung, U. Il; Sakai, T. *Macromolecules* **2011**, *44* (9), 3567–3571.
- (62) Matsunaga, T.; Sakai, T.; Akagi, Y.; Chung, U. Il; Shibayama, M. *Macromolecules* **2009**, *42* (4), 1344–1351.
- (63) Safronov, A. P.; Adamova, L. V.; Blokhina, A. S.; Kamalov, I. A.; Shabadrov, P. *A. Polym. Sci. - Ser. A* **2015**, *57* (1), 33–42.
- (64) Li, H.; Liu, B.; Zhang, X.; Gao, C.; Shen, J.; Zou, G. *Langmuir* **1999**, *15* (6), 2120–2124.
- (65) Choi, C. H. J.; Zuckerman, J. E.; Webster, P.; Davis, M. E. *Proc. Natl. Acad. Sci. U. S. A.* **2011**, *108* (16), 6656–6661.
- (66) Akagi, Y.; Gong, J. P.; Chung, U. Il; Sakai, T. *Macromolecules* **2013**, *46* (3), 1035–1040.
- (67) Macosko, C. W.; Miller, D. R. *Macromolecules* **1976**, *9* (2), 199–206.
- (68) Miller, D. R.; Macosko, C. W. *Macromolecules* **1976**, *9* (2), 206–211.
- (69) Akagi, Y.; Matsunaga, T.; Shibayama, M.; Chung, U. Il; Sakai, T. *Macromolecules* **2010**, *43* (1), 488–493.
- (70) Horkay, F.; Basser, P. J.; Hecht, A. M.; Geissler, E. *Macromol. Biosci.* **2002**, *2* (5), 207–213.

- (71) Horkay, F.; Tasaki, I.; Basser, P. J. *Biomacromolecules* **2000**, *1* (1), 84–90.
- (72) Kozlovskaya, V.; Sukhishvili, S. A. *Macromolecules* **2006**, *39* (18), 6191–6199.
- (73) Horkay, F.; Tasaki, I.; Basser, P. J. *Biomacromolecules* **2001**, *2* (1), 195–199.
- (74) Saeed Al-Anbakey, A. M. *J. Atoms Mol.* **2014**, *4* (February 2014), 1–6.
- (75) Ilavský, M.; Mikeš, J.; Dušek, K. *Polym. Bull.* **1980**, *3* (8–9), 481–487.
- (76) Mori, T.; Tanaka, K. *Acta Metall.* **1973**, *21* (5), 571–574.
- (77) Eshelby, J. D.; Trans, P.; Lond, R. S. *Philos. Trans. R. Soc. London. Ser. A, Math. Phys. Sci.* **1951**, *244* (877), 87–112.
- (78) Kern, W. *Phys. Chem.* **1938**, *181A(1)*, 249–282.
- (79) Fowler, R. H.; Guggenheim, E. A. *Statistical Thermodynamics*; Cambridge University Press, 1939.
- (80) Manning, G. S.; Ray, J. J. *Biomol. Struct. Dyn.* **1998**, *16* (2), 461–476.
- (81) Yu, X.; Tanaka, A.; Tanaka, K.; Tanaka, T. *J. Chem. Phys.* **1992**, *97* (10), 7805–7808.
- (82) Nagasawa, M.; Murase, T.; Kondo, K. *J. Phys. Chem.* **1965**, *69* (11), 4005–4012.
- (83) Laguecir, A.; Ulrich, S.; Labille, J.; Fatin-Rouge, N.; Stoll, S.; Buffle, J. *Eur. Polym. J.* **2006**, *42* (5), 1135–1144.
- (84) Nishi, K.; Fujii, K.; Chung, U. Il; Shibayama, M.; Sakai, T. *Phys. Rev. Lett.* **2017**, *119* (26), 1–6.

## **Chapter 3. Effect of nonlinear elasticity on the swelling behaviors of Tetra-PAA-PEG gels in monovalent salt solutions**

### **3.1. Introduction**

In Chapter 2, I investigated the swelling behaviors of Tetra-PAA-PEG gel under tuned external solutions and validated the model that combining Tanaka's model with Manning's counterion condensation theory (F-R-D-M model) for describing the swelling behaviors of Tetra-PAA-PEG gel. The elastic free energy in this model is described as the Neo-Hookean function.<sup>1,2</sup> Neo-Hookean model has been considered as a model for ideal polymer networks with infinite extensibility and without structural defects, where the regular network composed of the Gaussian chains with uniform length is assumed.<sup>2-5</sup> In chapter 2, even though the experimental results can be roughly reproduced by the predictions from the F-R-D-D model, there are still some deviation existing in high  $Q$  region, where the effect of finite extensibility of the polymer chain on the elasticity of the polymer network became significant. In this condition, Neo-Hookean model no long can be applicable for describing the elastic free energy of the polymer chain. Skouri et al.<sup>6</sup> investigated the swelling and elastic properties of polyacrylic acid gels, they found the shear modulus can be described by Flory's model that derived from Gaussian statistics of the chains within not too high swelling ratios but failed in high swelling ratios range. There is an upturn in shear modulus under large deformation due to the non-Gaussian elasticity of the polymer network with highly stretched conformation. The similar phenomenon has also been reported for

polyelectrolyte gels of hydrolyzed polyacrylamide.<sup>7</sup> To account for non-Gaussian chain effect for the description of the mechanical behavior of the polyelectrolyte gel, some studies adopt the Gent model and found this model could capture the non-Gaussian chain effect well.<sup>8,9</sup> Therefore, the predictions from the modification of F-R-D-M model by considering the non-Gaussian chain effect is supposed to approach the experimental results.

However, in chapter 2, I only utilized the Tetra-PAA-PEG gel with one network strand length and the deformation of the gel does not reach to the limitation. Thus, I need to design Tetra-PAA-PEG gels with different network strand lengths and investigate the effect of non-linear elasticity on the swelling behaviors.

Here, I can follow the similar strategy of designing Tetra-PEG gel. The mechanical and swelling properties of Tetra-PEG gel can be controlled by tuning the molecular weight and molar ratio to achieve. Due to the similar network structure, end groups and same description of elasticity method between Tetra-PEG gel and Tetra-PAA-PEG gel at non-ionized state.<sup>10</sup> The mechanical and swelling properties of Tetra-PAA-PEG gels are supposed to be controlled by tuning the molecular weight and concentration of Tetra-PAA-MA and Tetra-PEG-SH.<sup>11-14</sup> Thus, the swelling ratios of Tetra-PAA-PEG gels with different PEG segment length are expected to be in a wide range, and the applicability of F-R-D-M model at large swelling ratio can be revealed.

In chapter 3, I tune the molecular weight of Tetra-PEG-SH to investigate the effect of the neutral segment lengths on the mechanical and swelling properties of the Tetra-PAA-PEG gel. The concentration of Tetra-PAA-MA is also set to a specific value, and

the molar ratio of Tetra-PAA-MA to Tetra-PEG-SH is controlled to 1:1 by adjusting the concentration of Tetra-PEG-SH to obtain the same crosslink density. Comparing the experimental swelling behaviors of the Tetra-PAA-PEG gels with predictions by F-R-D-M model, the effect of the nonlinear elasticity on the description of elastic free energy is revealed.

### 3.2. Materials and Methods

#### A. Fabrication of Tetra-PAA-PEG Gels

Tetrathiol-terminated poly(ethylene glycol) (Tetra-PEG-SH) was purchased from NOF Corporation (Tokyo, Japan). Tetramaleimide-terminated poly(acrylic acid) (Tetra-PAA-MA) was prepared from the Tetraazide-terminated poly(*tert*-butyl acrylate) (Tetra-PtBuA-N<sub>3</sub>). The details of the preparation of Tetra-PAA and Tetra-PEG precursors were reported previously.<sup>13,15-17</sup> Constant amounts of Tetra-PAA-MA and Tetra-PEG-SH were dissolved in citrate-phosphate buffer solution, of which the pH and ionic strength were 5.9 and 100mM, respectively. The Tetra-PAA-PEG gels fabricated using Tetra-Tetra-PEG-SH with  $M_w$  of 1.0, 2.0 and  $4.0 \times 10^4$  g mol<sup>-1</sup> are called 10K Tetra-PAA-PEG gel, 20K Tetra-PAA-PEG gel and 40K Tetra-PAA-PEG gel, respectively. The  $M_w$  of Tetra-PAA-MA of all the Tetra-PAA-PEG gels were  $1.9 \times 10^4$  g mol<sup>-1</sup>. To obtain the consistent initial fixed ion concentration, the same prepolymer molar concentrations and tune the strand lengths of PEG, the concentration of Tetra-PAA-MA was fixed 60.0 g L<sup>-1</sup> for all types of Tetra-PAA-PEG gel. In contrast, the concentrations of Tetra-PEG-SH were set to be 32.3, 64.6, and 129.3 g L<sup>-1</sup> for 10K, 20K, and 40K Tetra-PAA-PEG gel, respectively. Equal amounts of the prepolymer solutions were mixed for 30 s and poured into the silicone mold at room temperature. In this study, at least 48 h was given for each reaction to complete.

#### B. Rheological Measurements after Gelation

The gel samples were prepared as disk films and set at the measuring plate of a rheometer (MCR301; Anton Paar, Graz, Austria) with a parallel plate fixture having a

diameter of 25 mm. The diameter and thickness of the samples at the as-prepared state were 40.0 mm and 1.0 mm, respectively. The angular frequency ( $\omega$ ) dependences of the storage modulus ( $G'$ ) and loss modulus ( $G''$ ) were measured with a strain amplitude ( $\gamma$ ) of 1.0% at 25 °C. The oscillatory shear strain amplitudes were found within the range of the linear viscoelasticity for all the tests.

### C. Swelling Experiments

The gel samples for swelling ratio measurements were prepared as rectangular films (length: 5.0 mm, thickness: 2.0 mm, width: 3.0 mm). The pH of external solutions was set from 2.0 to 11.0, then, the specimens were immersed in the solutions for 48 h to reach the equilibrium swelling state at 25 °C. The pH of external solutions was deviated from the setting value due to the existence of the carboxyl groups on the Tetra-PAA-MA polymer; thus, I titrated an HCl (pH = 2.0) or NaOH (pH = 12.0) solution into the external solutions to adjust the pH to the setting values. In the ionic strength dependence measurement, the ionic strengths of external solutions were tuned from 10 to 1000 mM by adding different amounts of NaCl. The effect of Na<sup>+</sup> and Cl<sup>-</sup> (introduced by pH adjustment) on the ionic strength of external solutions can be neglected compared with the ionic strength tuning by NaCl.

The swelling ratio of the Tetra-PAA-PEG gel was investigated by measuring the volume change of the sample by using the encoded stereo microscopes (M165 C, Leica Co.). In this study, the swelling ratio ( $Q$ ) was defined by using the initial volume of gel sample  $V_0$  and the swollen volumes of gel sample  $V_s$ :  $Q = V_s/V_0$ . Generally, the swelling of the gels is an isotropic deformation. The volume change was estimated by

using the change of the initial side length of gel sample at as-prepared state  $L_0$  and the side length of gel sample at equilibrium swelling state  $L_s$ , thus the swelling ratio  $Q$  was expressed as:  $Q = (L_s/L_0)^3$ .  $L_0$  was 5.0 mm, while  $L_s$  were in the range of 2.2-17.3 mm depending on the external solutions conditions.

### 3.3. Results and Discussion

#### A. Effect of neutral segments lengths on the swelling behaviors

Figure 3-1 shows the pH dependence of the swelling ratios of 10K, 20K, and 40K Tetra-PAA-PEG gel in NaCl solution with ionic strength of 2 and 10 mM. The swelling ratios of all the Tetra-PAA-PEG gels increased with increasing pH. They reached a plateau when  $\text{pH} > 7.0$ , which corresponds to the pH dependence of the ionization of acrylic acid on the polymer chains. On the other hand, the swelling ratios decreased with increasing the ionic strengths. The pH-dependence and ionic strength-dependence of the swelling ratios indicate the presence of the ionic pressure by the Donnan equilibrium, by which the distribution of mobile ions inside and outside the gels is determined. It is worth noting that the salt concentrations are larger than the fixed ions' concentration, where Donnan equilibrium works well.

The swelling ratios of 10K Tetra-PAA-PEG gel were twice larger than the swelling ratios of 20K Tetra-PAA-PEG gel and 40K Tetra-PAA-PEG gel under the same external conditions. These swelling behaviors were in contrast to the normal Tetra-PEG gel system, where the swelling ratios of 20K Tetra-PEG gel were larger than those of 10K Tetra-PEG gel under the same  $\phi_0$ .<sup>12</sup> This contradiction will be explained by the balance between  $\Pi_{el}$  and  $\Pi_{mix}$  of Tetra-PAA-PEG gel in section B.

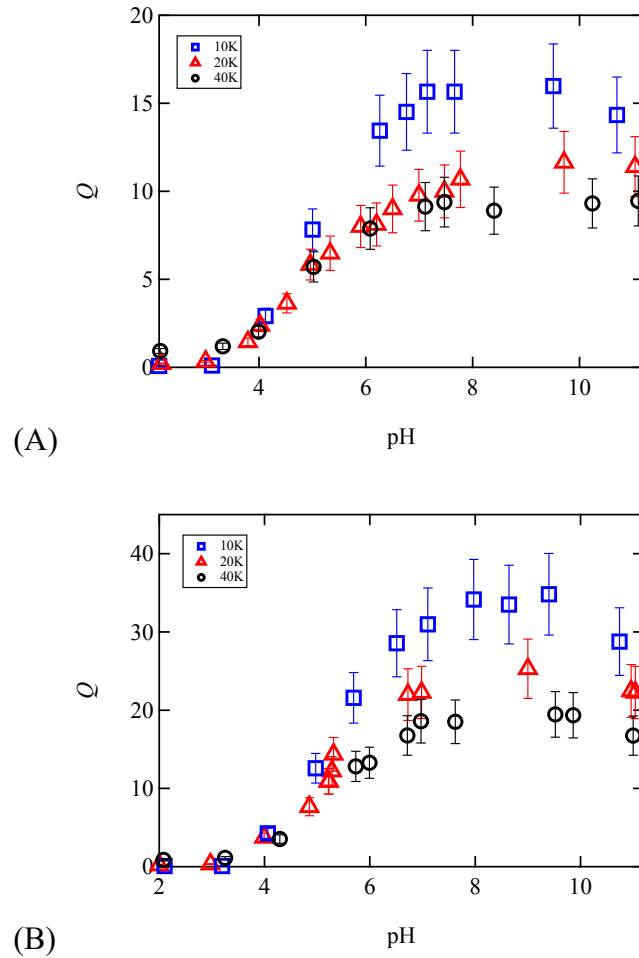


**Figure 3-1.** The pH-dependence of the swelling ratio of 10K (blue), 20K (red), and 40K (black) Tetra-PAA-PEG gel in salt solutions with different ionic strengths. (A) 10 mM, (B) 2 mM.

### B. Effect of neutral segments lengths on the mechanical properties

As I mentioned in the theoretical part, the balance among  $\Pi_{el}$ ,  $\Pi_{mix}$  and  $\Pi_{ion}$  determines the swelling ratio of the polyelectrolyte gels. Here, I utilized the same concentrations of the PAA units among the 10K, 20K, and 40K Tetra-PAA-PEG gels. Under the same  $Q$ ,  $\Pi_{ion}$  are consistent for all the Tetra-PAA-PEG gels. Thus, the sum of  $\Pi_{el}$  and  $\Pi_{mix}$  determines the order of the swelling ratios.  $\Pi_{el}$  is determined by the

shear modulus at as-prepared state and the swelling ratio. Figure 3-2 shows the molecular weight-dependence of the shear moduli of the Tetra-PAA-PEG gel.  $G_0$  increased with  $M_w$ , which exhibits opposite tendency against the rubbery elasticity theory.<sup>2,18-20</sup> In general, the shear modulus is determined by the number density of the crosslinks, which is inversely proportional to the network strand length. This opposite tendency is attributed to the difference distance from the overlapping concentration at the as-prepared state. According to our previous studies,<sup>21,22</sup> the shear modulus deviates from the classical rubbery elasticity theory, depending on the concentration normalized by the overlapping concentration of the prepolymers. In our system, the molar concentration of the crosslinks was set to be identical, while the strand length of the PEG part was different. As a result, the total concentration increased with increasing the network strand length. (See sections 1 and 2 of Appendix)

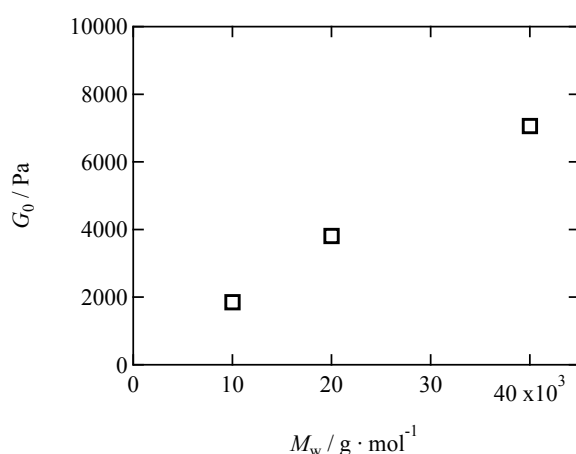


**Figure 3-2.** The molecular weight ( $M_w$ )-dependence of the shear modulus ( $G_0$ ) of Tetra-PAA-PEG gels.

On the other hand,  $\Pi_{\text{mix}}$  is determined by  $\chi$  parameter, the initial polymer concentration, and the swelling ratio. The  $\chi$  parameter was experimentally estimated from  $Q$  at pH > 8.0 and 1500 mM NaCl conditions, where the effects of the hydrogen bond between the PAA and PEG chains,<sup>23-25</sup> and the electrostatic potential from the fixed ions are negligible. The swelling ratios were almost constant under high ionic strength conditions shown in Figure 3-3. Under this condition, the swelling pressure is composed only of the elastic and mixing pressures, which is given as

$$\Pi = \Pi_{\text{el}} + \Pi_{\text{mix}} = 0 \quad (3-1)$$

$\Pi_{\text{el}}$  is derived from the elastic free energy, when assuming the elastic free energy has Neo-Hookean type potential,<sup>2,26</sup>  $\Pi_{\text{el}}$  is expressed as

$$\Pi_{\text{el}} = -G_0 Q^{-\frac{1}{3}} \quad (3-2)$$

$\Pi_{\text{mix}}$  can be obtained using the lattice approximation based on the Flory-Huggins theory as<sup>2,27,28</sup>

$$\Pi_{\text{mix}} = -\frac{RT}{V_1} \left[ \ln \left\{ 1 - \left( \frac{\phi_0}{Q} \right) \right\} + \left( \frac{\phi_0}{Q} \right) + \chi \left( \frac{\phi_0}{Q} \right)^2 \right] \quad (3-3)$$

where  $V_1$  is the molar volume of the solvent, and  $\chi$  is the Flory-Huggins interaction parameter. Substituting equations (3-2) and (3-3) into equation (3-1), the  $\chi$  parameter was obtained and expressed as

$$\chi = -\frac{\frac{G_0 V_1}{RT} Q^{-\frac{1}{3}} + \ln \left\{ 1 - \left( \frac{\phi_0}{Q} \right) \right\} + \left( \frac{\phi_0}{Q} \right)}{\left( \frac{\phi_0}{Q} \right)^2} \quad (3-4)$$

The  $\chi$  parameters were calculated to be 0.46, 0.46, 0.45 for 10K, 20K, and 40K Tetra-PAA-PEG gels, respectively. It is worth noting that adding NaCl has no strong effect on the  $\chi$  parameter.<sup>29</sup>

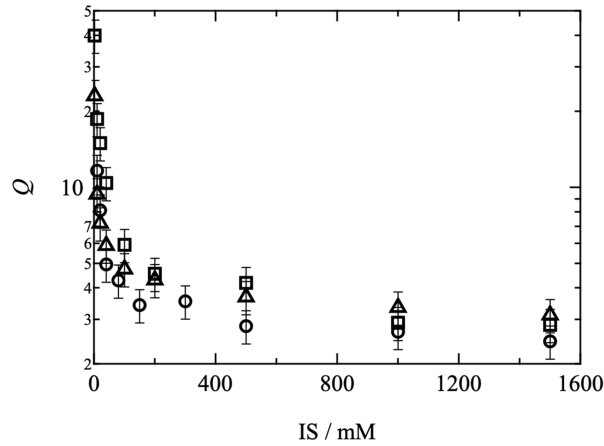


**Figure 3-3.** Ionic strength-dependence of swelling ratios of Tetra-PAA-PEG gels in NaCl solutions. 10K Tetra-PAA-PEG gel (squares), 20K Tetra-PAA-PEG gel (circles), 40K Tetra-PAA-PEG gel (triangles). The pH of outer solutions for 10K, 20K, and 40K Tetra-PAA-PEG gels were 8.6, 9.7 and 8.0, respectively.

Using the values of the shear moduli and the estimated  $\chi$  parameter, I can simulate  $\Pi_{el}$  and  $\Pi_{mix}$  as a function of  $Q$ , shown in Figure 3-4. When  $Q$  is larger than approximate 3.0, the elastic pressure overcomes the mixing pressure. Under the high swelling region, the elastic pressure dominates the order of the swelling behaviors, which is the main reason of the abnormal order of  $Q$  among the Tetra-PAA-PEG gels.

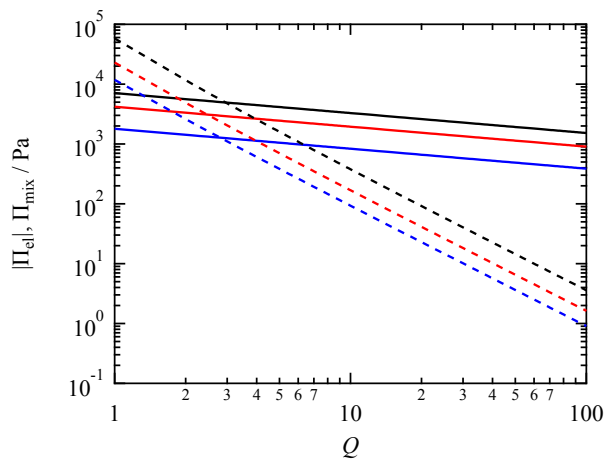


**Figure 3-4.** The absolute value of elastic pressure  $|\Pi_{el}|$  (solid lines) and mixing pressure  $\Pi_{mix}$  (dashed lines) of 10K (blue), 20K (red), and 40K (black) Tetra-PAA-PEG gel as a function of swelling ratio  $Q$ .

Figure 3-5 (A) compares the experimental results of 10K, 20K, and 40K Tetra-PAA-PEG gels with the predictions by the Flory-Rehner model considering both the Donnan equilibrium and Manning's counterion condensation effect (the F-R-D-M model) under ionic strength 10 mM. The F-R-D-M model predictions can well reproduce all the swelling behaviors of 10K, 20K, and 40K Tetra-PAA-PEG gels, which indicates the validity of the F-R-D-M model. Thus, even though the lengths of PEG segments of 10K, 20K, and 40K Tetra-PAA-PEG gels were different, the estimation of  $\zeta$  only depend on the distance between the neighboring fixed ionic groups of the Tetra-PAA-MA polymer.

Figure 3-5 (B) shows the comparison of experimental results of 10K, 20K, and 40K Tetra-PAA-PEG gels with the F-R-D-M model predictions under ionic strength of 2 mM. The swelling behaviors of 20K and 40K Tetra-PAA-PEG gels still correspond well with the F-R-D-M model predictions, while the experimental results of 10K Tetra-PAA-PEG gel are downwardly deviated from the theoretical line. I will discuss the deviation in Section C.

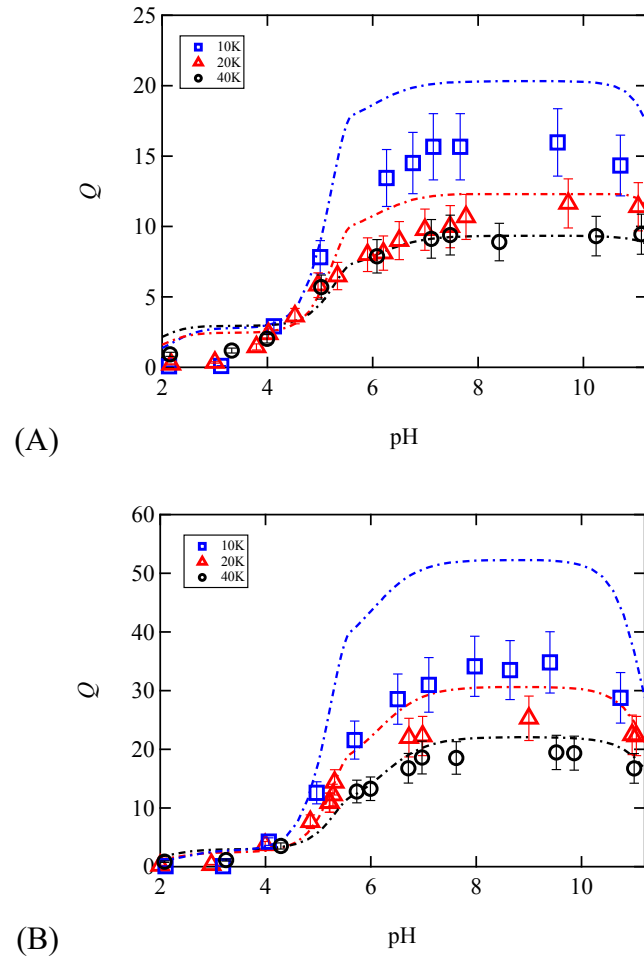


**Figure 3-5.** Comparison of the experimental results with the predictions by the Flory-Rehner model with considering both the Donnan equilibrium and Manning's counterion condensation effects (dashed lines). The ionic strength of salt solutions: (A) 10 mM, (B) 2 mM. The predictions result of 10K (blue), 20K (red), and 40K (black) Tetra-PAA-PEG gels are represented from top to bottom.

### C. Effect of finite extensibility of polymer chains on the swelling behaviors

The downward deviation of experimental  $Q$  of 10K Tetra-PAA-PEG gel under ionic strength of 2mM from prediction line can be attributed to the failure to describe the elastic pressure. The Neo-Hookean model described the elastic free energy utilized here,

which considers the elastic free energy of the ideal polymer networks with infinite extensibility.<sup>2-4</sup> Notably, the  $Q$  of 10K Tetra-PAA-PEG gel in a salt solution with the ionic strength of 2mM were much larger than the  $Q$  of Tetra-PAA-PEG gel in other external conditions; the maximum was even up to 35. Under such a large deformation, the distribution function of segments cannot follow the Gaussian description, and the Neo-Hookean model is no longer applicable for describing the elastic free energy of Tetra-PAA-PEG gel.

To consider the effect of the finite extensibility of the network strands, I adopt the Gent model, which describes the effect of finite extensibility by the minimum addition to the Neo-Hookean model.<sup>30</sup> According to the Gent model, the elastic free energy  $\Delta F_{el}$  is expressed as

$$\Delta F_{el} = -\frac{V_0 G_0}{2} (I_m - 3) \ln \left( 1 - \frac{I_1 - 3}{I_m - 3} \right) \quad (3-5)$$

where  $V_0$  is the volume at the as-prepared state.  $I_1$  is the first invariant of Green's deformation tensor,  $I_m$  is the maximum value of  $I_1$  where the stress becomes infinite, and  $I_1$  is expressed as<sup>31</sup>

$$I_1 = \alpha_x^2 + \alpha_y^2 + \alpha_z^2 \quad (3-6)$$

where  $\alpha_i$  is the elongation ratio in the  $i$  axis ( $i=x, y, z$ ) of the gel at the swollen state.

The elongation ratios are obtained by assuming isotropic deformation, which are given as

$$\alpha_x = \alpha_y = \alpha_z = \alpha = Q^{\frac{1}{3}} = \left( \frac{V}{V_0} \right)^{\frac{1}{3}} \quad (3-7)$$

where  $V$  is the volume of gel at swollen state.  $I_m$  is the maximum value of  $I_1$  under the ultimate elongation ratio  $\alpha_{max}$  is expressed as

$$I_m = \alpha_{\max}^2 + 2\alpha_{\max}^{-1} \quad (3-8)$$

According to the classical concept of elastomers,  $\alpha_{\max}$  was given as<sup>32</sup>

$$\alpha_{\max} = \frac{aN_e}{aN_e^{1/2}} = N_e^{1/2} \quad (3-9)$$

where  $a$  is the Kuhn length and  $N_e$  is the segment number of the network strand between the neighboring elastically effective junctions.  $N_e$  of Tetra-PAA-PEG gel was given as

$$N_e = \frac{M_{\text{PAA}}b_{\text{PAA}}}{4m_{\text{PAA}}a_{\text{PAA}}} + \frac{M_{\text{PEG}}b_{\text{PEG}}}{4m_{\text{PEG}}a_{\text{PEG}}} \quad (3-10)$$

where  $M_{\text{PAA}}$  is the molecular weight of Tetra-PAA-MA prepolymer,  $M_{\text{PEG}}$  is the molecular weight of Tetra-PEG-SH prepolymer,  $m_{\text{PAA}}$  is the molecular weight of a monomeric PAA unit,  $m_{\text{PEG}}$  is the molecular weight of a monomeric PEG unit,  $b_{\text{PAA}}$  is the monomer length of PAA,  $b_{\text{PEG}}$  is the monomer length of PEG,  $a_{\text{PAA}}$  and  $a_{\text{PEG}}$  are the Kuhn segment size of PAA and PEG, respectively. Substituting the equations (3-9) and (3-10) into eq. (3-8),  $I_m$  is estimated. Table 3-1 summarizes the calculated results of  $N_e$ ,  $\alpha_{\max}$  and  $I_m$ .

**Table 3-1.** The molecular weight of Tetra-PEG-SH ( $M_{\text{PEG}}$ ), of Tetra-PAA-MA ( $M_{\text{PAA}}$ ), the degree of polymerization between the neighboring elastically effective junctions of polymer network ( $N_e$ ) of prepolymers inside Tetra-PAA-PEG gels, the ultimate elongation ratio ( $\alpha_{\text{max}}$ ) and the maximum value of  $I_1$  under the ultimate elongation ratio ( $I_m$ ) of 10K, 20K, and 40K Tetra-PAA-PEG gels.

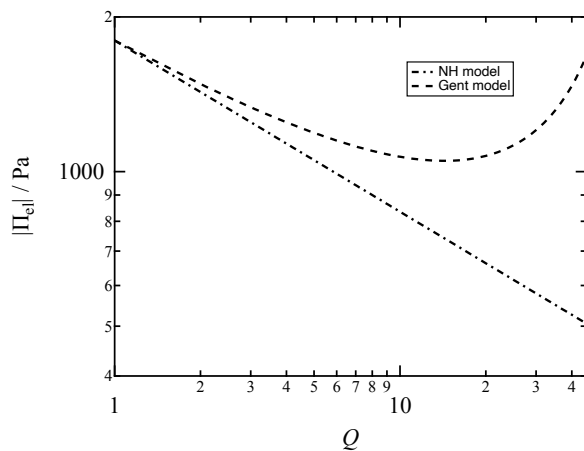
Samples	$M_{\text{PEG}}$ [g/mol]	$M_{\text{PAA}}$ [g/mol]	$N_e$ [-]	$\alpha_{\text{max}}$ [-]	$I_m$ [-]
10K Tetra-PAA-PEG gel	$1.0 \times 10^4$	$1.9 \times 10^4$	53	7.3	53
20K Tetra-PAA-PEG gel	$2.0 \times 10^4$	$1.9 \times 10^4$	81	9.0	81
40K Tetra-PAA-PEG gel	$4.0 \times 10^4$	$1.9 \times 10^4$	$1.4 \times 10^4$	12	$1.4 \times 10^4$

The elastic pressure is obtained by derivation of  $\Delta F_{\text{el}}$  of the Gent model (The detailed procedure is shown in the Appendix 3) and is given as

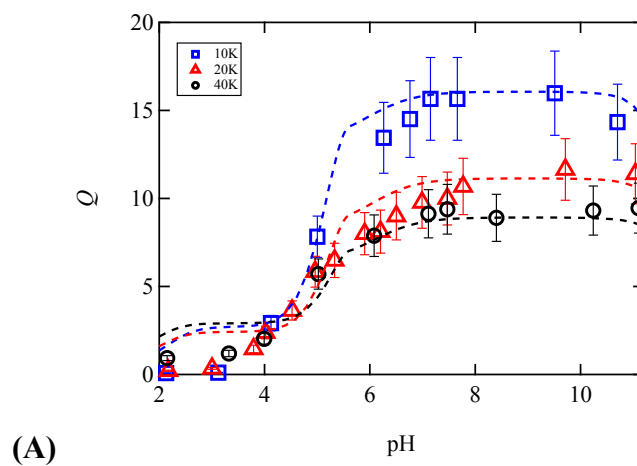
$$\Pi_{\text{el}} = -\frac{I_m - 3}{I_m - I_1} G_0 Q^{-\frac{1}{3}} \quad (3-11)$$

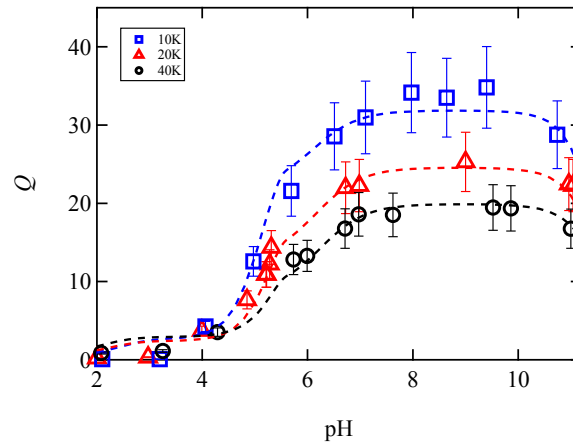
It is worth noting that  $I_m$  is invariable as calculated above, while  $I_1$  is a function of elongation ratio and is affected by the change of  $Q$ . Thus,  $\Pi_{\text{el}}$  is still a function of  $Q$  and  $G_0$ . Figure 3-6 shows the swelling ratio dependence of the elastic pressure of 10K Tetra-PAA-PEG gel predicted by the Neo-Hookean and the Gent model. The Gent model prediction is larger than the Neo-Hookean model prediction, and the gap between  $|\Pi_{\text{el}}|$  of two models becomes significant with the increase of the  $Q$ . In the higher  $Q$  than 20, the Gent model predicts 1.6 times larger values than the Neo-Hookean model. This larger deviation results in the failure to describe the F-R-D-M model for 10K Tetra-

PAA-PEG gel.



**Figure 3-6.** Swelling ratio ( $Q$ ) dependence of the elastic pressure ( $|\Pi_{e1}|$ ) of 10K Tetra-PAA-PEG gel. The dashed-dotted-dashed line represents  $|\Pi_{e1}|$  predicted by the Neo-Hookean model, dashed line represents  $|\Pi_{e1}|$  predicted by the Gent model.





**(B)** Comparison of the experimental results with the predictions by the F-R-D-M model adopting the Gent model for describing the elastic free energy (dashed lines). The ionic strength of salt solutions: (A) 10 mM, (B) 2 mM. The predictions result of 10K (red), 20K (blue), and 40K (black) Tetra-PAA-PEG gels are represented from top to bottom.

Figure 3-7 shows compares the experimental results with the predictions by the F-R-D-M model adopting the Gent model for describing the elastic free energy. The predictions can well reproduce the swelling behaviors of all the Tetra-PAA-PEG gels in all external conditions. The correspondence is even better than the prediction by the F-R-D-M model adopting the Neo-Hookean model for describing the elastic free energy under the low  $Q$  region. This good correspondence indicates the validity of the Gent model for describing the elastic free energy of Tetra-PAA-PEG gel under large deformation. In Chapter 2, I considered the effect of counterion condensation on describing the distribution of mobile ions inside and outside the gel. The swelling behaviors of 20K Tetra-PAA-PEG gel was well reproduced by the F-R-D-M model

adopting the Neo-Hookean model for describing the elastic free energy. It is because the swelling ratios were in relatively small range. However, for the Tetra-PAA-PEG gel undergoing a large size deformation under the low ionic strength, the description of elastic free energy should be modified by the Gent model.

#### D. Applicability of the modified F-R-D-M model for the conventional polyelectrolyte gels

The modified F-R-D-M model can reproduce well the swelling behaviors of Tetra-PAA-PEG gel system under various external solution, which is benefit from the similar network structure as Tetra-PEG gel (a near ideal network structure). All the crosslinks are homogeneously distributed inside Tetra-PAA-PEG gel, and all the fixed ions are also well controlled heterogeneously distributed only on the Tetra-PAA polymer network strands. However, the distribution of crosslink and fixed ions of conventional polyelectrolyte gels are not well controlled and heterogeneously distributed inside the gel due to the random polymerization fabrication method. Here, I want to test the applicability of the modified F-R-D-M model to the conventional polyelectrolyte gel. Figure 3-8 compares the experimental results of polyacrylic acid gel with the predictions by the modified F-R-D-M model. The details of the polyacrylic acid gel can be found in Horkay's research.<sup>29</sup> Within the pure polyacrylic acid gel, the distance between the ionized neighboring fixed ions is constant under external solution with high pH. When all the crosslinks are assumed to be homogeneously distributed inside the gel, which is an ideal condition,  $I_m$  is calculated to be 410 based on the average number of the network strand between the neighboring elastically effective junctions.

It is not surprised to find a deviation between the predictions by the modified F-R-D-M model and the experimental results. This deviation can be attributed to the random and heterogeneous distribution of crosslinks, which resulted in the non-uniform network strand length. The short network strands with small polymerization degree exhibit lower ultimate elongation ratio  $\alpha_{\max}$  compared with long network strands, and bulk  $\alpha_{\max}$  was determined by the short network strands. Thus, the  $I_m$  should be decreased compared with the case all the crosslinks are homogeneously distributed inside the gel. The dotted-dashed-dotted line represents the predictions by the modified F-R-D-M model considering the effect of heterogeneous distribution and  $I_m$  is assumed to be 80 for fitting the experiment results. The experimental results can be well reproduced by the predictions from the modified F-R-D-M model, which indicated the applicability of the F-R-D-M model to conventional polyelectrolyte gel. It's worth noting that the heterogeneity inside the conventional polyelectrolyte can lead to the non-uniform of the network strand lengths, resulting in the misestimating of  $\alpha_{\max}$ . In this case, the value of  $\alpha_{\max}$  determined by the stretching measurement is a valuable method for solving this problem.

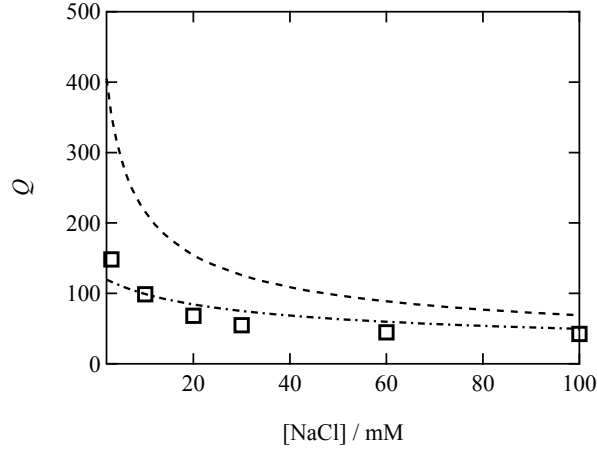


**Figure 3-8.** Comparison of the experimental results of polyacrylic acid gels with the predictions by the modified F-R-D-M model (dashed line) and the modified F-R-D-M model considering the effect of heterogeneity on the network strand lengths (dotted-dashed-dotted line). The data of the swelling ratios of polyacrylic acid gels refer to Horkay *et al.*<sup>29</sup>

On the other hand, the conventional copolymer polyelectrolyte gels consist of both neutral segments and ionic segments, which are more complicated. The distribution of fixed ions on the network strands is random and cannot be controlled. This problem can be solved by introducing a parameter  $a$  to consider this uncontrollable distribution of fixed ions. The distance between the ionized neighboring fixed ions of heterogeneous gel  $b_{ave}$  can be expressed by

$$b_{ave} = ab \quad (3-12)$$

where  $b$  is the distance between the neighboring ionized fixed ions of pure polyacrylic acid gels

$$b = \frac{L_{PAA}}{n_{PAA}} (10^{pK_a - pH} + 1) \quad (3-13)$$

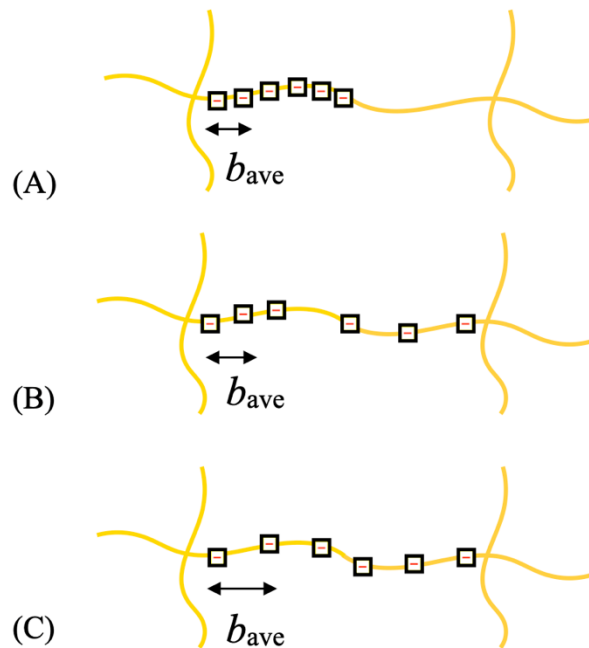


**Figure 3-9.** Schematic illustration of the distribution of fixed ions on the heterogeneous conventional polyelectrolyte gel.

Figure 3-9 shows the typical situations of the distribution of fixed ions on the network strands in the conventional copolymer polyelectrolyte gels. In the situation (A), which is a limitation condition, all the fixed ions are localized within a certain area and the neighboring groups of each fixed ions are also the fixed ions. In this case,  $a = 1$ , which is the same as the conventional polyacrylic acid gel. In the situation (C), all the fixed ions are localized homogeneously on all the polymer chains, and the distance between the neighboring fixed ions increase to a large value. If the molar ratio of the ionic segments is extremely low in the copolymer gel, which is also a limitation condition,  $a$  and  $b_{ave}$  tend to be infinite. Under such condition, this copolymer gel is a weakly

charged polyelectrolyte gel, the counterion condensation cannot occur around all the fixed ions and the swelling behaviors of this copolymer gel can be described by the F-R-D model. In the situation (B), which is an intermediate situation between situations (A) and (C), all the ionic segments are randomly and heterogeneously distributed. In this case, the  $b_{\text{ave}}$  in different area is also different, and I can use the parameter  $a$  to fit the experiment result to understand the distribution of fixed ions inside the gel. Compared with some conventional structure analysis method, such as small angle X-ray scattering (SAXS) or small angle neutron scattering (SANS), I believe the swelling measurement is also a potential method for understand the heterogeneity inside the conventional gel. Unfortunately, I cannot find sufficient data for this analysis yet. In the future, I plan to induce some controllable heterogeneity into the gel, then design a new method for investigating the network structure heterogeneity inside the polyelectrolyte gel based on the swelling measurement.

### 3.4. Conclusion

I successfully fabricated Tetra-PAA-PEG gel with tuned neutral segment lengths. Then, I investigated the swelling behaviors of the Tetra-PAA-PEG gels under various external conditions. The major findings are as follows: (i) The swelling ratios increased with increasing pH and decreasing ionic strength; (ii) the swelling ratios decreased with increasing the network strand lengths; (iii) The swelling behaviors the Tetra-PAA-PEG gels under ionic strength of 10 mM were well reproduced by the F-R-D-M model predictions, indicates the validity of the Neo-Hookean model for describing the elastic free energy under appropriate deformation; (iv) The swelling behaviors of 10K Tetra-PAA-PEG gel under ionic strength of 2 mM were smaller than the F-R-D-M model predictions. With the modification of the elastic free energy by the Gent model, the swelling behaviors corresponded well with the modified F-R-D-M model predictions, indicating the validity of the Gent model for describing the elastic free energy of gel under high deformation. These findings indicate that the modified F-R-D-M model is more valid for describing the swelling behaviors of highly charged polyelectrolyte gel with a wide range of segment lengths.

## Appendix

### 1. Overlapping polymer volume fraction of the blend system of Tetra-PAA and Tetra-PEG

Constant amounts of Tetra-PAA-MA was dissolved in a citrate-phosphate buffer solution to obtain the polymer solution with concentration ranging from 0 to 120 g L<sup>-1</sup>. The pH and ionic strength of the buffer solution were 5.9 and 100 mM, respectively. The effect of ionization of acrylic acid was suppressed by applying the buffer solution as a solvent. The viscosity  $\eta$  of the polymer solutions was measured by a rheometer (MCR301; Anton Paar, Graz, Austria) with a cone plate at a constant shear rate of 100 s<sup>-1</sup>. All the experiments were performed at 25 °C. The specific viscosity  $\eta_{sp}$  was expressed as

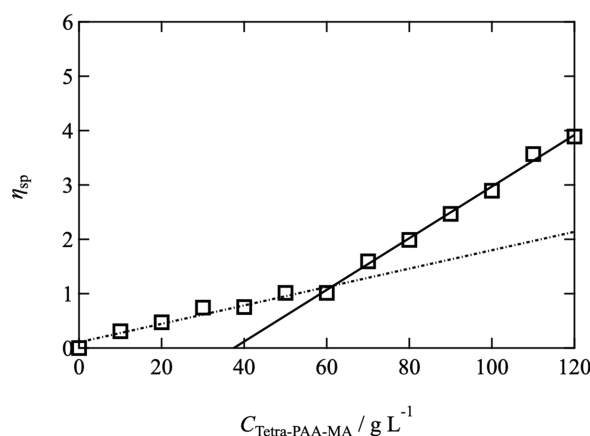
$$\eta_{sp} = \frac{\eta - \eta_0}{\eta_0} \quad (\text{A-3-1})$$

where  $\eta_0$  is the viscosity of the buffer solution.

Supporting figure 1 shows the specific viscosity  $\eta_{sp}$  of Tetra-PAA-MA polymer solutions as a function of polymer concentration. From the crossover of the two fitting lines, the  $C_{PAA}^*$  of the Tetra-PAA-MA polymer was estimated to be 60 g L<sup>-1</sup>, and the overlapping polymer volume fraction  $\phi_{PAA}^*$  was calculated to be 0.050. Tetra-PAA-PEG gel was fabricated from Tetra-PAA-MA and Tetra-PEG-SH prepolymers, thus the blend overlapping polymer volume fraction  $\phi_{blend}^*$  of Tetra-PAA-PEG gel was determined by  $\phi^*$  and  $\phi$  of both Tetra-PAA-MA and Tetra-PEG-SH prepolymers inside Tetra-PAA-PEG gel, which was given as

$$\phi_{blend}^* = f_{PEG}\phi_{PEG}^* + f_{PAA}\phi_{PAA}^* \quad (\text{A-3-2})$$

where  $\phi_{\text{PEG}}^*$  was the overlapping polymer volume fraction of Tetra-PEG prepolymer, which were already measured by our previous research.  $f_{\text{PEG}}$  and  $f_{\text{PAA}}$  were the volume fraction of Tetra-PEG-SH and Tetra-PAA-MA to the total polymer volume, respectively.



**Supporting figure 1.** Specific viscosity of Tetra-PAA-MA polymer solutions as a function of polymer concentration. The overlapping concentration  $C^*$  was estimated to be the point at the intersection of the fitting lines of lower concentration and high concentration.

Supporting table 1 shows the total polymer volume fraction  $\phi_{\text{total}}$  and overlapping polymer volume fraction  $\phi_{\text{blend}}^*$  of 10K, 20K, and 40K Tetra-PAA-PEG gel, respectively.  $\phi_{\text{total}}$  of 10K Tetra-PAA-PEG gel was smaller than the  $\phi_{\text{blend}}^*$ , while  $\phi_{\text{total}}$  of 20K and 40K Tetra-PAA-PEG gel was slightly larger than the  $\phi_{\text{blend}}^*$ .

**Supporting table 1.** Polymer volume fraction ( $\phi_{\text{PEG}}$ ) of Tetra-PEG-SH, polymer volume fraction ( $\phi_{\text{PAA}}$ ) of Tetra-PAA-MA, total polymer volume fraction ( $\phi_{\text{total}}$ ) of

prepolymers inside Tetra-PAA-PEG gels and overlapping polymer volume fraction ( $\phi_{\text{blend}}^*$ ) of 10K, 20K, and 40K Tetra-PAA-PEG gels.

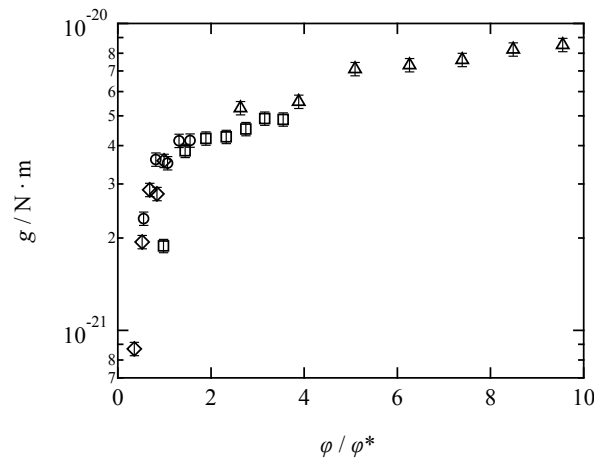
Samples	$\phi_{\text{PEG}} [-]$	$\phi_{\text{PAA}} [-]$	$\phi_{\text{total}} [-]$	$\phi_{\text{blend}}^* [-]$
10K Tetra-PAA-PEG gel	0.014	0.025	0.039	0.054
20K Tetra-PAA-PEG gel	0.027	0.025	0.052	0.042
40K Tetra-PAA-PEG gel	0.053	0.024	0.077	0.025

## 2. Calculation of $G_0/G_{\text{af}}$

According to our previous studies,<sup>13</sup>  $G_0$  of the Tetra-PEG gel did not obey the simple rubber elasticity theories<sup>22</sup> due to the negative energetic contribution<sup>21</sup>.  $G_0$  is given as

$$G_0 = g(\nu - \mu) \quad (\text{A-3-3})$$

where  $\nu$  is the number per prepolymer of the elastically effective network strands,  $\mu$  is the number per prepolymer of the active cross-link and  $g$  is a pre-factor related to the energetic contribution. Our previous studies suggested that  $g$  is a function of  $\phi/\phi^*$  shown in Supporting figure 2.



**Supporting figure 2.** The value of  $g$  as a function of  $\phi/\phi^*$  of Tetra-PEG gels (5K, rhombus; 10K, circle; 20K, square; 40K, triangle). The data of Tetra-PEG

gels are replotted from Akagi et al.<sup>22</sup> with permission.

Supporting figure 3 shows the reaction conversion of 10K, 20K, and 40K Tetra-PAA-PEG gels. The reaction conversion was in the range of 0.81-0.90. Adopting the Bethe approximation,  $\nu$  and  $\mu$  can be calculated as a function of the reaction conversion ( $p$ ).<sup>33,34</sup> Under the stoichiometric mixing condition, the AB-type reaction can be instead by presuming that the reaction is an AA-type reaction of the 4-armed prepolymer. Thus, the probability of one arm of a 4-armed prepolymer was not connected to the percolated network,  $P(F)$ , is expressed as

$$P(F) = \left(\frac{1}{p} - \frac{3}{4}\right)^{\frac{1}{2}} - \frac{1}{2} \quad (\text{A-3-4})$$

Using equation (A-3-4), the probability of 3-functional or 4-functional crosslink (i.e.,  $P(X_3)$  or  $P(X_4)$ ) can be derived from a 4-armed prepolymer as

$$P(X_3) = \binom{4}{3} \cdot P(F) \cdot [1 - P(F)]^3 \quad (\text{A-3-5})$$

$$P(X_4) = [1 - P(F)]^4 \quad (\text{A-3-6})$$

Thus,  $\mu$  and  $\nu$  can be expressed as:

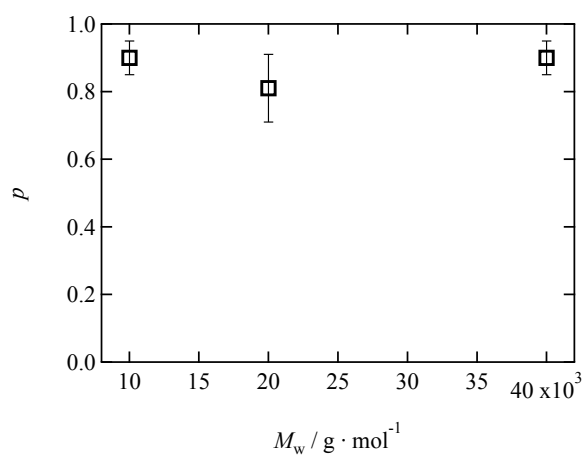
$$\mu = P(X_3) + P(X_4) \quad (\text{A-3-7})$$

$$\nu = \frac{3}{2} \cdot P(X_3) + 2 \cdot P(X_4) \quad (\text{A-3-8})$$

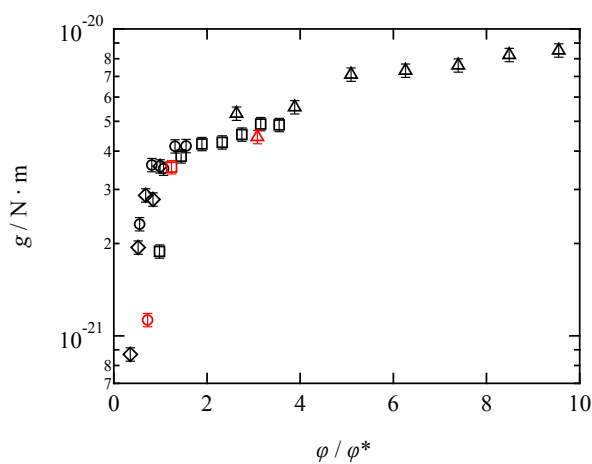
$g$  for the Tetra-PAA-PEG gel was obtained by inserting equations (A-3-7) and (A-3-8) into equation (A-3-3).

The obtained values of  $g$  were plotted in Supporting figure 4, which obeys the master curve of the Tetra-PEG gels. These agreements support that the reduction of  $G_0$  of the Tetra-PAA-PEG gels with shorter network length can be explained by the

distance from  $\phi^*$ .



**Supporting figure 3.** The reaction conversion ( $p$ ) of 10K, 20K and 40K Tetra-PAA-PEG gels.



**Supporting figure 4.** The value of  $g$  as a function of  $\phi/\phi^*$  of Tetra-PEG gels (black: 5K, rhombus; 10K, circle; 20K, square; 40K, triangle) and Tetra-PAA-PEG gel (red: 10K, circle; 20K, square; 40K, triangle).

### 3. Calculation of $\Pi_{el}$ of Gent model

$\Pi_{el}$  was defined as a change in the elastic free energy ( $\Delta F_{el}$ ) when changing the number

of solvent molecules ( $n_B$ ) with a constant number of polymers in the system ( $n_A$ ), and was expressed as

$$\Pi_{el} = -\frac{1}{V_1} \left( \frac{\partial \Delta F_{el}}{\partial n_B} \right)_{n_A} \quad (\text{A-3-9})$$

where  $N_A$  is Avogadro's constant,  $V_1$  is the molar volume of the solvent, thus  $N_A/V_1$  is the number of solvent molecules in a unit volume. According to Gent model, the elastic free energy  $\Delta F_{el}$  is expressed as

$$\Delta F_{el} = -\frac{V_0 G_0}{2} (I_m - 3) \ln \left( 1 - \frac{I_1 - 3}{I_m - 3} \right) \quad (\text{A-3-10})$$

where  $G_0$  and  $V_0$  are the shear modulus and volume of the gel at as-prepared state.  $I_1$  is the first invariant of the Green's deformation tensor,  $I_m$  is the maximum value of  $I_1$  where the stress becomes infinite, and  $I_1$  is expressed as

$$I_1 = \alpha_x^2 + \alpha_y^2 + \alpha_z^2 \quad (\text{A-3-11})$$

where  $\alpha_i$  is the elongation ratio in the  $i$  axis ( $i=x, y, z$ ) of the gel at swollen state. The elongation ratios are obtained by assuming isotropic deformation, which are given as

$$\alpha_x = \alpha_y = \alpha_z = \alpha = Q^{\frac{1}{3}} = \left( \frac{V}{V_0} \right)^{\frac{1}{3}} \quad (\text{A-3-12})$$

where  $Q$  and  $V$  are the swelling ratio, the volume at swollen state, respectively. Substituting equations (A-3-10), (A-3-11) and (A-3-12) into equation (A-3-9), the following equation is obtained

$$\Pi_{el} = -\frac{1}{V_1} \left( \frac{\partial \Delta F_{el}}{\partial n_B} \right)_{n_A} = -\frac{1}{V_1} \left( \frac{\partial \Delta F_{el}}{\partial \alpha} \right)_{n_A} \left( \frac{\partial \alpha}{\partial n_B} \right)_{n_A} = -\frac{3\alpha V_0 G_0}{V_1} \frac{I_m - 3}{I_m - I_1} \left( \frac{\partial \alpha}{\partial n_B} \right)_{n_A} \quad (\text{A-3-13})$$

Here,

$$\alpha^3 = \frac{V}{V_0} = \frac{V_0 + n_B V_1}{V_0} \quad (\text{A-3-14})$$

Therefore,  $\Pi_{el}$  can be rewritten as

$$\Pi_{el} = -\frac{I_m - 3}{I_m - I_1} G_0 Q^{-\frac{1}{3}} \quad (\text{A-3-15})$$

In equation (A-3-15), the term of  $G_0 Q^{-\frac{1}{3}}$  is equal to the shear modulus at the swollen state. Thus,  $\Pi_{el}$  is experimentally validated by measuring the shear modulus.

## Reference

- (1) Flory, P. J.; Rehner, J. *J. Chem. Phys.* **1943**, *11* (11), 521–526.
- (2) Flory, P. J. *Principles of Polymer Chemistry*; Cornell University Press, 1953.
- (3) Treloar, L. R. G. *The Physics of Rubber Elasticity*; Oxford University Press, USA, 1975.
- (4) Wall, F. T. *J. Chem. Phys.* **1942**, *10* (7), 485–488.
- (5) Katashima, T.; Urayama, K.; Chung, U. Il; Sakai, T. *Soft Matter* **2012**, *8* (31), 8217–8222. <https://doi.org/10.1039/c2sm25340b>.
- (6) Skouri, R.; Schosseler, F.; Munch, J. P.; Candau, S. J. *Macromolecules* **1995**, *28* (1), 197–210.
- (7) Schröder, U. P.; Oppermann, W. *Macromolecular Symposia*; Wiley Online Library, 1993; Vol. 76, pp 63–74.
- (8) Li, J.; Suo, Z.; Vlassak, J. J. *Soft Matter* **2014**, *10* (15), 2582–2590.
- (9) Miquelard-Garnier, G.; Creton, C.; Hourdet, D. *Soft Matter* **2008**, *4* (5), 1011–1023.
- (10) Tang, J.; Katashima, T.; Li, X.; Mitsukami, Y.; Yokoyama, Y.; Sakumichi, N.; Chung, U.; Shibayama, M.; Sakai, T. **2020**, *53* (19), 8244–8254.
- (11) Fujiyabu, T.; Yoshikawa, Y.; Chung, U. il; Sakai, T. *Sci. Technol. Adv. Mater.* **2019**, *20* (1), 608–621.
- (12) Matsunaga, T.; Sakai, T.; Akagi, Y.; Chung, U. Il; Shibayama, M. *Macromolecules* **2009**, *42* (4), 1344–1351.
- (13) Yoshikawa, Y.; Sakumichi, N.; Chung, U. Il; Sakai, T. *Soft Matter* **2019**, *15* (25),

- 5017–5025.
- (14) Akagi, Y.; Sakurai, H.; Gong, J. P.; Chung, U. Il; Sakai, T. *J. Chem. Phys.* **2013**, *139* (14), 1–7.
- (15) Sakai, T.; Matsunaga, T.; Yamamoto, Y.; Ito, C.; Yoshida, R.; Suzuki, S.; Sasaki, N.; Shibayama, M.; Chung, U. Il. *Macromolecules* **2008**, *41* (14), 5379–5384.
- (16) Oshima, K.; Fujimoto, T.; Minami, E.; Mitsukami, Y. *Macromolecules* **2014**, *47* (21), 7573–7580.
- (17) Hayashi, K.; Okamoto, F.; Hoshi, S.; Katashima, T.; Zujur, D. C.; Li, X.; Shibayama, M.; Gilbert, E. P.; Chung, U. Il; Ohba, S.; et al. *Nat. Biomed. Eng.* **2017**, *1* (3), 1–7.
- (18) Flory, P. J. *J. Chem. Phys.* **1977**, *66* (12), 5720–5729.
- (19) James, H. M.; Guth, E. *J. Chem. Phys.* **1953**, *21* (6), 1039–1049.
- (20) Flory, P. J. *Polymer (Guildf)*. **1979**, *20* (November), 1317–1320.
- (21) Yoshikawa, Y.; Sakumichi, N.; Chung, U.; Sakai, T. **2019**, 1–11.
- (22) Akagi, Y.; Gong, J. P.; Chung, U. Il; Sakai, T. *Macromolecules* **2013**, *46* (3), 1035–1040.
- (23) Cohen, Y.; Prevys, V. *Acta Polym.* **1998**, *49* (10–11), 539–543.
- (24) Khutoryanskiy, V. V.; Dubolazov, A. V.; Nurkeeva, Z. S.; Mun, G. A. *Langmuir* **2004**, *20* (9), 3785–3790.
- (25) Yu, X.; Tanaka, A.; Tanaka, K.; Tanaka, T. *J. Chem. Phys.* **1992**, *97* (10), 7805–7808.
- (26) Onuki, A. *Adv. Polym. Sci.* **1993**, *109*, 63–121.

- (27) Huggins, M. L. *Ann. N. Y. Acad. Sci.* **1942**, *43* (1), 1–32.
- (28) Flory, P. J. *J. Chem. Phys.* **1942**, *10* (1), 51–61.
- (29) Horkay, F.; Tasaki, I.; Basser, P. J. *Biomacromolecules* **2000**, *1* (1), 84–90.
- (30) Gent, A. N. *Rubber Chem. Technol.* **1996**, *69* (1), 59–61.
- (31) Rivlin, R. S. *Philos. Trans. R. Soc. London. Ser. A, Math. Phys. Sci.* **1948**, *241* (835), 379–397.
- (32) Obukhov, S. P.; Rubinstein, M.; Colby, R. H. *Macromolecules* **1994**.
- (33) Macosko, C. W.; Miller, D. R. *Macromolecules* **1976**, *9* (2), 199–206.
- (34) Miller, D. R.; Macosko, C. W. *Macromolecules* **1976**, *9* (2), 206–211.

## **Chapter 4. Swelling behaviors of Tetra-PAA-PEG gel in divalent salt solutions**

### **4.1. Introduction**

In Chapter 3, I found the validation of the modified F-R-D-M model for describing the swelling behaviors of Tetra-PAA-PEG gels even under large deformation by adopting the Gent model for describing the finite extensibility effect on the network strands. Thus, the swelling behaviors of Tetra-PAA-PEG gel in monovalent salt solution under various conditions were understood.

However, the description of the swelling behaviors in divalent salt remain unclear. The investigation of swelling behaviors of polyelectrolyte gel in divalent salt has attracted little attention compared with monovalent salt due to the complicated interaction inside gel system.<sup>1,2</sup> Different from the monovalent salt, which only influences the ionic pressure inside the gel system, the divalent salt can also coordinate with the acrylic acid group. Horkay and co-workers<sup>2,3</sup> investigated the swelling behaviors of the fully neutralized polyacrylic acid hydrogels immersed in the solutions of monovalent salts and divalent salts. In this research, they found the monovalent ions only influence the ionic contribution to the total pressure, while divalent ions influence both the ionic and mixing contributions. In other words, monovalent salts have no effect on the interaction between polymer and solvent, while divalent salts significantly influence the interaction between polymer and solvent. They also deduced that the calcium ion cannot form stable cross-link with acrylic acid groups by uniaxial compression measurements and concluded there is no enhancement of elasticity.

However, the mechanical measurement of their research is a static measurement, the contribution to the elasticity of gel by the crosslink between calcium ions and carboxyl groups cannot be detected if the lifetime of temporary cross-link shorter than the duration of the measurement. Some studies indicated the calcium ion can form crosslink with PAA and stabilize PAA hydrogels by preventing the dissolution of the gel.<sup>4</sup> Infrared spectroscopy has also distinguished several stable forms of calcium ion binding to the carboxyl groups.<sup>5</sup> In Zhou's study, they mentioned that  $\text{Ca}^{2+}$  acting as ionic secondary crosslinking forming bridges between neighboring PAA chains and enhanced the elasticity of the gel.<sup>6</sup> Thus, the description of the effect of divalent salt on the mechanical and swelling properties of polyelectrolyte gels remain unclear.

Tetra-PAA-PEG gel possesses a regular network structure with uniformly distributed cross-linking points and is a model for testing the theoretical model. Modified F-R-D-M model works well for describing the swelling behaviors of Tetra-PAA-PEG gel in monovalent salt solution, while the Manning's counterion condensation theory can be applied for the precise estimation of the effective fixed ion concentration. Manning also described the estimation method of the effective fixed ion concentration in divalent salt system.<sup>7-9</sup> For example, if Tetra-PAA-PEG gel is immersed in the external solution with monovalent salt, the condensation can occur when the ionization degree of fixed ions is 0.34. In the case of divalent salt, the condensation can occur under even lower ionization degree of fixed ions. By precisely understand the distribution of calcium ions inside the Tetra-PAA-PEG gel based on the counterion condensation and Donnan equilibrium effect, the molecular mechanism of

the interaction between  $\text{Ca}^{2+}$  and PAA and the swelling behaviors of the gel in divalent salt solution can be understood.

In Chapter 4, I investigated the pH dependence of swelling ratios of Tetra-PAA-PEG in  $\text{CaCl}_2$  salt solutions with concentrations of 0.1 and 100 mM. By considering the short lifetime of aggregation structure between calcium ions and acrylic acid groups, I performed the dynamic rheological measurement to measure the frequency dependence of the shear modulus. By comparison the experimental shear modulus with the predictions from the theoretical model, the molecular mechanism of the effect of calcium ions on the mechanical and swelling properties of Tetra-PAA-PEG gel is revealed.

## 4.2. Experimental

### A. Fabrication of Tetra-PAA-PEG Gels

Tetrathiol-terminated poly(ethylene glycol) (Tetra-PEG-SH) was purchased from NOF Corporation (Tokyo, Japan). Tetramaleimide-terminated poly(acrylic acid) (Tetra-PAA-MA) was prepared from the Tetraazide-terminated poly(*tert*-butyl acrylate) (Tetra-PtBuA-N<sub>3</sub>). The details of the preparation of Tetra-PAA and Tetra-PEG precursors were reported previously.<sup>10-13</sup> Molecular weight ( $M_w$ ) of Tetra-PEG-SH and Tetra-PAA-MA were  $2.0 \times 10^4$  and  $1.9 \times 10^4$  g mol<sup>-1</sup>, respectively. Constant amounts of Tetra-PAA-MA and Tetra-PEG-SH were dissolved in citrate-phosphate buffer solution, of which the pH and ionic strength were 5.9 and 100mM, respectively. To obtain the same molar concentration, the concentration of Tetra-PEG-SH and Tetra-PAA-MA were set to 64.7 and 60.0 g L<sup>-1</sup>, respectively. Equal amounts of the prepolymer solutions were mixed for 30 s and poured into the silicone mold at room temperature for 48 h until the reaction completion.

### B. Swelling Experiments

The gel samples for swelling ratio measurements were prepared in silicon mold with rectangular shape (length: 5.0 mm, thickness: 2.0 mm, width: 3.0 mm). As for the pH dependence measurement, I prepared two groups solutions with pH tuned from 2.0 to 11.0, the volume of the solutions was 50 mL, which is much larger compared with the size of gel samples. The concentration of CaCl<sub>2</sub> in two groups solutions were respectively controlled to 0.1 mM and 100 mM by adding different amounts of CaCl<sub>2</sub> salt. The specimens were immersed into the solutions for 48h to reach the equilibrium

swelling state at 25 °C. The pH of external solutions was deviated from the setting value due to the existence of the carboxyl groups on the Tetra-PAA-MA polymer, thus I titrated an HCl (pH = 2.0) or NaOH (pH = 12.0) solution into the external solutions to adjust the pH to the setting values. In the case of divalent salt concentration dependence measurement, the salt concentration of CaCl<sub>2</sub> in the external solutions were tuned from 0.1 to 100 mM by adding different amounts of CaCl<sub>2</sub> at pH 11, under which the ionization degree of carboxyl groups was larger than 0.99.

The swelling ratio of the Tetra-PAA-PEG gel was investigated by measuring the volume change of the samples by using the encoded stereo microscopes (M165 C, Leica Co.). In this study, the swelling ratio ( $Q$ ) was defined by using the initial volume of gel sample  $V_0$  and the swollen volumes of gel sample  $V_s$ :  $Q = V_s/V_0$ . Generally, the swelling of the gels is an isotropic deformation. The volume change was estimated by using the change of the initial side length of gel sample at as-prepared state  $L_0$  and the side length of gel sample at equilibrium swelling state  $L_s$ , thus the swelling ratio  $Q$  was expressed as:  $Q = (L_s/L_0)^3$ .  $L_0$  was 5.0 mm, while  $L_s$  were in the range of 4.3-13.7 mm depending on the external solutions conditions.

### C. Rheological Properties of the swollen and deswollen gels

The Tetra-PAA-PEG gel samples were prepared in a silicon mold with disk shape. The diameter and thickness of the samples at as-prepared state were 35.0 mm and 1.0 mm, respectively. The gel samples were immersed into the CaCl<sub>2</sub> salt solutions with salt concentration of 0.1 and 100 mM under pH = 11 for 48h to reach the equilibrium swelling state at 25 °C. The swollen and deswollen gel samples were set at the

measuring plate of a rheometer (MCR301; Anton Paar, Graz, Austria) with a parallel plate fixture having a diameter of 25 mm. The angular frequency ( $\omega$ ) dependences of the storage modulus ( $G'$ ) and loss modulus ( $G''$ ) were measured with a strain amplitude ( $\gamma$ ) of 1.0% at 25 °C. The oscillatory shear strain amplitudes were found within the range of the linear viscoelasticity for all the tests.

#### D. Small-angle X-ray scattering (SAXS)

The gel samples were transferred into custom-made SAXS cells (1 mm thick) that were then tightly sealed with glass windows (30  $\mu\text{m}$  thick). The scattering profiles were obtained using a SAXSpoint 2.0 instrument (Anton Paar, Austria), equipped with an EIGER R 1M detector. Each sample was irradiated with an X-ray beam having a wavelength of 0.154 nm for 20 min at a sample-to-detector distance of 0.50 m. The sample chamber was kept under vacuum ( $< 0.005$  Pa) during the measurements to eliminate ambient scattering. The samples were held at  $25.0 \pm 0.1^\circ\text{C}$  during these measurements. All the SAXS profiles were corrected for the exposure time, transmittance, sample thickness, cell background, and also normalized to the absolute intensity with a custom-made data reduction package Red2D (<https://github.com/hurxl/Red2D>) on a scientific data analysis software (Igor Pro 8, WaveMetrics, USA).

### 4.3. Result and discussions

#### A. Effect of pH on the swelling behaviors (divalent salt)

Figure 4-1 shows the pH dependence of the swelling ratios of Tetra-PAA-PEG gel in  $\text{CaCl}_2$  salt solutions with concentration of 0.1 mM. The  $Q$  of Tetra-PAA-PEG gel increased with increasing pH, reaching a plateau when  $\text{pH} > 7.0$ , which corresponds to the pH dependence of the ionization of acrylic acid groups on the polymer chains. This swelling behavior in divalent salt solution is similar to the swelling behaviors of Tetra-PAA-PEG gel in monovalent salt solution, indicating the distribution of mobile ions that follow the Donnan equilibrium. In Chapter 3, the swelling behaviors of Tetra-PAA-PEG gel in monovalent salt solution can be well reproduced by the modified F-R-D-M model predictions. Thus, I also apply the modified F-R-D-M model to predict the swelling behaviors in divalent salt solution. Here, the  $\chi$  parameter in divalent salt solution is assumed to be the same as in monovalent salt solution. The effective fixed ions concentration in monovalent salt solution is expressed as

$$[\text{COOH}]_{0, \text{effective}} = \frac{[\text{COOH}]_0}{2\xi} \quad (4-1)$$

It is important to note that adding salt to solvent can influence the value of Bjerrum length by changing the dielectric constant. However, this effect can be neglected, since the maximum concentration of  $\text{CaCl}_2$  salt is only 100 mM in this study.<sup>14,15</sup>

Dashed line represents the predictions by the modified F-R-D-M model using equation (4-1) to estimate the effective fixed ions concentration. Unfortunately, there is a significant gap between the modified F-R-D-M model predictions and the experimental results. This deviation can be attributed to the overestimation of the

effective fixed ions concentration. According to the Manning's theory, the counterion with larger valence can cause the stronger divergence of the phase integral,<sup>8</sup> and the divalent counterions will condense on the fixed ions until the net value of critical parameter  $\zeta$  is lowered to the value 0.5, while the monovalent counterions can only lower the critical parameter  $\zeta$  to 1.0. Thus, the final effective concentration of fixed ions in divalent salt solution is half of that in monovalent salt solution, and the effective fixed ions concentration is expressed as

$$[\text{COOH}]_{0, \text{effective}} = \frac{[\text{COOH}]_0}{4\zeta} \quad (4-2)$$

It is worth noting that the counterion condensation can occur under lower pH in divalent salt solution compared with in monovalent salt solution, because the average contour distance between the neighboring fixed charges  $b$  is govern by the ionization degree of fixed ions.

Dashed-dotted-dashed line represents the predictions by the modified F-R-D-M model using the equation (4-2) to estimate the effective fixed ions concentration. With the modification of the effective fixed ions concentration, the modified F-R-D-M model predictions can well reproduce the swelling behaviors of Tetra-PAA-PEG gels in  $\text{CaCl}_2$  salt solutions with salt concentration of 0.1 mM, suggesting the validity of the modified F-R-D-M model for describing the swelling behaviors of Tetra-PAA-PEG gel in divalent salt.

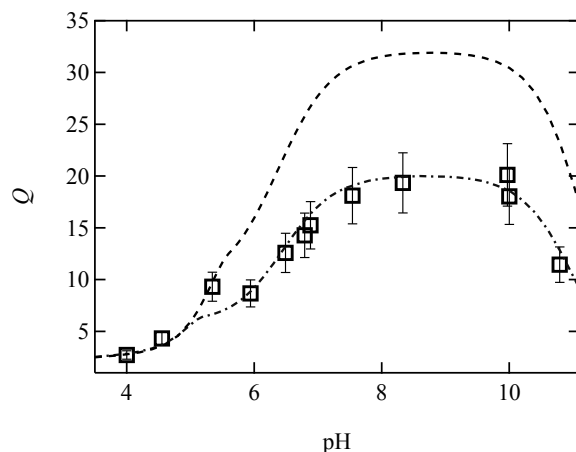


**Figure 4-1.** pH dependence of the swelling ratios of Tetra-PAA-PEG gel in  $\text{CaCl}_2$  salt solutions with salt concentrations of 0.1 mM. The dashed line and dashed-dotted-dashed line represent the predictions by the modified F-R-D-M model that using equation (4-1) and (4-2) to estimate the effective fixed ion concentration, respectively.

Figure 4-2 shows the pH dependence of the swelling ratios of Tetra-PAA-PEG gel in  $\text{CaCl}_2$  salt solutions with concentration of 100 mM. The swelling ratios of Tetra-PAA-PEG gel were less than 1.0 under the whole pH range, which are 3 times smaller than the swelling ratios of Tetra-PAA-PEG gel in monovalent salt solution with the same ionic strength. The experimental results significantly deviated from the modified F-R-D-M model predictions using equation (4-2) to estimate the effective fixed ion concentration. However, this deviation under high salt concentration does not mean the invalidity of the modified F-R-D-M model for describing the swelling behaviors of Tetra-PAA-PEG gel in divalent salt, while the model predictions can well reproduce the experimental results in low salt concentration. This deviation is attributed to the

formation of aggregation structure between  $\text{Ca}^{2+}$  and PAA, which disturbed the estimation of elastic pressure and mixing pressure within the modified F-R-D-M model.

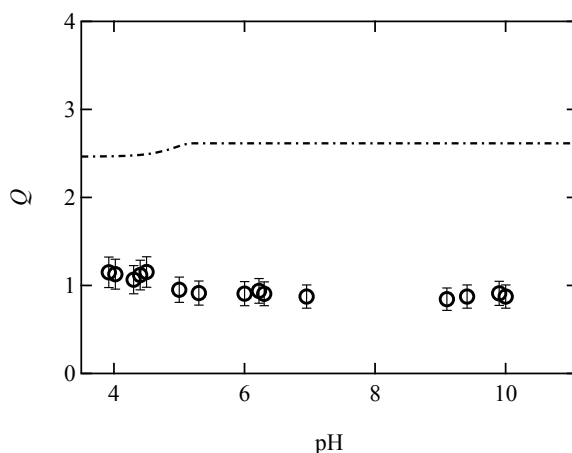


**Figure 4-2.** pH dependence of the swelling ratios of Tetra-PAA-PEG gel in  $\text{CaCl}_2$  salt solutions with concentrations of 100 mM (circles). The dashed line represents the predictions by the modified F-R-D-M model that using equation (4-2) to estimate the effective fixed ions concentration.

#### B. Effect of divalent salt concentration on the swelling behaviors

Figure 4-3 shows the  $\text{CaCl}_2$  salt concentration-dependence of the swelling ratios of Tetra-PAA-PEG gel in salt solutions at  $\text{pH} = 11$ , the acrylic acid groups on the polymer chains are totally dissociated under this pH condition. The  $Q$  of Tetra-PAA-PEG gel decreased with the increase of salt concentration, and the  $Q$  reduced much compared with the  $Q$  of Tetra-PAA-PEG gel in monovalent salt solution. Here, I plot the modified F-R-D-M model predictions against salt concentration and compare with the experimental results. The swelling ratios of Tetra-PAA-PEG gel under 0.1 mM salt

concentration corresponds well with the predictions, which is consistent with the pH dependence measurement result of Tetra-PAA-PEG gel in divalent salt solution with concentration of 0.1 mM. When the salt concentration was larger than 0.1 mM, the gap between the predictions and experimental results became significant with the increase of salt concentration. This deviation also suggests the formation of aggregation structure. With the increase of the salt concentration in the external solution, the amount of  $\text{Ca}^{2+}$  that diffuse into the gel also increase. Thus, more aggregation structure is formed and the deviation increases with increasing salt concentration.

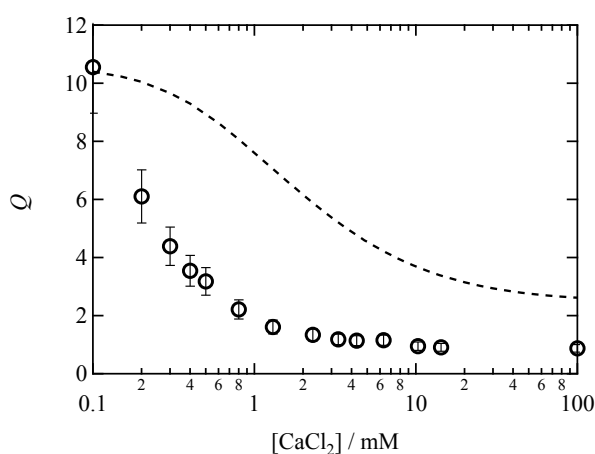


**Figure 4-3.**  $\text{CaCl}_2$  concentration-dependence of the swelling ratios of Tetra-PAA-PEG gel in salt solutions at pH = 11.

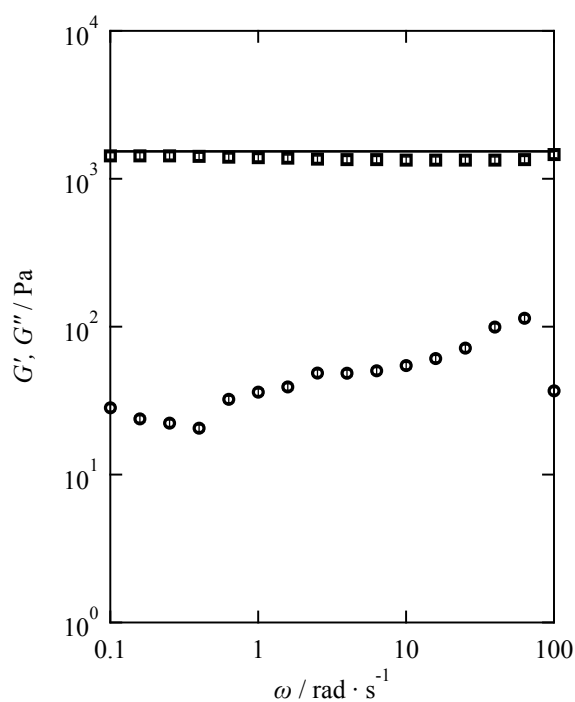
### C. Effect of divalent salt concentration on the mechanical properties

To verify the existence of the aggregation structure, the mechanical measurement was performed. Figure 4-4 shows the angular frequency dependence of the storage modulus ( $G'$ ) and loss modulus ( $G''$ ) of the Tetra-PAA-PEG gel in the  $\text{CaCl}_2$  salt solutions with different salt concentrations at pH = 11. I plot the prediction of  $G'$  by Flory's model,

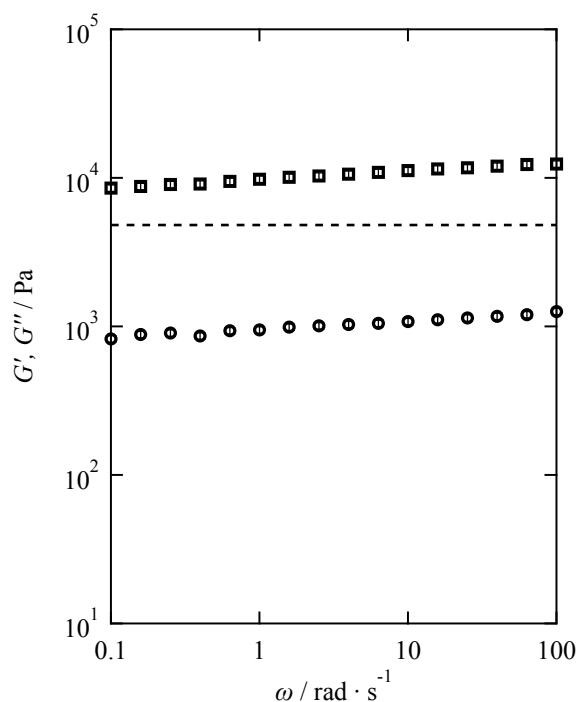
which successfully described the elasticity of the Tetra-PAA-PEG gel in monovalent salt solution, the expression is given as

$$\Pi_{el} = -G_0 Q^{-\frac{1}{3}} \quad (4-3)$$

The experimental  $G'$  of Tetra-PAA-PEG gel in divalent salt solution with concentration 0.1 mM can be well reproduced by the theoretical line, which indicates there is no effect of divalent salt on the elasticity. However, the experimental  $G'$  of Tetra-PAA-PEG gel in divalent salt solution with concentration 100 mM deviated from the theoretical line in the whole  $\omega$  range. The experimental  $G'$  is 1.8 times larger values than the predictions at 0.1  $\text{rad s}^{-1}$ . This deviation suggests the formation of aggregation, leading to the enhancement of the elasticity of the gel.



(A)



(B)

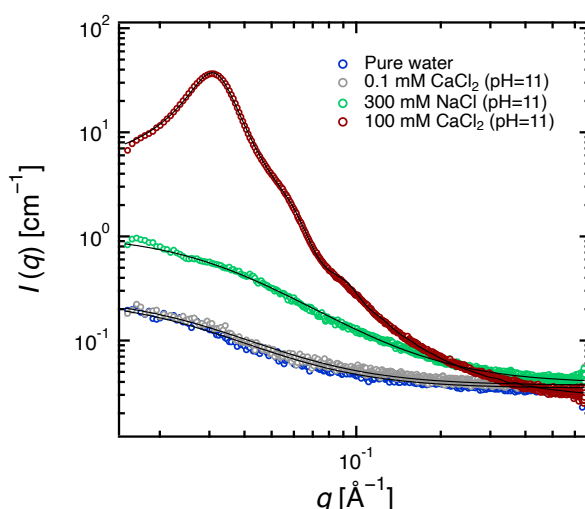
**Figure 4-4.** Angular frequency dependence ( $\omega$ ) of the storage modulus  $G'$  (squares) and loss modulus  $G''$  (circles) of the Tetra-PAA-PEG gel in the  $\text{CaCl}_2$  salt solutions with different concentration of (A) 0.1 and (B) 100 mM, respectively. pH of external solutions is set to 11. The solid line and dashed line represent the predicted results from Flory's model.

Figure 4-5 shows the SAXS profiles of the gel in pure water, gel with 0.1 mM  $\text{CaCl}_2$ , gel with 300 mM NaCl, and gel with 100 mM  $\text{CaCl}_2$ . To prevent the effect of high ionic strength on the spectrum of Tetra-PAA-PEG gel in 100 mM  $\text{CaCl}_2$  solution, I also measured the SAXS profile for Tetra-PAA-PEG gel in 300 mM NaCl solution that has the same ionic strength. For the gel samples without a peak in the profile, a power-law decrease in the scattering intensity was observed. These profiles are qualitatively similar to those previously reported for pure tetra-PEG<sup>16</sup> and pure tetra-PAA<sup>17</sup>

hydrogels. Scattering from such relatively homogeneous semi-dilute gels is dominated by concentration fluctuations and is expressed by the Ornstein-Zernike (OZ) function.

$$I(q) = \frac{I(0)}{1 + (q\xi)^2} + I_{\text{BKG}} \quad (4-4)$$

where  $I(0)$  is the scattering intensity at the limit of  $q = 0$ ,  $\xi$  is the correlation length associated with the concentration fluctuation of the gel network, and  $I_{\text{BKG}}$  is the background scattering. Good agreement between the observed intensity and the OZ function was observed, indicating that the polymer chains are molecularly or homogeneously dispersed in the solvent. Indeed, it was expected that these gel samples have no significant aggregation because little to no  $\text{CaCl}_2$  salt was added.



**Figure 4-5.** Small angle X-ray scattering (SAXS) profiles for the Tetra-PAA-PEG gel samples in different external solutions: pure water (blue), 0.1 mM  $\text{CaCl}_2$  solution (gray), 300 mM  $\text{NaCl}$  solution (green), 100 mM  $\text{CaCl}_2$  solution (brown). The solid lines (pure water, 0.1 mM  $\text{CaCl}_2$  solution and 300 mM  $\text{NaCl}$  solution) for indicate fitting based on the Ornstein-Zernike (OZ) function. The solid lines (100 mM  $\text{CaCl}_2$  solution) indicate fitting based on the polydisperse “fuzzy”

sphere model.

For the gel sample with 100 mM CaCl<sub>2</sub>, a peak was observed which can be attributed to the structure factor or the correlation between the domains of aggregates formed upon the addition of divalent salt. Using the  $q$  value of the peak  $q_{\text{peak}}$ , the interdomain distance  $d$  can be calculated using Bragg's law:  $d = 2\pi/q_{\text{peak}}$ . The calculated value of  $d$  was 205.2 Å. To obtain quantitative information on the aggregate structure, a polydisperse sphere model with fuzzy interface was used to fit the data. For this model, the experimentally observed scattering intensity is described as

$$I(q) = N P(q) S(q) \quad (4-5)$$

where

$$N = \frac{\phi_{\text{HS}}}{V_{\text{HS}}} \quad (4-6)$$

$$V_{\text{HS}} = \frac{4}{3}\pi R_{\text{HS}}^3 (1 + 3p^2) \quad (4-7)$$

$N$  is the number density of the hard spheres,  $\phi_{\text{HS}}$  is the volume fraction,  $V_{\text{HS}}$  is the mean volume,  $R_{\text{HS}}$  is the mean radius with a Gaussian distribution, and  $p$  is the polydispersity.  $P(q)$  is the form factor representing scattering from individual domains and is given by

$$P(q) = \int_0^{\infty} f(R_c) |F(q, R_c)|^2 dR_c \quad (4-8)$$

Where

$$F(q, R_c) = \frac{4}{3}\pi R_c^3 \Delta\rho \frac{3(\sin(qR_c) - qR_c \cos(qR_c))}{(qR_c)^3} \quad (4-9)$$

$R_c$  is the radius of the domain core assuming tetra-PAA aggregates primarily constitute the core,  $f(R_c)$  is the Gaussian distribution function for  $R_c$ , and  $\Delta\rho$  is the scattering

length density (SLD) difference between the polymer and the solvent. Note that the difference in SLD between PEG ( $1.04 \times 10^{-5} \text{ \AA}^{-2}$ ) and PAA ( $1.03 \times 10^{-5} \text{ \AA}^{-2}$ ) is negligibly small and is also smaller than that between H<sub>2</sub>O ( $9.47 \times 10^{-6} \text{ \AA}^{-2}$ ) and either PEG or PAA. Therefore, SAXS is not able to discriminate between PEG and PAA and it is assumed that the domains have a uniform SLD.  $S(q)$  is the structure factor representing correlation between domains for which the hard sphere case was used, as given by the Percus-Yevick approximation<sup>18</sup> through the direct correlation function  $c_0$

$$S(q) = \frac{1}{1 - Nc_0(q)} \quad (4-10)$$

$$\begin{aligned} Nc_0(q) = & x^{-3}(A(\sin x - x \cos x) + B[(2/x^2 - 1)x \cos x + 2 \sin x - 2/x] \\ & - (\phi_{\text{HS}} A/2)[24/x^3 + 4(1 - 6/x^2) \sin x \\ & - (1 - 12/x^2 + 24/x^4)x \cos x]) \end{aligned} \quad (4-11)$$

$$A = -24\phi_{\text{HS}} \frac{(1 + 2\phi_{\text{HS}})^2}{(1 - \phi_{\text{HS}})^4} \quad (4-12)$$

$$B = 36\phi_{\text{HS}}^2 \frac{(2 + \phi_{\text{HS}})^2}{(1 - \phi_{\text{HS}})^4} \quad (4-13)$$

$$x = qD_{\text{HS}} \quad (4-14)$$

where  $D_{\text{HS}}$  is the mean diameter of the hard spheres.

Model fitting using the entire  $q$  range in the present study well reproduced the scattering profile of the gel sample with 100 mM CaCl<sub>2</sub>. This excellent agreement between the model and the experimental data indicates that the system undergoes microphase separation into polymer-rich domains and a matrix consisting of the remaining polymers and the solvent. The values of the structural parameters  $R_c = 52.9 \text{ \AA}$ ,  $R_{\text{HS}} = 99.8 \text{ \AA}$ ,  $N = 6.6 \times 10^{-8} \text{ \AA}^{-3}$ , and  $p = 0.27$  were then obtained from the

model fitting. The length scales  $R_c$  and  $R_{HS}$  of the domains are much smaller than the visible light wavelength ( $\sim 4-7 \times 10^3 \text{ \AA}$ ), which agrees with the observation that the gels are transparent. Since the  $R_g$  of tetra-PEG ( $M_w = 20\text{k g/mol}$ ,  $64.7 \text{ g/L}$ ) is around  $25 \text{ \AA}$  and is much smaller than  $d = 205.2 \text{ \AA}$  in this study,<sup>19</sup> it is likely that several tetra-PAA chains are collapsed to form a single domain. Because of the chain connectivity, this must be accompanied by the contraction of tetra-PEG chains.

The aggregation structure has two effects to leading to the deviation between the theoretical predictions and experiment results of the swelling and mechanical measurements. The first effect is that aggregation structure behaves as elastic hard cores and enhances the elasticity of the gel. The second effect is that aggregation structure can decrease the solvated polymer fraction, resulting in the decrease of mixing pressure. Both two effects can lead to the deviation between the predictions and the experimental results. Thus, the modified F-R-D-M model can successfully predict the swelling behaviors of Tetra-PAA-PEG gel in divalent salt solution at low concentration, in which no aggregation structure is formed. In the case of high salt concentration, the existence of aggregation structure can lead to the misestimation of the pressure.

Conventional studies that consider the divalent salt can only change the  $\chi$  parameter of the system and have no effect on the elasticity. However, according to my study on the Tetra-PAA-PEG gel in divalent salt system, the aggregation structure can form under high ionic strength condition and significantly enhance the elasticity of gel. Also, the validation of the modified F-R-D-M model for predicting the swelling behaviors of Tetra-PAA-PEG gel in divalent salt solution is verified.

#### 4.4. Conclusion

In this chapter, I investigated the swelling behaviors of 20K Tetra-PAA-PEG gel in divalent salt solution with different pH values and salt concentrations. Then, I measured the mechanical properties of gel to deduce the formation of aggregation structure. My major findings are as follows: (i) The swelling behaviors of Tetra-PAA-PEG gel in divalent salt solution of 0.1 mM concentration can be well reproduced by the modified F-R-D-M model, while the swelling behaviors of Tetra-PAA-PEG gel in divalent salt solution of 100 mM concentration deviated from the predictions by the F-R-D-M model; (ii) The swelling ratio of Tetra-PAA-PEG gel deviated from the predictions by the F-R-D-M model with the increase of the divalent salt concentration; (iii) The shear modulus of Tetra-PAA-PEG gel in divalent salt solution of 0.1 mM concentration can be well reproduced by the predictions, while the shear modulus under 100 mM concentration has a strong frequency dependence and deviated from the predictions, indicating the formation of aggregation structure that contribute to the elasticity; (iv) The SAXS measurement results support no aggregation structure formed in 0.1 mM concentration and aggregation structure formed in 100 mM concentration. The aggregation structure can lead to the enhancement of the elasticity and decrease the osmotic pressure. These findings indicate the validation of the modified F-R-D-M model for describing the swelling behaviors of Tetra-PAA-PEG gel in divalent salt solution, and the formation of aggregation structure strongly depend on the salt concentration of external solutions.

## Reference

- (1) Muta, H.; Kawauchi, S.; Satoh, M. *Colloid Polym. Sci.* **2003**, *282* (2), 149–155.
- (2) Horkay, F.; Tasaki, I.; Basser, P. J. *Biomacromolecules* **2000**, *1* (1), 84–90.
- (3) Horkay, F.; Basser, P. J.; Hecht, A. M.; Geissler, E. *Proc. Inst. Mech. Eng. Part H J. Eng. Med.* **2015**, *229* (12), 895–904.
- (4) Joachimiak, A.; Okrasa, L.; Halamus, T.; Wojciechowski, P. *Macromol. Symp.* **2005**, *222*, 203–208.
- (5) Bulo, R. E.; Donadio, D.; Laio, A.; Molnar, F.; Rieger, J.; Parrinello, M. *Macromolecules* **2007**, *40* (9), 3437–3442.
- (6) Zhou, C.; Qian, S. S.; Li, X. J.; Yao, F.; Forsythe, J. S.; Fu, G. D. *RSC Adv.* **2014**, *4* (97), 54631–54640.
- (7) Nordmeier, E.; Dauwe, W. *Polym. J.* **1991**, *23* (11), 1297–1305.
- (8) Manning, G. S. *Polyelectrolytes* **1974**, *00* (2), 9–37.
- (9) Manning, G. S. *Q. Rev. Biophys.* **1978**, *11* (2), 179–246.
- (10) Sakai, T.; Matsunaga, T.; Yamamoto, Y.; Ito, C.; Yoshida, R.; Suzuki, S.; Sasaki, N.; Shibayama, M.; Chung, U. Il. *Macromolecules* **2008**, *41* (14), 5379–5384.
- (11) Oshima, K.; Fujimoto, T.; Minami, E.; Mitsukami, Y. *Macromolecules* **2014**, *47* (21), 7573–7580.
- (12) Yoshikawa, Y.; Sakumichi, N.; Chung, U. Il; Sakai, T. *Soft Matter* **2019**, *15* (25), 5017–5025.
- (13) Hayashi, K.; Okamoto, F.; Hoshi, S.; Katashima, T.; Zujur, D. C.; Li, X.; Shibayama, M.; Gilbert, E. P.; Chung, U. Il; Ohba, S.; et al. *Nat. Biomed. Eng.*

- 2017, *I* (3), 1–7.
- (14) Gavish, N.; Promislow, K. *Phys. Rev. E* **2016**, *94* (1), 12611.
- (15) Mollerup, J. M.; Breil, M. P. *AIChE J.* **2015**, *61* (9), 2854–2860.
- (16) Matsunaga, T.; Sakai, T.; Akagi, Y.; Chung, U.-I.; Shibayama, M. *Macromolecules* **2009**, *42* (4), 1344–1351.
- (17) Morishima, K.; Li, X.; Oshima, K.; Mitsukami, Y.; Shibayama, M. *The Journal of Chemical Physics* **2018**, *149* (16), 163301–163309.
- (18) Ashcroft, N. W.; Lekner, J. *Physical Review* **1966**, *145* (1), 83–90.
- (19) Matsunaga, T.; Sakai, T.; Akagi, Y.; Chung, U.-I.; Shibayama, M. *Macromolecules* **2009**, *42* (16), 6245–6252.

## Chapter 5. Summary and Conclusion

This dissertation attempts to discuss two fundamental questions from experimental viewpoint: (1) how does the heterogeneous distribution of the fixed ions influence the swelling behaviors of polyelectrolyte gels; and (2) how are the swelling behaviors of highly charged polyelectrolyte gels based on the theoretical models.

From the viewpoint, a polyelectrolyte gel (Tetra-PAA-PEG gel) with di-block copolymer network structure fabricated by thiol-terminated poly(ethylene glycol) (Tetra-PEG-SH) and maleimide-terminated poly(acrylic acid) (Tetra-PAA-MA) via click chemistry was chosen as the model system, since the network structure owns tetrafunctional crosslinking points and a uniform strand length, which is similar to Tetra-PEG gel system that corresponds to nearly-deal network with good controllability of the network structures. This dissertation focuses on understanding of the heterogeneous distribution of acrylic acid groups on the swelling behaviors of Tetra-PAA-PEG gel in various external solutions. The principal results and conclusions are summarized below.

In Chapter 2, I investigated the optimized gelation condition for fabricating Tetra-PAA-PEG gel, and performed the swelling measurements for Tetra-PAA-PEG gel under various pH and ionic strength conditions in monovalent salt solution to validate the conventional polyelectrolyte theories. I discuss the deviation from the conventional models and proposed new model modified by counterion condensation theory for describing the swelling behaviors of highly charged polyelectrolyte gel. The major

findings are as follow:

1. The reaction between thiol and maleimide end groups is controlled by the pH of buffer solution, the gelation time can be optimized to 10 mins by setting the pH of buffer solution to 5.9.
2. The experimental storage modulus  $G'$  of Tetra-PAA-PEG gel can be reproduced by the phantom network model.
3. The conventional polyelectrolyte model (Flory-Rehner model combined with Donnan theory) cannot describe the swelling behaviors of Tetra-PAA-PEG gel.
4. I modified the conventional polyelectrolyte model by combining with counterion condensation theory (F-R-D-M model), which successfully describe the swelling behaviors of Tetra-PAA-PEG gel.

In Chapter 3, I fabricated the Tetra-PAA-PEG gels with the different neutral segment lengths while controlling the consistent fixed ion concentrations and crosslink density. The effect of neutral segment lengths on the mechanical and swelling properties is investigated by performing the rheological and swelling measurements. I discuss the deviation of experimental swelling ratios from the predictions by the F-R-D-M model under relatively large deformation and modified the F-R-D-M model by adopting the Gent model to describe the effect of finite extensibility of the network strands. The major findings are as follow:

1. The shear modulus is deviated from the classical rubbery elasticity theory, depending on the concentration normalized by the overlapping concentration of the

prepolymers.

2. The F-R-D-M model successfully describe the swelling behaviors of Tetra-PAA-PEG gel under relatively small deformations, but failed to describe the swelling behaviors under relatively large deformations.
3. I modified the F-R-D-M model by adopting the Gent model that consider the finite extensibility of network strands instead of the Neo-Hookean model, and successfully describe the swelling behaviors under larger deformation.

In Chapter 4, I investigated the swelling behaviors of Tetra-PAA-PEG gel in divalent salt solutions under various conditions. The major finding are as follows:

1. The modified F-R-D-M model predictions can well reproduce the swelling behaviors of Tetra-PAA-PEG gel in  $\text{CaCl}_2$  salt solution with relatively low concentration (0.1 mM).
2. The elastic modulus of Tetra-PAA-PEG gel in  $\text{CaCl}_2$  salt solution with relatively low concentration (0.1 mM) was well reproduced by the Flory's model, but deviated from the Flory's model in  $\text{CaCl}_2$  salt solution with relatively high concentration (100mM).
3. SAXS measurement result indicate the deviation in relative relatively high concentration is attributed to the formation of aggregation structure, which enhances the elasticity of the gel and decreases the mixing pressure.

In conclusion, I established the prepared condition of Tetra-PAA-PEG gel, and

evaluated the structure analysis, mechanical and swelling properties using this gel. This gel possesses well controlled heterogeneous distribution of fixed ions inside the gel system, and is a good model for investigating the relationship between the distribution of fixed ions and swelling behaviors. In monovalent salt system, the swelling behaviors can be well described by Flory-Rehner model considering both the Donnan equilibrium and Manning's counterion condensation effects under relatively small deformation. By adopting the Gent model instead of the Neo-Hookean model, the swelling behaviors under relatively high deformation can also be well described (the modified F-R-D-M model). In divalent salt system, the swelling behaviors can be well described by the modified F-R-D-M model under relatively low salt concentration condition. Calcium ion and acrylic acid groups can form aggregation under relatively high salt concentration, enhancing the elasticity of the gel and decrease the mixing pressure.

Through the investigation on the Tetra-PAA-PEG gels, the model for describing the swelling behaviors of highly charged polyelectrolyte gel is defined. These findings will help better understand the relationship between the distribution of fixed ions and the swelling behaviors of polyelectrolyte gels in various external solutions.

## List of publications

1. **J. Tang**, T. Katashima, X. Li, Y. Mitsukami, Y. Yokoyama, N. Sakumichi, U. Chung, M. Shibayama, T. Sakai. "Swelling Behaviors of Hydrogels with Alternating Neutral/Highly Charged Sequences." *Macromolecules*, 53.19 (2020): 8244-8254.
2. **J. Tang**, T. Katashima, X. Li, Y. Mitsukami, Y. Yokoyama, N. Sakumichi, U. Chung, M. Shibayama, T. Sakai. "Effect of Nonlinear Elasticity on the Swelling Behaviors of Highly Swollen Polyelectrolyte Gels." *Gels*, Submitted.
3. **J. Tang**, T. Katashima, C. I. Gupit. X. Li, Y. Mitsukami, Y. Yokoyama, N. Sakumichi, U. Chung, M. Shibayama, T. Sakai. "Swelling Behaviors of Hydrogels with Alternating Neutral/Highly Charged Sequences in divalent salt solution." To be submitted.

## List of presentations

1. **Jian Tang**, C. I. Gupit, Xiang Li, Takuya Katashima and Takamasa Sakai.  
"Swelling behaviors of polyelectrolyte gel based on Tetra-arm homopolymers." 29<sup>th</sup>  
Annual Meeting of MRS-J (Yokohama (Japan)) 27<sup>th</sup>-29<sup>th</sup> Nov. 2019.
2. **Jian Tang**, Xiang Li, Mitsukami Yoshiro, Yuki Yokoyama, Takuya Katashima,  
Mitsuhiro Shibayama, Takamasa Sakai. "Swelling behaviors of polyelectrolyte gel  
based with high charge density." 69<sup>th</sup> SPSJ Annual Meeting (Fukuoka (Japan)) 27<sup>th</sup>-  
29<sup>th</sup> May. 2020.
3. **Jian Tang**, Takuya Katashima, Xiang Li, Mitsukami Yoshiro, Yuki Yokoyama,  
Naoyuki Sakumichi, Ung-il Chung, Mitsuhiro Shibayama, Takamasa Sakai.  
"Swelling Behaviors of Hydrogels with Alternating Neutral/Highly Charged  
Sequences." 3<sup>th</sup> Glowing Polymer Symposium in Kanto (Online (Japan)) 28<sup>th</sup> Nov.  
2020.